1.0	4.5	2.8	2.5
	5.0	3.2	2.2
	5.6		
	6.3	3.6	
1.1		4.0	2.0
			1.8
1.25	1.4		1.6

MICROCOPY RESOLUTION TEST CHART
NATIONAL BUREAU OF STANDARDS-1963-A

AFGL-TR-82-0234

ANALYSIS OF A POLARIZATION DIVERSITY
WEATHER RADAR DESIGN

J.S. Ussailis
L.A. Leiker
R.M. Goodman IV
J.I. Metcalf

Georgia Tech Research Institute
Georgia Institute of Technology
Atlanta, Georgia 30332

AD A121666

Final Report
1 October 1980 - 30 June 1982

2 July 1982

DTIC
SELECT
NOV 2 2 1982

A

DTIC FILE COPY

82 11 22 102

REPORT DOCUMENTATION PAGE		READ INSTRUCTIONS BEFORE COMPLETING FORM
1. REPORT NUMBER AFGL-TR-82-0234	2. GOVT ACCESSION NO. A̶ᴅ̶-̶	3. RECIPIENT'S CATALOG NUMBER
4. TITLE *(and Subtitle)* Analysis of a Polarization Diversity Weather Radar Design		5. TYPE OF REPORT & PERIOD COVERED Final 10/1/80-6/30/82
		6. PERFORMING ORG. REPORT NUMBER
7. AUTHOR(*s*) J.S. Ussailis, L.A. Leiker, R.M. Goodman IV, and J.I. Metcalf *		8. CONTRACT OR GRANT NUMBER(*s*) F19628-81-K-0027
9. PERFORMING ORGANIZATION NAME AND ADDRESS Georgia Tech Research Institute Georgia Institute of Technology Atlanta, Georgia 30332		10. PROGRAM ELEMENT, PROJECT, TASK AREA & WORK UNIT NUMBERS 62101F 678100
11. CONTROLLING OFFICE NAME AND ADDRESS Air Force Geophysics Laboratory Hanscom AFB, Massachusetts 01731 Monitor/Graham M. Armstrong/LYR		12. REPORT DATE 2 July 1982
		13. NUMBER OF PAGES 141
14. MONITORING AGENCY NAME & ADDRESS(*if different from Controlling Office*)		15. SECURITY CLASS. *(of this report)* UNCLASSIFIED
		15a. DECLASSIFICATION/DOWNGRADING SCHEDULE

16. DISTRIBUTION STATEMENT *(of this Report)*

Approved for public release; distribution unlimited

17. DISTRIBUTION STATEMENT *(of the abstract entered in Block 20, if different from Report)*

18. SUPPLEMENTARY NOTES

* Air Force Geophysics Laboratory /LYR

19. KEY WORDS *(Continue on reverse side if necessary and identify by block number)*

Polarization diversity radar	Polarization isolation
Circular polarization diversity	Polarization diversity modification for
Linear polarization diversity	coherent Doppler radar
Integrated cancellation ratio	

20. ABSTRACT *(Continue on reverse side if necessary and identify by block number)*

This report focuses not only on a design for a pulse-to-pulse polarization diversity modification of the Air Force Geophysics Laboratory (AFGL) S-band Doppler weather radar, but also upon the meteorological and technical requirements of such a radar. The theoretical aspects of and physical limitations imposed by the polarization diversity requirement are presented independently of this design and as a result are applicable towards the development of any similar system. The antenna modification could also be applied towards the

DD ₁ FORM ₇₃ 1473   EDITION OF 1 NOV 65 IS OBSOLETE

general case, excepting the condition imposed in this design that the present twenty-four foot diameter reflector be retained. Formulae are developed to demonstrate the various uncertainties for the system as a whole and the antenna in particular. Tradeoffs between the various meteorological measurement goals vs available and constructible radio frequency components are presented.

Accession For

NTIS GRA&I

DTIC TAB

Unannounced

Justification

By

Distribution

Availability

Avail and/or

special

A

TABLE OF CONTENTS

iii

TABLE OF CONTENTS (continued)

TABLE OF CONTENTS (continued)

TABLE OF CONTENTS (continued)

LIST OF FIGURES

vii

LIST OF FIGURES (continued)

LIST OF TABLES

SECTION 1
INTRODUCTION

This report will focus not only on a design for a pulse-to-pulse polarization diversity modification of the Air Force Geophysics Laboratory (AFGL) S-band Doppler weather radar, but also upon the meteorological and technical requirements of such a radar. The theoretical aspects of and physical limitations imposed by the polarization diversity requirement, detailed in Section 2, are presented independently of this design and as a result are applicable towards the development of any similar system. The antenna modification, specified in Section 3, could also be applied towards the general case, excepting the condition imposed in this design that the present AFGL twenty-four foot diameter reflector be retained. These two sections do support the thesis that the system is constructible, but performance would be slightly reduced from the anticipations of the meteorological community. Formulae are developed to demonstrate the various uncertainties for the system as a whole and the antenna in particular. Trade-offs between the various meteorological measurement goals vs available and constructible radio frequency components are presented in detail in Section 4. A summary (Section 5) and lists of recommended components and vendors (Appendices A and B) conclude this report.

SECTION 2
BACKGROUND

2.1 INTRODUCTION

Backscattered radar signals in general are characterized by a scattering matrix of four complex coefficients which correspond to the four possible transmit-receive polarization combinations for a given pair of orthogonal antenna polarizations. The diagonal terms correspond to transmitting and receiving with the antenna polarization, e.g., L-L and V-V. The off-diagonal terms correspond to receiving with an antenna polarized othogonal to the transmit antenna polarization, e.g., L-R and H-V. These coefficients are complex because they contain magnitude and phase information. The diagonal terms are usually denoted by S_{11} and S_{22} or S_{HH} and S_{VV} and the off-diagonal terms as S_{12} and S_{21} or S_{HV} and S_{VH}.

To determine the complete backscatter matrix of a radar target, one must transmit two orthogonal polarizations. In the case of meteorological targets, signal decorrelation due to random relative motions of the individual scatterers requires that the transmitted polarization be switched very rapidly, i.e., between radar pulses. This pulse-to-pulse polarization agility technique allows one to measure the relative magnitudes and phases of the scattering coefficients with maximum accuracy. If the transmit polarization is switched at a rate slower than the signal decorrelation rate then only the relative magnitudes and phases of the pair S_{11} and S_{12} and the pair S_{22} and S_{21} can be measured accurately; the magnitudes of S_{11} and S_{22}, for example, would each be derivable only as averages and their relative magnitude would be subject to the statistical uncertainties of both. The relative phase of these coefficients would be lost.

The physical parameters of interest manifest themselves in the anisotropy of the electromagnetic propagation and scattering

3

media. Orientation angles and relative dimensions of scatterers can be derived from the non-zero relative phase angles and relative magnitudes of the scattering coefficients. Attainment of these measurement objectives thus places stringent criteria on the accuracy of signal amplitude and phase measurement. In addition to the usual meteorological radar requirements of high receiver signal-tc-noise ratio, narrow beam, and low sidelobe power level, design criteria must be developed for uniformity of signal polarization across the radar beam, isolation of the two signals in the receiver, and minimization of magnitude and phase errors in the two receiver channels.

The scattering coefficients given above in terms of linear polarization can be expressed in terms of any pair of orthogonal base vectors by a matrix transformation. Circular and linear base vectors are most commonly used, in the interest of reducing the complexities of engineering and analysis. For certain classes of radar targets, the terms in the scattering matrix can be simplified if some of the parameters have known values or relative values. In meteorological scattering media, observed at 10 cm radar wavelength, the linearly cross-polarized signals (i.e., off-diagonal matrix terms) are usually of smaller amplitude than the co-polarized signals by a factor of 100 (20 dB) or more. If the symmetry axes of the medium are aligned with the local vertical and horizontal, as is often the case, the off-diagonal terms are due entirely to the distribution of canting angles of the individual scatterers. Under such conditions, the diagonal terms of the scattering matrix (defined relative to linearly polarized base vectors) are of greatest interest. The measurement of these quantities with linear polarization requires rapid switching between horizontal and vertical transmitted polarizations. The same quantities can be derived from received signals with polarizations identical and orthogonal to a transmitted circular polarization, without the requirement for rapid switching. If switched linear polarization is used for

4

determining the diagonal terms of the scattering matrix, then the sequentially received signals are within a few decibels of each other (horizontally polarized power is up to 5 dB greater than vertically polarized power in rain, but 2 or 3 dB less than the vertically polarized power in ice-phase media). If the circular polarization option is exercised, then the received signal in the transmission channel is typically 15 dB or more below the simultaneously received signal in the orthogonal channel. The purity of the transmitted polarization and the isolation of the received signals establish a lower limit on the capability of measuring the ratio of power in the two channels.

Information on the orientation state of the scattering medium (average canting angle and the extent to which the individual scatterers are preferentially aligned) can be obtained from the off-diagonal terms of the scattering matrix, if switched linear polarization is transmitted. Similar information can be obtained from the two circularly polarized received signals without switching polarization, although in this case there will be ambiguities if the scatterers are large (i.e., non-Rayleigh) or if differential propagation effects are present. These ambiguities can be resolved if the transmitted polarization is alternated between right and left circular.

If spectrum analysis techniques are to be used in analyzing the received signals, then the signal time series to be analyzed must comprise signal samples with uniform polarization characteristics. Such a time series can be generated from alternate radar pulses during operation with pulse-to-pulse polarization switching. Two sets of time series, corresponding to the two transmitted polarization states, can be generated during an observation interval. Each of these would have a sampling rate equal to half of the actual radar pulse repetition rate.

The meteorological concepts and engineering factors involved in this research area have been discussed in detail in several

technical reports and published papers, listed in the references following Appendix C.

2.2 LEVEL OF RECEIVED BACKSCATTER

The design requirements of a radar receiver are dependent upon the expected return signal characteristics. One of these characteristics, the received level of backscatter, is a function of range, cross section, and extent of the target. Furthermore, in the case of a polarization diversity, Doppler weather radar, the expected return is also dependent upon the size, shape, and composition of an extended conglomerate of relatively small targets. To perform the necessary calculations, we assume this conglomerate to be tenuous, homogeneous, uniform, and isotropic within the viewing cell. The requirements of both the receiver and the antenna will be functions of the aforementioned characteristics and must be defined to the quality of detail required by the research to be performed. The properties of the radar transmitter, while influenced by these target characteristics, will not be considered in this report, since (1) there is no provision to alter the existing transmitter and (2) the gathering of quality data is not so strongly influenced by the transmitter characteristics.

2.2.1 RECEIVED RADAR BACKSCATTER

To determine the anticipated returned power level presented to the receiver, one refers to the radar range equation[1]

$$P_r = P_t \frac{G_t G_r \sigma \lambda^2 F_t^2 \; F_r^2}{(4\pi)^3 \; r^4} \; . \qquad (1)$$

---

1   M. I. Skolnik, RADAR HANDBOOK, (New York, NY: McGraw-Hill, 1970) pp. 2-4.

where: G_t = gain of transmitting antenna

G_r = gain of receiving antenna

σ = cross section of target

λ = wavelength

F_t = pattern factor of transmitting antenna

= $\dfrac{\text{antenna gain at angle of target}}{\text{maximum antenna gain}}$

F_r = pattern factor of receiving antenna

r = range

P_t = transmitted power and

P_r = received power.

In the case of a radar with a common receive/transmit antenna, Equation (1) reduces to

$$P_r = P_t \frac{G^2 \ \sigma \ \lambda^2 \ F^2}{(4\pi)^3 \ r^4} \ . \tag{2}$$

The maximum radar range can also be determined. First, one must select an applicable signal-to-noise ratio for which reasonable signal processing can be expected. This can be expressed in terms of received power,

$$\frac{S}{N} = \frac{P_r}{P_N} \ .$$

where

S/N = signal to noise ratio necessary to operate the processor

P_N = composite power level of noise generated within receiver and noise temperature of the observed medium.

If the receiver is considered to be an ideal amplifier with a resistor operating at temperature T connected to its antenna terminals, then P_N becomes,

$$P_N = K_b B(T_{eff} + T_s) = K_b BT, \tag{3}$$

7

where

K_b = Boltzmann's constant,

B = receiver bandwidth,

T_{eff} = effective receiver noise temperature, and

T_s = observed median temperature.

So that the maximum range of the radar is,

$$r = P_t \left[\frac{G^2\ \sigma\ \lambda^2\ F^2}{(4\pi)^3 \left(\frac{S}{N}\right) K_b TB} \right]^{1/4} . \qquad (4)$$

Although Equations (1) and (4) are useful for determining the required transmitter power level, receiver bandwidth, acceptable signal-to-noise ratio, and antenna gain for a standard target tracking or search radar, their usefulness is cumbersome when assessing the requirements of a weather radar. As an example, what antenna gain or factor does one employ in these equations when the target completely fills the antenna main beam as well as many sidelobes? The expected backscatter level can be more easily calculated by dissecting the radar range equation into its component parts, analyzing each part individually, and finally reformulating the equation.

2.2.2 LEVEL OF BACKSCATTER RECEIVED BY A BEAM FILLING RADAR
2.2.2.1 Precipitation Cross Section
2.2.2.1.1 Reflectivity

Meteorological reflectivity, η, is defined as the total radar cross section (RCS) per unit volume. If one considers a spherical raindrop model and only Rayleigh scattering (D $\ll \lambda$), then the cross section can be analytically determined[2];

---

2   J. I. Metcalf, et al., "Design Study for a Coherent Polarization-Diversity Radar" Georgia Institute of Technology, Engineering Experiment Station, Final Report for the period 1 March 1979 – 11 April 1980. AFGL-TR-80-0262 Air Force Geophysics Laboratory, AD A096757.

i.e.,

$$\sigma = \frac{\pi^5}{\lambda^4} |\kappa|^2 D^6$$

so that

$$\eta = \frac{\pi^5}{\lambda^4} |\kappa|^2 \frac{D^6}{V} = \frac{\pi^5}{\lambda^4} |\kappa|^2 Z \times 10^{-10} , \qquad (5)$$

where

$$\kappa = \frac{\epsilon - 1}{\epsilon + 2}$$

ϵ = precipitation dielectric constant,

D = raindrop diameter,

V = volume of reflecting cell,

Z = reflectivity factor expressed in mm^6/m^3, and

λ is expressed in cm

Given a Marshall-Palmer raindrop distribution[3]

$$\eta = (2 \times 10^{-8}) \frac{\pi^5}{\lambda^4} |\kappa|^2 R^{1.6}, \qquad (6)$$

where R is the rainfall rate in mm/hr. The rainfall reflectivity can be reduced to

$$\eta = \frac{A}{\lambda^4} , \qquad A = (2 \times 10^{-8}) \pi^5 R^{1.6} . \qquad (7)$$

Empirically, similar relationships have been determined[4] for other forms of precipitation. Since $|\kappa|^2$ numerically equals 0.93 for water and 0.197 for ice, and since the radar frequency is fixed at a mean frequency of 2.74 GHz, these relationships can be presented in simplified form (Table 1).

---

3 Ibid

4 Ibid

TABLE 1.   METEOROLOGICAL REFLECTIVITY OF VARIOUS PHENOMENA
AT 2.74 GHz*

Reflectivity, η in units m^{-1}	Weather Phenomena
$4.04 \times 10^{-10} R^{1.6}$	rain
$8.55 \times 10^{-10} R^{2}$	snow
$4.27 \times 10^{-9} R^{0.97}$	hail
$9.70 \times 10^{-14} M^{2}$	water clouds
$2.05 \times 10^{-14} M^{2}$	ice clouds

* M is in grams of melted water/cubic meter and R is
the melted rainfall rate in millimeters/hour.

2.2.2.1.2 Effective Antenna Beamwidth

Prior to calculating the expected precipitation backscatter
power level, one must determine an average incident beam power
level and corresponding effective antenna beamwidth. One cannot
employ the maximum effective radiated power (ERP) or antenna gain
as usually defined within the radar range equation, as these
levels are definable only at the center of the main beam.
Likewise one cannot assume the antenna beamwidth is the usually
stated half-power beamwidth (HPBW), since the anticipated target
normally extends beyond this angle. One approach to the problem
is to determine an antenna gain that is averaged over the entire
main beam between the first null beamwidth (FNBW). In the case
of cylindrically symmetric parabolic antennas, the minus 6 dB
beamwidth can be taken as a good approximation to the effective
filled beamwidth over which the main beam power is averaged.
Within this beamwidth, it is also safe to approximate the one-
coordinate antenna pattern P(θ) as the exponential function,

$$P(\theta) = e^{-(a\theta)^2} \qquad\qquad (8)$$

where   a   = C/θ_{3dB},

           θ =   displacement angle from the center of the main beam, and

          θ_{3dB} =   half power beam angle.

C can be determined from the definition of HPBW,

$$P(\theta_{3dB}) = -\frac{1}{2} = e^{-(C)^2}$$

or   C = 0.83.

The average beam power is defined over both coordinates as

$$P(\theta,\phi) = \frac{\displaystyle\int_{\theta,\phi} e^{-(a\theta)^2} e^{-(a\phi)^2} d\theta d\phi}{\displaystyle\int_{\theta,\phi} d\theta d\phi}.$$

The solution of $\int_\theta e^{-(a\theta)^2} d\theta$ is straighforward:

let $t/\sqrt{2} = a\theta$, so that $t = a\sqrt{2}\,\theta$ and $d\theta = \dfrac{1}{a\sqrt{2}} dt$ then

$$\int_\theta e^{-(a\theta)^2} d\theta = \frac{1}{a\sqrt{2}} \int e^{-t^2/2} dt.$$

From a table of integrals[5] we find a solution for the Error Function,

---

5   H. B. Dwight, <u>Tables of Integrals and Other Mathematical Data</u>, Fourth Edition (New York, NY: The Macmillian Co., 1969) p. 136.

$$\text{Erf } \frac{x}{\sqrt{2}} = \frac{1}{\sqrt{2\pi}} \int_{-x}^{x} Q^{-t^2/2} \, dt$$

$$= x\left(\frac{2}{\pi}\right)^{1/2} \left[1 - \sum_{N=1}^{\infty} \frac{x^{2N} (-1)^N}{2^N (N)(2N+1)} \right].$$

so that

$$\int_{\theta} e^{-(a\theta)^2} \, d\theta = 2\theta \left[1 - \sum_{N=1}^{\infty} \frac{(a\theta)^{2N} (-1)^N}{N (2N+1)} \right].$$

The antenna pattern average then becomes

$$\overline{P(\theta,\phi)} = \left[1 + \sum_{N=1}^{\infty} \frac{(a\theta)^{2N} (-1)^N}{N (2N+1)} \right] \left[1 + \sum_{M+1}^{\infty} \frac{(a\theta)^{2M} (-1)^M}{M (2M+1)} \right]. \qquad (9)$$

Equation (9) may be placed in dB space and simplified by symmetry to

$$P_O = 10 \text{ LOG } \overline{(P(\theta,\phi))} = 20 \text{ LOG } \overline{(P(\theta))}$$

$$= 20 \text{ LOG } \left[1 + \sum_{N=1}^{\infty} \frac{(a\theta)^{2N}(-1)^N}{N (2N+1)} \right]. \qquad (10)$$

The average antenna gain is then the product of the peak antenna gain and Equation (9). This average gain is asumed to exist over part of or the entire main beam, with θ the bound over which the average is taken. It is instructive to conceptualize a one-dimensional average gain for targets so distant that they act as slightly extended backscatterers in the vertical direction and filled beam backscatterers in the horizontal direction. Of course, employment of one set of bracketed terms in Equation (9) fulfills this requirement.

The average gain may also be described by a reduction of the measured antenna gain by Equation (10); this reduced level is now assumed to be a cylindrical beam with beamwidth ±θ. Both the

one- and two-dimensional gain reductions for various beamwidth angles were determined for a 24-foot symmetric paraboloid by a simple computer program (Appendix C) and are reproduced in Table 2. Note that the -6 dB beamwidth approximates the results of Probert-Jones[6]. Furthermore, the results agree with the Georgia Tech clutter models which employ the half power gain and an effective beamwidth of

$$\theta_{eff} = \sqrt{2} \ HPBW \ ;$$

this approximation will be employed in subsequent calculations.

TABLE 2. ANTENNA GAIN REDUCTION VS FILLED BEAM BEAMWIDTH

Effective Beamwidth	Subtended Angle	One Dim. Gain Reduction	Two Dim. Gain Reduction
-1/4 dB	0.31°	0.08 dB	-0.16 dB
-3	1.09	0.92	1.83
-6	1.50	1.60	3.20
-10	2.00	2.50	5.00
first null	2.80	3.70	7.40

2.2.2.1.3 Scattering Cross Section For Target At Near and Intermediate Ranges

The scattering cross section of a homogeneous conglomerate of small non-absorbent particles may now be determined. Consider a cell within a cylindrically symmetric antenna beam (Figure

---

6   J. R. Probert-Jones, "The Radar Equation in Meteorology," Quart. J. Roy. Meteor. Soc., 88, 1960, pp. 485-495.

1). The volume of scatters in this cell is given by the volume of a cylinder of diameter θ_{eff} length corresponding to $c\tau/2$, where c is the velocity of light and τ is the transmitted pulse width. This cylindrical approximation is acceptable because (1) the cell's range, r, is much greater than its extent and (2) application of the previous effective beamwidth calculation yields a cylindrical beam. The cell's volume is then

$$V = \pi \left[\frac{r\theta_{eff}}{2} \right]^2 \left[\frac{c\tau}{2} \right]$$

with θ expressed in radians. The scattering cross-section becomes,

$$\sigma = \frac{\pi}{8} \left[r\theta_{eff} \right]^2 c\tau\eta \tag{11}$$

which can be approximated for a 24 foot symmetrical paraboloid and a 1.0 microsecond pulse width as

$$\sigma \simeq 8.5 \times 10^{-2} \ r^2 \eta \tag{12}$$

where η is given in Table 1 for various meteorological targets.

Note that this discussion is valid only for targets that fill the entire main beam. In the case of weather radar, such approximations lose validity as r increases to an intermediate range where beamfilling becomes less likely due to a lessened vertical target extent; this extent depends, of course, upon the precipitation medium. The radar's usefulness can continue, in range, beyond a point at which targets of almost any nature can only fill the beam horizontally. These beamfilling factors 'ave an impact upon the radar range equation.

2.2.2.1.4 Scattering Cross Section for Targets at Far Range

In a previous subsection, the two-dimensional average beam power correction factor was determined for a model cylindrical

14
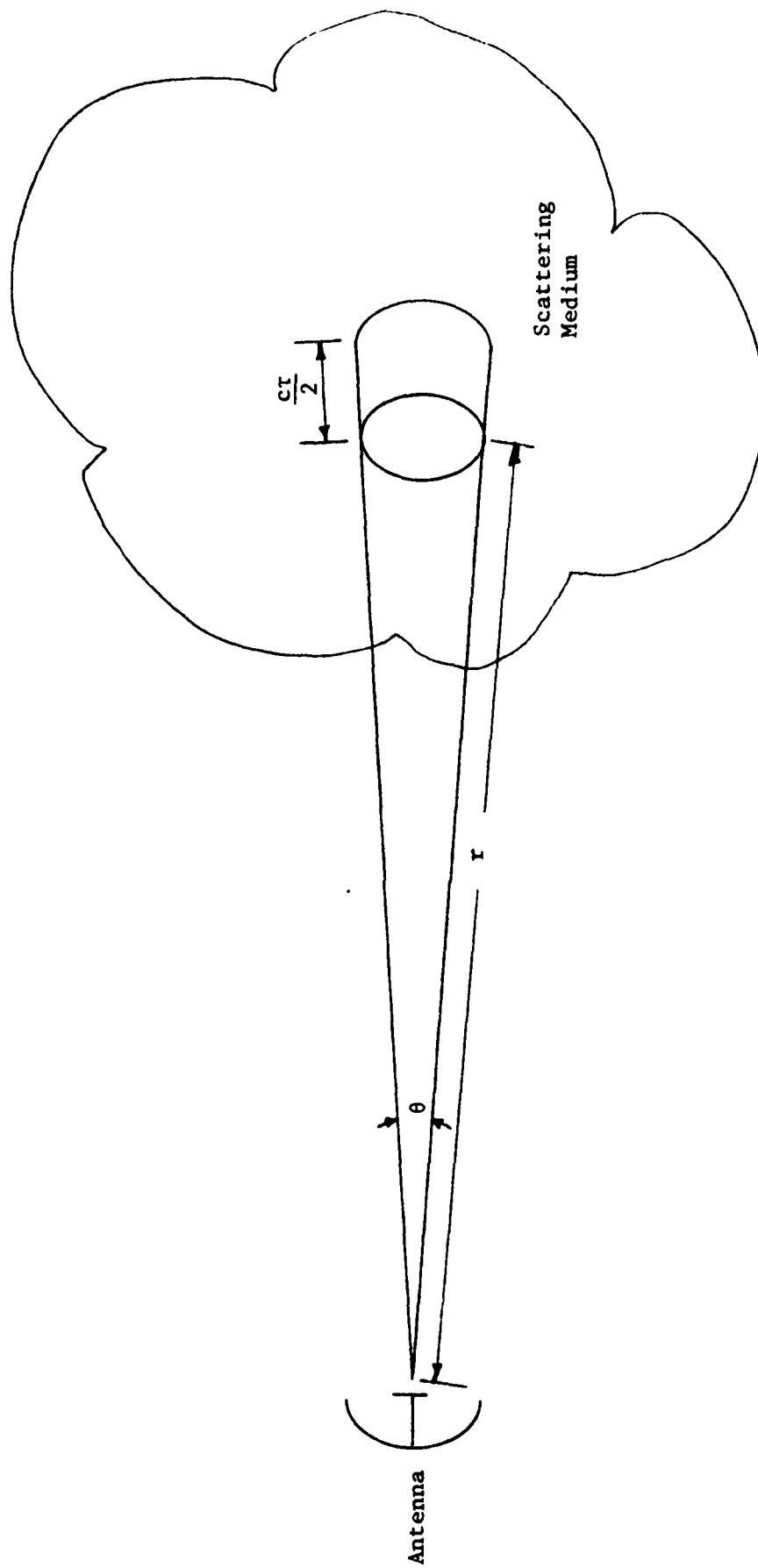
Figure 1. Volume of scatters in a beamfilling radar.

15

beam of radius approximately equal to the -6 dB beamwidth angle of a symmetric parabolic antenna. In that subsection the one-dimensional average beam power correction factor was also calculated; that calculation will be useful in the far range approximation.

Assume that a cell of interest is sufficient by far in range so that the lower edge is occluded by the horizon and the upper cell edge is within the cylindrical radar beam (Figure 2). In this limiting case, the cell volume is given by assuming an approximate rectangular, rather than circular, cross section so that

$$V \approx (a_2 - a_1)(r\theta_{eff})(c\tau/2). \tag{13}$$

where a_1 and a_2 are the lower and upper beam edges, respectively. The scattering cross section then becomes,

$$\sigma = (a_2 - a_1)(r\theta_{eff})(c\tau/2)\eta. \tag{14}$$

As will be shown, the energy returned to the radar in this case varies as r^{-3}, instead of the r^{-2} law normally assumed for beam-filling radars. Furthermore, the one dimensional average antenna gain correction is valid as the vertical dimension is now bounded by the target extent, rather than the antenna beamwidth.

2.2.2.2 Beam Filling Radar Range Equation

Equation (2) may now be altered for this class of radar. If we note that:

$$G^2 F^2 = (G_{3dB})^2$$
$$\sigma = \pi/8 \; (\rho\theta_{eff})^2 \; c\tau\eta$$

for the near and intermediate ranges, then Equation (2) becomes

16
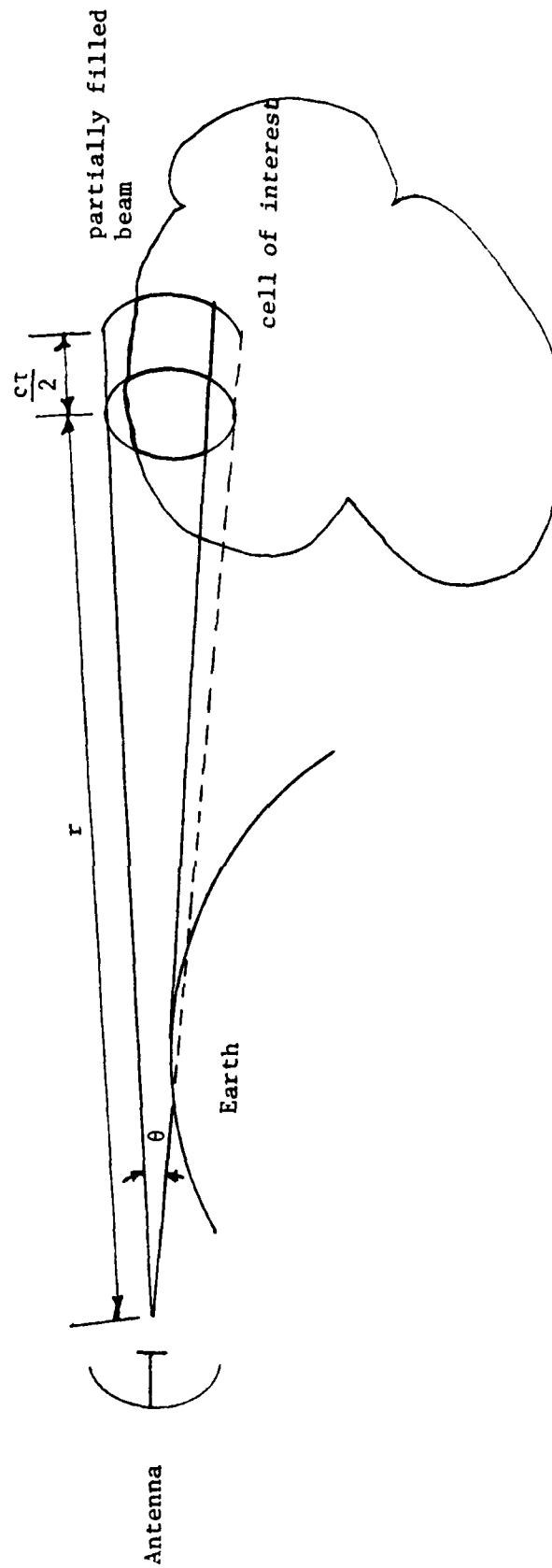
Figure 2. Partially filled radar beam in a limiting far range case.

$$P_r = P_t \ \frac{c\tau}{512\pi^2} \ \frac{\left[G_{3dB} \ \lambda \ \theta_{eff}\right]^2 \ \eta}{r^2}$$

$$= 18.1 \ \frac{P_t \ \tau \ \left[G_{3dB} \ \lambda \ \theta'\right]^2}{r^2} \ \eta \ .$$

(15)

with $\theta' = \sqrt{2}$ HPBW now expressed in degrees. For the far range, employing the results of the previous paragraph yields

$$P_r = 1.32 \times 10^3 \ \frac{P_t \tau \theta' \left[a_2 - a_1\right] \left[G_{3dB} \ \lambda\right]^2}{r^3} \eta.$$

(16)

The return energy is proportional to the inverse square or inverse cube of range depending upon the beamfilling conditions. Since a-priori the extent of beamfilling is unknown, other means which will supply knowledge of cell conditions must be employed to determine this extent. Polarization diversity can make a contribution in determination of the type and extent of the observed cell. First, however an examination must be performed to understand the range at which partial beamfilling might occur. Obviously, cell cross section for a cylindrical symmetric antenna is proportional to $(r\theta_{eff})^2$. If a 200 kilometer range, 113 meter antenna altitude, and 1.6 degree effective antenna beamwidth are considered (i.e., the AFGL radar), then elevation beamfilling occurs for cells from approximately 1600 to 5600 meters altitude. Specific conditions will determine whether beamfilling occurs and whether the inverse square or inverse cube law should be applied. The path loss (space loss plus reflectivity "loss") vs various precipitation and precipitation rates are plotted in Figures 3 through 7; here it was assumed that the inverse cube law is applicable for ranges $>$ 100 km and the inverse square law is applicable for lesser ranges. Such sharp delineation does not occur in nature.

18
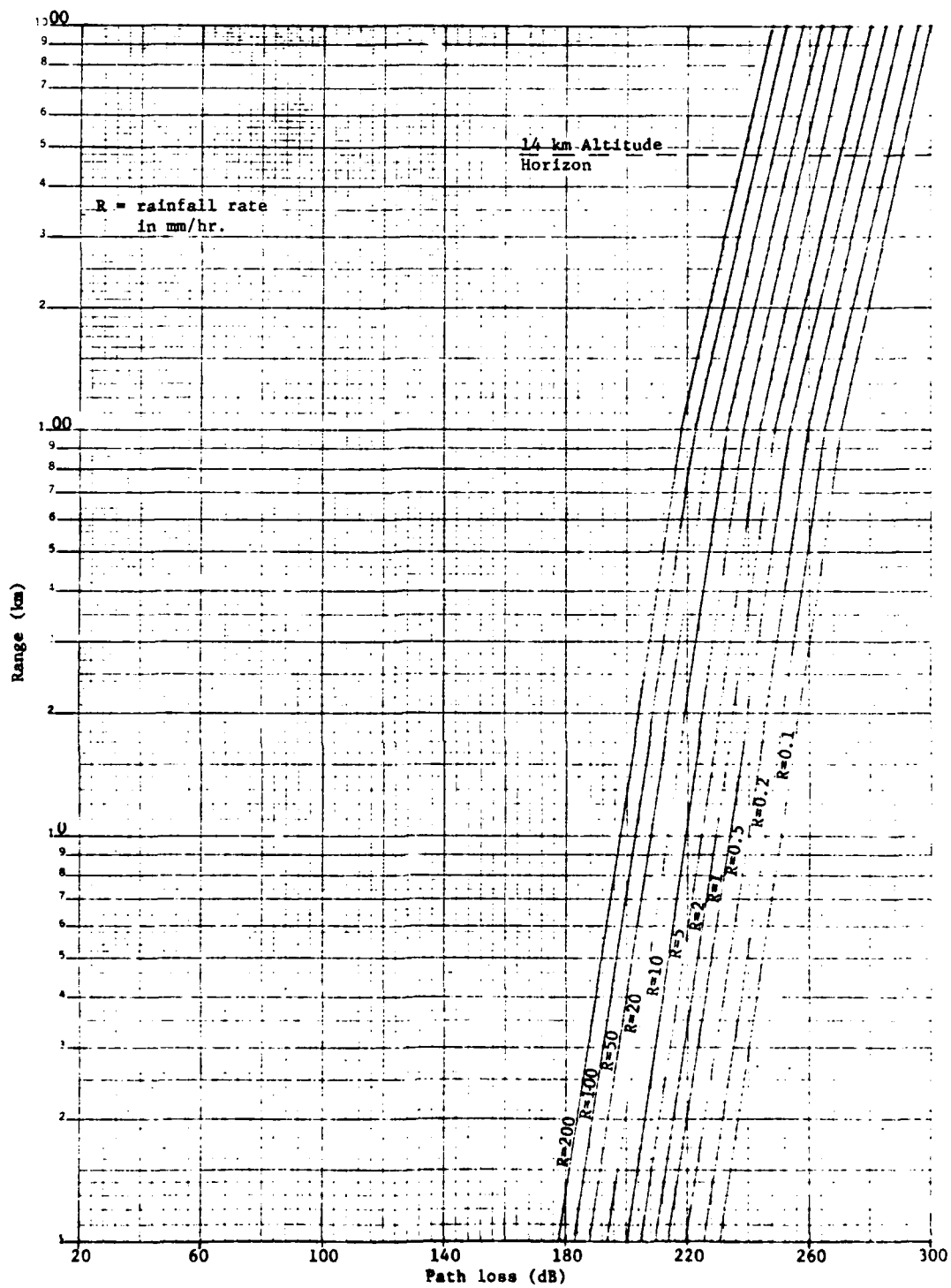
Figure 3. Path loss at various ranges and rainfall rates.
$\lambda = 10.9$ cm

19
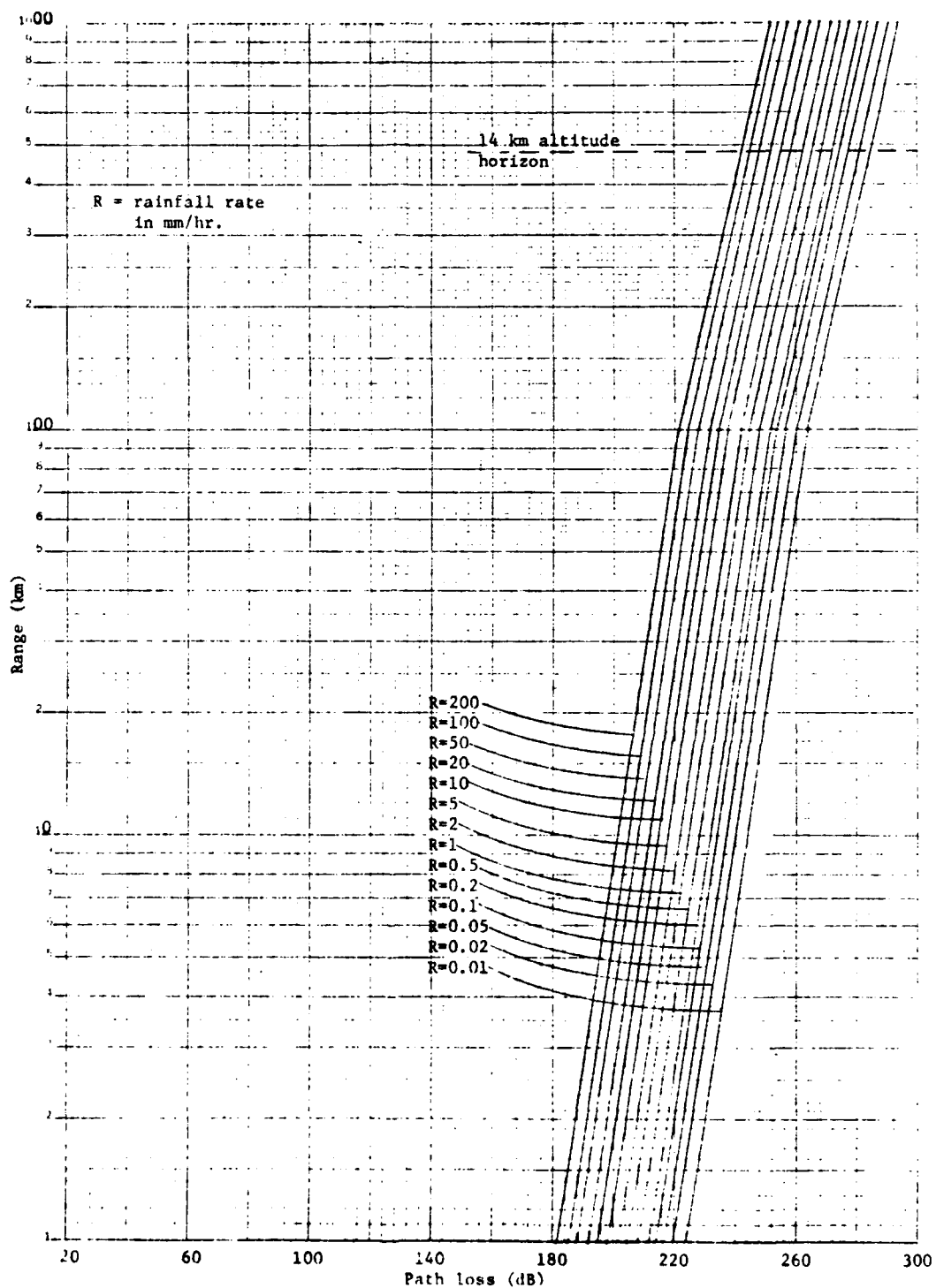
Figure 4.   Path loss at various ranges and hail rates.
$\lambda = 10.9$ cm

20
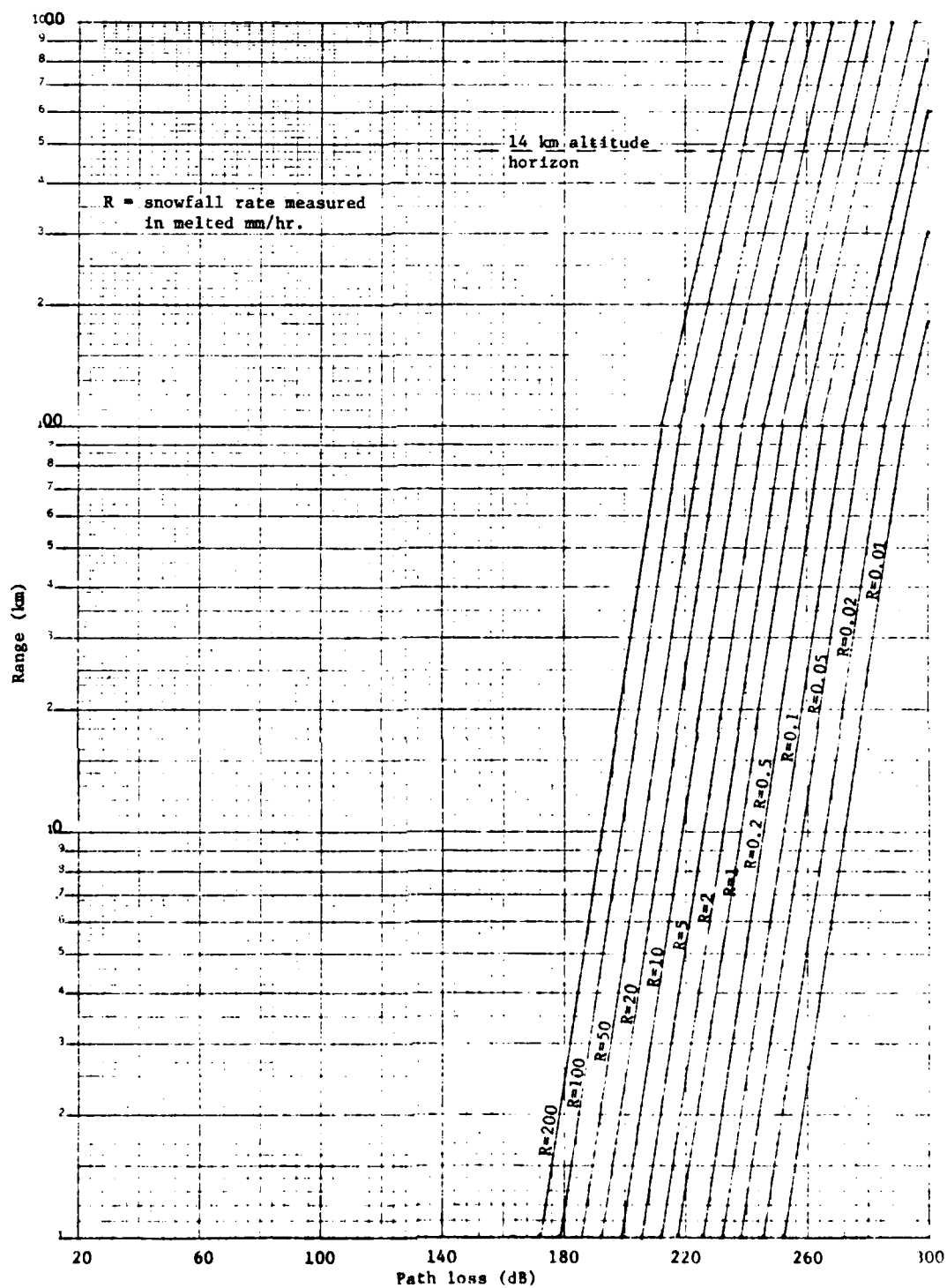
Figure 5.   Path loss at various ranges and snowfall rates.
$\lambda = 10.9$ cm

21
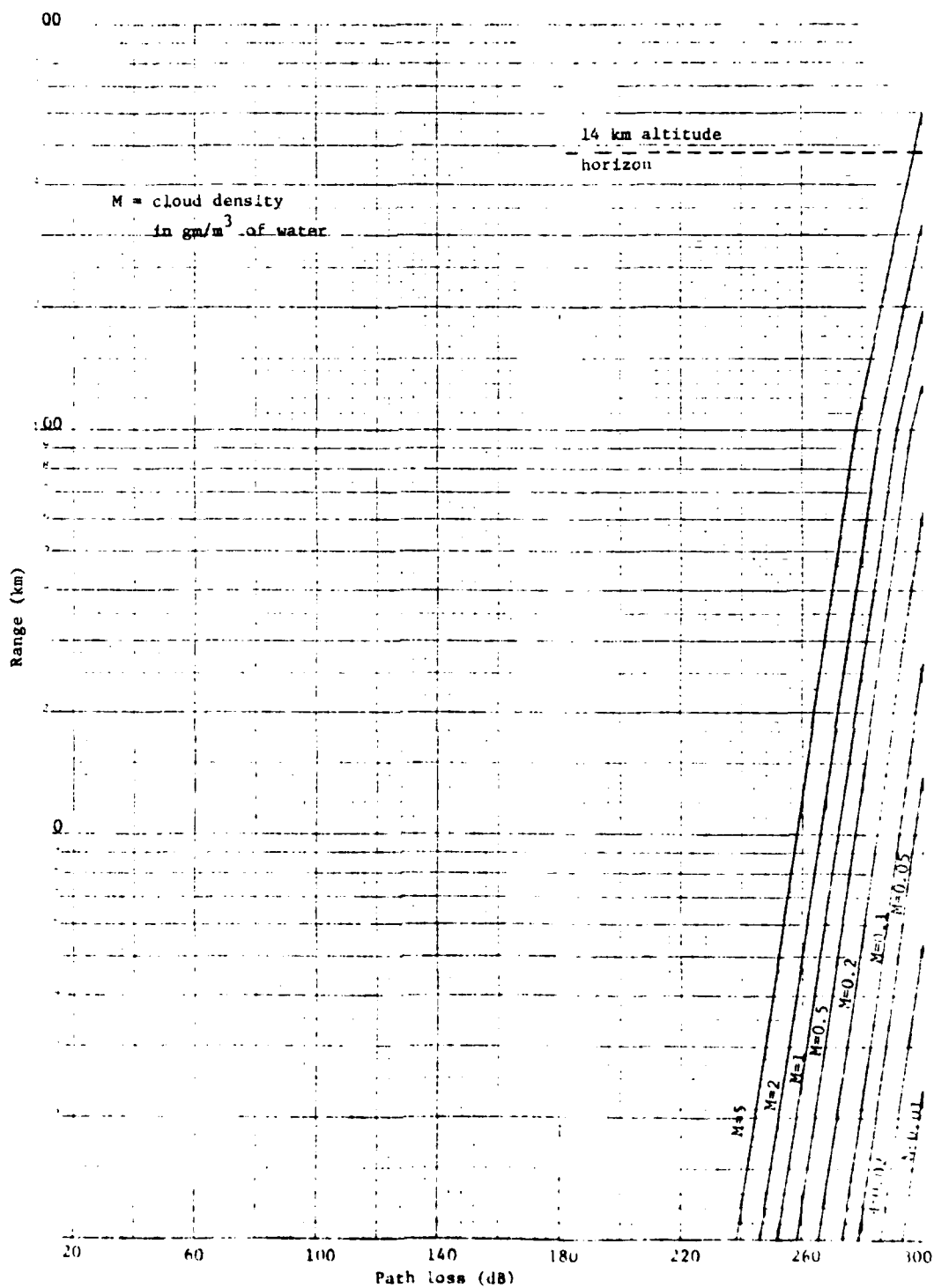
Figure 6.   Path loss at various ranges and water cloud densities.
λ = 10.9 cm

22
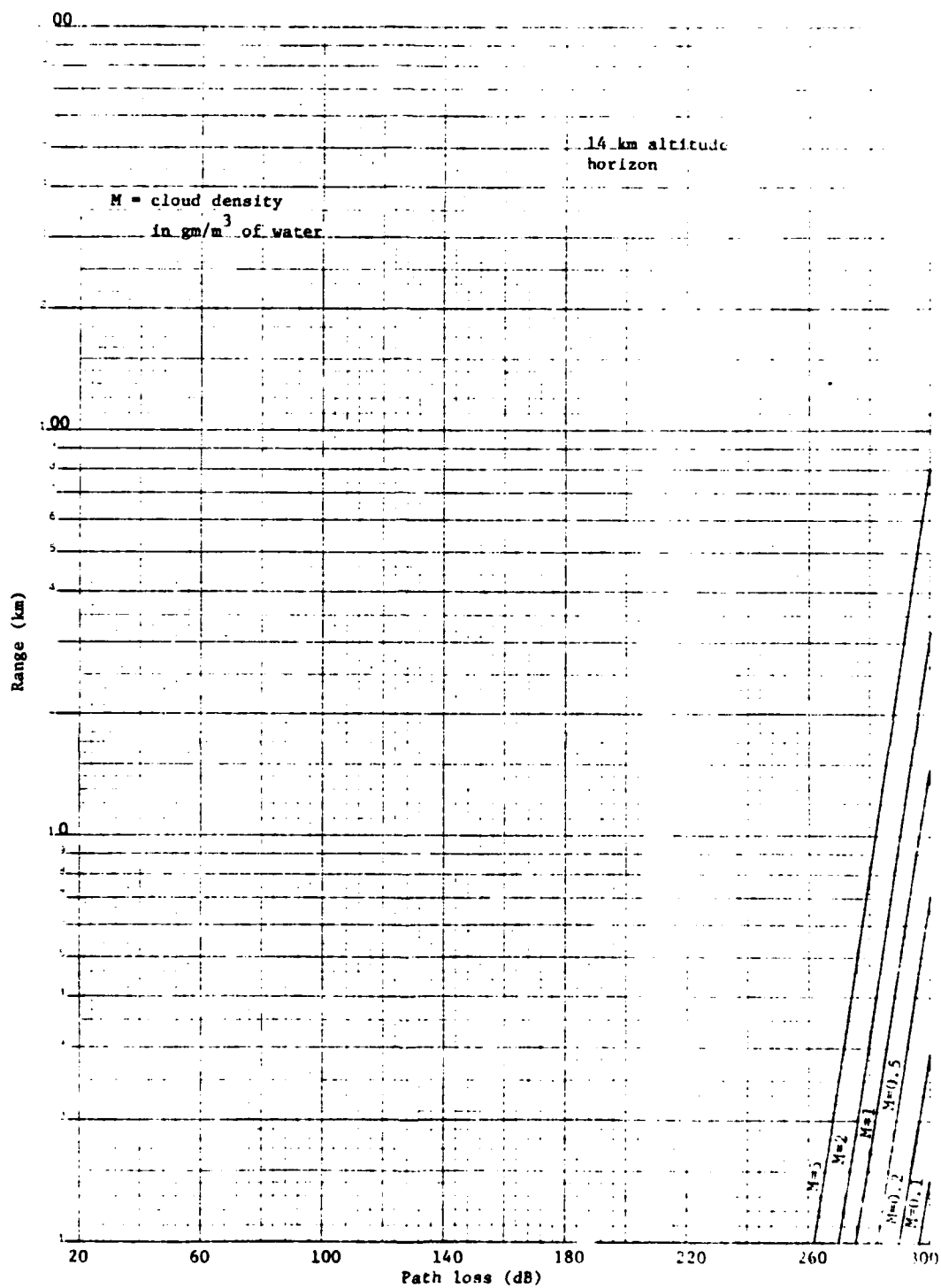
Figure 7. Path loss at various ranges and ice cloud densities.
$\lambda = 10.9$ cm

23

The aforementioned graphs are a result of the specific considerations of the AFGL radar where it is instructive to separate the path loss from the antenna gain and transmitter power. This will enable investigation of transmitter power reduction in order to reduce the cost of some high priced microwave components, as well as investigations of various values of lessened antenna gain due to subreflector shaping to improve polarization isolation.

From Equation (15), the filled beam path loss becomes,

$$PL = 18.1 \frac{\tau(\lambda\theta')^2}{r^2} \eta \ .$$

Given the AFGL radar conditions of $\tau = 1.0$ μs, $\lambda = 10.9$ cm, and $\theta' = 1.54$ degrees,

$$PL = 62.9 \text{ dB} + 10 \text{ LOG}_{10}\left[\frac{\eta}{r^2}\right] \ .$$

Finally, the received power can be calculated from

$$\left(P_r\right)_{dBm} = \left(P_t\right)_{dBm} + \left(2G_{3dB}\right)_{dB} - \left[62.9 + 10 \text{ LOG}_{10}\left(\frac{\eta}{r^2}\right)\right]_{dB}$$

and overall system performance is given by

$$(S/N)_{dB} = P_t + 2G_{3dB} - \left[62.9 + 10 \text{ LOG}_{10}\left(\frac{\eta}{r^2}\right)\right] - 10 \text{ LOG}_{10} K_b TB$$

From this expression and a knowledge of the target and extent of beamfilling, the range of the target can be determined from measurement of the receiver signal-to-noise ratio.

2.5   POLARIZATION DIVERSITY REQUIREMENTS

In this section, the requirements for pulse-to-pulse polarization diversity measurements will be undertaken. In

24

other reports[7,8] the ramifications of polarization diversity measurements have been shown; however, the implementation and quantitative results thereof have not been previously alluded to. Here, we will define and bound some overall system errors as well as discuss the matrix formulation and equivalence of circular and linear polarization diversity.

2.3.1 SYSTEM PHASE AND AMPLITUDE ERROR

As a starting point, one must determine the fundamental measurables of a polarization diversity weather radar, as contrasted with some other remote sensing polarimetric device such as a radio astronomy observatory. Two classes of polarization diversity weather radar systems exist: (1) dual circular which measures the backscatter of the transmitted and orthogonal polarizations and (2) dual linear which measures backscatter of only the transmitted polarization. In the past, the former systems have been polarization switched on a burst (or group) to burst basis to analyze the average backscatter matrix (i.e., relativity slow speed switching of the transmitted polarization has been employed), while the latter systems have utilized pulse-to-pulse polarization switching of the transmitted signal to measure only the diagonal elements of the matrix. The proposed AFGL 10 cm polarization diversity radar will offer pulse-to-pulse switching for evaluating the entire backscatter matrix in both circular and linear polarization measurement schemes. The antenna, microwave package, and RF through detection portions of the receiver will have phase and amplitude uncertainties imposed upon them by the desired quanitative results. The word "uncertainty" ,rather than the more common

---

7   J. I. Metcalf, "Interpretation of Simulated Polarization Diversity Radar Spectral Functions", submitted to Radio Science, 1982.

8   Metcalf, et al., Op. cit.

term "error", will be used throughout this report to distinguish between that part of the "error" (such as phase change as a function of amplitude change) which can be eliminated by post-detection software from that part of the error which is random or attained from unmeasurable quantities such as differential thermal effects. Most of these analyses will be devoted to the circular polarization mode of operation, as here two of the most difficult to achieve performance requirements exist: less than one degree channel-to-channel phase tracking uncertainty and greater than 35 dB between-channel isolation.

In the circular polarization diversity weather radar format, the measurable backscatter quantities are:[9,10]

$W_1 = \langle E_1 E_1^* \rangle$ = total power received in the transmission channel

$W_2 = \langle E_2 E_2^* \rangle$ = total power received in the orthogonal channel

$\bar{\alpha}$ = mean slant angle of the polarization ellipse or precipitation canting angle with respect to local vertical

$|\rho|$ = crosscorrelation function or fraction of oriented backscatterers.

These measurables are closely related to Stokes parameters[11,12] as employed in other polarimetric systems; for historical reasons, they will be retained in this analysis.

9   G. C. McCormick and A. Hendry, "Principles for the Radar Determination of the Polarization Properties of Precipitation," Radio Science, Vol. 10, No. 4, April 1975, pp. 421-434.

10   J. I. Metcalf and J. D. Echard, "Coherent Polarization-Diversity Radar Techniques in Meteorology," J. Atmos. Sci., Vol. 35, No. 10, October 1978, pp. 2010-2019.

11   M. H. Cohen, "Radio Astronomy Polarization Measurements," Proc of IRE, Vol. 46, Jan. 1958, pp. 172-182

12   J. D. Kraus, Radio Astronomy, (New York, NY: McGraw-Hill, 1966) Chapter 4

2.3.2 CANCELLATION RATIO AND INTEGRATED CANCELLATION RATIO

The integrated cancellation ratio (ICR) usually offers a measurement of circular polarization radar antenna performance as a clutter suppressor. Offutt[13] presented a somewhat difficult definition:

> ICR "is defined as the ratio of radar power received with circular polarization to the radar power received with linear polarization when the antenna in both instances is completely surrounded by an infinite number of randomly distributed small symmetric targets."

This definition is clarified by noting that in each instance the antenna is configurable for either circular or linear polarization, and is employed in each configuration to both transmit and receive signals to an infinite, uniform, homogeneous, isotropic assembly of spherically symmetric scatterers whose diameters are much less than the wavelength of transmission. Since the returned power level in the linear polarization configuration is exactly the same as the returned power level in the orthogonal channel of the antenna configured to receive both circular polarizations, the definition of ICR might be changed to read:

> Integrated cancellation ratio is defined as the ratio of radar power received in the tranmission channel to the power received in the orthogonal channel of a circular polarized radar antenna immersed in an infinite, homogeneous, isotropic assemblage of spherical scatterers whose diameters are much less than the transmission wavelength.

Note that this is a two-way measurement. Later it will be shown that another quantity, one-way integrated cancellation ratio, is often employed in the literature; furthermore, it will be shown that one-way and two-way ICR differ by 6 dB. Two additional items are of interest within the framework of this definition:

---

13   Jasik, editor, <u>Microwave Antenna Handbook</u>, See Section 17.8 by Warren B. Offutt.

(1) ICR is only definable for a circularly polarized antenna (an alternate definition, integrated cross-polarization ratio (ICPR) which is applicable for linearly polarized antennas will be presented in Section 3) and (2) if cross-channel mixing should occur, as it does in many microwave antenna feed assemblies, than only total system ICR may be considered.

Another useful quantity is the one-way, single point measurement, cancellation ratio (CR). CR is defined as the ratio of co-polarized to cross-polarized energy transmitted by a circularly polarized antenna towards a point in space. Offutt defines CR in a somewhat similar manner as the received signal from a radar employing precipitation clutter suppression[14]. Consider right circular polarization as the dominant polarization from an antenna capable of transmitting dual circular polarization. We define ρ as the ratio of the electric fields,

$$\rho = \frac{E_R}{E_L}$$

Then the cancellation ratio becomes,

$$CR = 10 \ LOG \ \frac{P_R}{P_L} = 20 \ LOG \ \rho. \tag{17}$$

Axial ratio is defined for linear horizontal and vertical polarization as E_H/E_V, or in the general case as E_{max}/E_{min} where E_{max} and E_{min} are the major and minor axes of the polarization ellipse. The polarization state is then described by the ratio of the major axis to the minor axis and the tilt angle between vertical and the major axis. However, the polarization state can also be represented in terms of two counter-rotating vectors and a phase angle between them (Figure 8).

---

14   Ibid

28
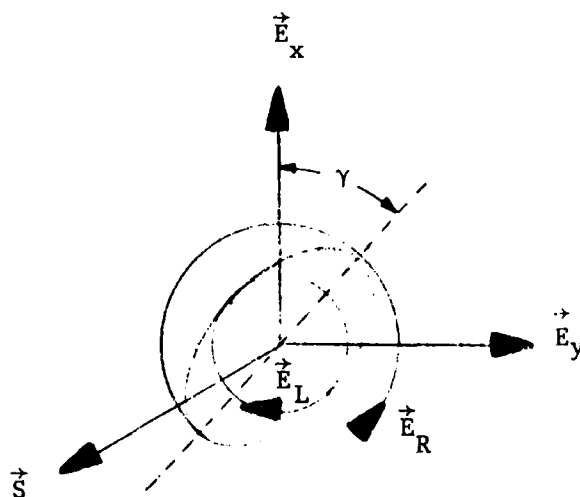
Figure 8. Generalized polarization ellipse derived
from orthogonal circular polarizations.

If these unit vectors for circular polarization are given in terms of linear polarization by:

$$\hat{R} = \frac{1}{\sqrt{2}} (\hat{x} + j\hat{y})$$

$$\hat{L} = \frac{1}{\sqrt{2}} (\hat{x} - j\hat{y})$$

then the axial ratio for circular polarization becomes,*

$$AR = \frac{E_L + E_R}{E_L - E_R}$$

so that, in terms of axial ratio, the cancellation ratio is,

$$CR = 20 \log \frac{AR - 1}{AR + 1} . \tag{18}$$

As an electromagnetic wave leaves an antenna, it contains a certain quantity of unwanted polarization as well as a dominant desired polarization. Even if the wave is perfectly reflected (i.e., its relative polarization state is unchanged), it is further corrupted by its return into the antenna. These degrees of polarization corruption are given by the axial ratio, E_{max}/E_{min}, so that the total axial ratio must be the product of the transmission and reception axial ratios. In the case of a common transmission and reception antenna, AR is replaced by AR^2 in Equation (18) and the two-way cancellation ratio becomes,

$$CR|_{two-way} = 20 \log \frac{AR^2 - 1}{AR^2 + 1} \tag{19}$$

---

* In some of the literature, notably Cohen and Deschamps, the axial ratio is defined as E_{min}/E_{max}, which yields $AR = E_L - E_R/E_L + E_R$. In other texts (such as Jasik), the term ellipticity is synonymous with axial ratio.

30

The difference between two-way and one-way cancellation ratio is

$$\Delta CR = CR_{\text{two-way}} - CR_{\text{one-way}}$$

$$= 20 \text{ LOG } \frac{(AR + 1)^2}{AR^2 + 1} \quad ,$$

which for small axial ratios is approximately 6 dB.

Following Allan, Markell, and McCormick[15], the ICR can be simply calculated by employing the antenna pattern, $G(\Omega)$, as a weighting function and integrating the electric field ratio over all space

$$ICR = 10 \text{ LOG } \frac{\int_{\Omega} \rho(\Omega)^2 \, G(\Omega)^2 \, d\Omega}{\int_{\Omega} G(\Omega)^2 \, d\Omega} \quad .$$

Here as before, the squared electric field ratio denotes the two-way property of ICR.

Offutt presents ICR in a somewhat different, but equivalent, form[16]

$$ICR = \frac{\displaystyle\sum_{\theta,\phi} (P_{max} - P_{min})^2 \sin\theta}{\displaystyle\sum_{\theta,\phi} (P_{max} + P_{min})^2 \sin\theta}$$

where P_{min} and P_{max} are the minimum and maximum power values received by a rotating dipole located at some far field points θ,ϕ all of which are equidistant from the apex of the antenna.

Note that with respect to the antena terminals, the two-way cancellation ratio is a relevant measurable term; as in the case of observation of an extended collection of targets, two-way CR

15   L. E. Allan, R. C. Markell, and G. C. McCormick, "A Variable Polarization Antenna" National Research Council of Canada Publication ERB-768, June 1967.

16   Jasik, Op. cit.

becomes indistinguishable from ICR. Furthermore, the two-way CR is directly degraded by the channel-to-channel crosstalk of the feed assembly and of the receiver; in fact, it is not possible to isolate feed assembly crosstalk from other contributions to the ICR. Therefore, the feed channel-to-channel isolation requirement must equal or exceed the ICR requirement. As addressed in Section 4, the receiver isolation must also be somewhat greater than the ICR for its crosstalk effects to be unnoticed.

2.3.3   INTER-CHANNEL RECEIVER AMPLITUDE UNCERTAINTY
2.3.3.1   Circular Polarization

In the circular polarization mode of operation, the received parameter most sensitive to error is the circular depolarization ratio (CDR)[17] given by,

$$ CDR = \frac{W_1}{W_2} = \frac{\langle E_1 E_1^* \rangle}{\langle E_2 E_2^* \rangle} $$

where E_1 and E_2 are the measured components of the scattered electric field, with E_1 being the component received by the channel of transmission. The overall requirement is that CDR must be measurable to within 0.1 dB. Since the measured parameter at the output of each channel of the receiver is not the total power, but the voltages E_1 and E_2, we can then define the ratio of the measured receiver voltages as

$$ r = \frac{E_1 e^{j\phi_1}}{E_2 e^{j\phi_2}} . $$

Obviously, the measurement tolerance of CDR becomes a measurement tolerance of r;

$$ \delta(r) = \delta \left[\frac{W_1}{W_2}\right]^{1/2} = \delta(CDR)^{1/2} < (0.1dB)^{1/2} = 1.037, $$

---

17   J. I. Metcalf, personal communication, 1982

so that the error function becomes

$$\frac{dr}{r} < 0.037 .$$

Prior to determining an expression for the error function, we note that two cases exist: (1) only the receiver channel-to-channel differential error is considered, while the antenna isolation is assumed to be infinite, or equivalently ICR=$-\infty$ and (2) the one-way ICR is assumed to be real, but small.

2.3.3.1.1 Case 1, ICR = $-\infty$

Let $r = \frac{E_1}{E_2} e^{j\phi}$ where $\phi = \phi_1 - \phi_2$

then

$$\frac{dr}{r} = \frac{E_2}{E_1} e^{-j\phi} \quad d \left[\frac{E_1}{E_2} e^{j\phi} \right]$$

$$= \frac{dE_1}{E_1} + jd\phi - \frac{dE_2}{E_2} ,$$

or

$$\frac{dE_1}{E_1} - \frac{dE_2}{E_2} = \frac{dr}{r} - jd\phi. \tag{20}$$

The absolute value of the left side of the above expression is the minimum required differential amplitude uncertainty between the two receiver channels. Using the previously determined values of CDR measurement tolerance and channel-to-channel phase uncertainty, the minimum required unmeasurable component of channel-to-channel amplitude error must be

$$\left| \frac{dE_1}{E_1} - \frac{dE_2}{E_2} \right| < \left| 0.037 - j \left[\frac{3}{2} \text{ degrees} \right] \left[\frac{2\pi}{360} \frac{\text{radians}}{\text{degrees}} \right] \right| = 0.045,$$

or expressed as dB error, the receiver channels must track within

differential uncertainty <0.38 dB.

33

2.3.3.1.2 Case 2, ICR << 1

Let E_{1i}, E_{2i} be the intrinsic backscattered voltages received at the antenna, and let f be the isolation between the antenna terminals*, then the voltage ratio at the receiver output is

$$r = \frac{\left[E_{1i} + fE_{2i} \right] e^{j\phi_1}}{\left[E_{2i} + fE_{1i} \right] e^{j\phi_2}} \quad ,$$

which may be reduced to

$$r = \frac{\left[E_{1i} + fE_{2i} \right]}{E_{2i}} e^{j\phi} \quad \text{since it is assumed } E_{2i} \gg E_{1i}.$$

Using $\frac{dr}{r} = d(\ln(r))$ and differentiation by parts, we obtain

$$\frac{dr}{r} = jd\phi + \frac{dE_{1i}}{E_{1i} + fE_{2i}} - \frac{E_{1i}dE_{2i}}{E_{2i}\left[E_{1i} + fE_{2i} \right]} + \frac{E_{2i}df}{E_{1i} + fE_{2i}} \quad . \tag{21}$$

However, E_{1i} and E_{2i} are not the observables at the receiver output as they contain the system uncertainty which separates E_1 and E_2 from E_{1i} and E_{2i}. By definition, those uncertainties are unmeasurable. Therefore, we may enforce the implication

$$dE_{1i} \rightarrow dE_1$$
$$dE_{2i} \rightarrow dE_2,$$

after which, we can translate Equation (21) into a form similar to Equation (20)

$$\frac{dE_1}{E_1} - \frac{dE_2}{E_2} + \frac{E_2}{E_1} df = \frac{dr}{r} - jd\phi \quad .$$

Again, employing our initial condition of observation of an infinite, uniform, homogeneous, isotropic collection of Rayleigh

---

* it can be shown that the one-way ICR is described by $|f|^2$

scattering spheres, and for the condition $E_2 \gg E_1$, the isolation is,

$$f = \frac{E_1}{E_2}$$

so that

$$\frac{dE_1}{E_1} - \frac{dE_2}{E_2} = \frac{dr}{r} - jd\phi - \frac{df}{f} \ . \tag{22}$$

As in Case 1, the minimum required unmeasurable component of channel-to-channel amplitude error must be

$$\text{differential uncertainty} < 10 \text{ Log} \left| \frac{dr}{r} - jd\phi - \frac{df}{f} \right| \ . \tag{23}$$

As an example, consider the conditions of Case 1, with additionally;

one-way ICR = 30 dB which implies a value, $f = 31.62$

uncertainty of ICR = 3 dB which implies a value, df = 1.41,

so that the differential amplitude uncertainty must be less than 0.23 dB for the circular depolarization ratio calculation to be valid within 0.1 dB.

2.3.3.2 Linear Polarization

Although, in the linear polarization mode of operation, measurements are performed in a fundamentally different manner, the inter-channel antenna isolation does effect overall system accuracy; furthermore, it can be shown that, as the antenna isolation degrades, the scattered energy increasingly appears more like that expected from a collection of homogeneous spherical targets than actual hydrometeors.

In the past, direct scattering measurements were made on the polarization of transmission, with no attempt to measure scattering of the orthogonal polarization as only one receiver channel was employed. The antenna output was switched between the local horizontal and vertical directions on a pulse-to-pulse

35

basis with the corresponding backscatter signal feed into the transmit/receive circulator. Obviously, with such a system, amplitude uncertainty of the post-circulator section of the receiver channel did not exist; all amplitude uncertainty error was contained within the switch, microwave hardware, feed assembly, and associated calibration network. If the present AFGL radar is to complement these experiments, then it requires a pre-circulator amplitude uncertainty equal to or less than the least expected differential reflectivity uncertainty of 0.1 to 0.3 dB[18],[19].

The isolation error of this mode affects the intrinsic horizontal and vertical electric fields in the same manner as circular polarization; however, it is preferable to begin this discussion, by considering the transmitted signal. During the previous discussion no attempt was made to consider the reduction of co-polarized transmitted energy due to a non-zero antenna isolation; it was assumed that this reduction was negligible. By conservation of energy, that condition is not wholly true. Consider an antenna transmitting a vertically polarized wave with a small, but non-trivial, horizontally polarized component which is due to the non-perfect antenna isolation. Then, the magnitude of the vertically polarized component must be reduced by the magnitude of the horizontally polarized component. After scattering, an identical effect occurs upon reception. These effects and impacts thereof can be easily demonstrated. Reconsider the aforementioned vertically polarized wave, the components are:

18   T. A. Seliga and V. N. Bringi, "Potential Use of Radar Differential Reflectivity Measurements at Orthogonal Polarizations for Measuring Precipitation," J. Appl. Meteor., Vol. 15, Jan. 1976, pp. 69-76.
19   V. N. Bringi, T. A. Seliga, and E. A. Mueller, "First Comparisons of Rain Rates Derived from Radar Differential Reflectivity and Disdrometer Measurements," IEEE GE-20 No. 2, April 1982, p 201.

$$|\vec{\hat{E}}_H| = fE \qquad \text{where } E = \text{total available electric field}$$

$$|\vec{\hat{E}}_V| = \sqrt{1 - f^2}\, E,$$

or in vector form

$$\vec{\varepsilon}_V = \begin{bmatrix} f \\ \sqrt{1-f^2} \end{bmatrix} \vec{\hat{E}}, \text{ where } \vec{\varepsilon}_V \text{ indicates predominant vertically} \atop \text{polarized transmitted electric field.}$$

Upon scattering and normalizing to the losses of propagation, which are assumed independent of polarization,

$$\vec{\varepsilon}_{SV} = S\,\vec{\varepsilon}_V = \begin{bmatrix} S_{HH} & S_{HV} \\ S_{VH} & S_{VV} \end{bmatrix} \begin{bmatrix} f \\ \sqrt{1-f^2} \end{bmatrix} \vec{\hat{E}}$$

$$= \begin{bmatrix} fS_{HH} + \sqrt{1-f^2}\, S_{HV} \\ fS_{VH} + \sqrt{1-f^2}\, S_{VV} \end{bmatrix} \vec{\hat{E}}\,.$$

Likewise, if a horizontally polarized wave is transmitted, the scattered field becomes

$$\vec{\varepsilon}_{SH} = S \begin{bmatrix} -\sqrt{1-f^2} \\ f \end{bmatrix} \vec{\hat{E}} = \begin{bmatrix} \sqrt{1-f^2}\, S_{HH} + fS_{HV} \\ \sqrt{1-f^2}\, S_{VH} + fS_{VV} \end{bmatrix} \vec{\hat{E}}\,.$$

At reception, both the horizontally polarized and vertically polarized components of either transmission condition must be considered. The non-infinite isolation at the antenna again imparts a reception matrix, R, identical to the transmission matrix.

$$R = \begin{bmatrix} \sqrt{1-f^2} & f \\ f & \sqrt{1-f^2} \end{bmatrix}\,.$$

The backscattered energy at the antenna terminals for vertically polarized transmission becomes

$$\vec{\epsilon}_{RV} = R\vec{E}_{SV} = \begin{bmatrix} \sqrt{1-f^2}[fS_{HH} + \sqrt{1-f^2}S_{HV}] + f[fS_{VH} + \sqrt{1-f^2}S_{VV}] \\ f[fS_{HH} + \sqrt{1-f^2}S_{HV}] + \sqrt{1-f^2}[fS_{VH} + \sqrt{1-f^2}S_{VV}] \end{bmatrix}\vec{E}. \quad (24)$$

Likewise, for horizontally polarized transmission

$$\vec{\epsilon}_{RH} = R\vec{E}_{SH} = \begin{bmatrix} \sqrt{1-f^2}[\sqrt{1-f^2}S_{HH} + fS_{HV}] + f[\sqrt{1-f^2}S_{VH} + fS_{VV}] \\ f[\sqrt{1-f^2}S_{HH} + fS_{HV}] + \sqrt{1-f^2}[\sqrt{1-f^2}S_{VH} + fS_{VV}] \end{bmatrix}\vec{E}. \quad (25)$$

In the linear polarization mode of operation, the upper and lower components of $\vec{\epsilon}_{RV}$ and $\vec{\epsilon}_{RH}$, respectively, are not measured, but are routed to a termination. Differential reflectivity is then calculated from the ratio of the remaining components of the Equations (24) and (25)

$$Z'_{DR} = 20 \, \text{Log} \, \frac{|\epsilon_{RH_1}|}{|\epsilon_{RV_2}|}$$

$$= 20 \, \text{Log} \, \frac{(1-f^2)S_{HH} + \sqrt{1-f^2}f(S_{HV} + S_{VH}) + f^2 S_{VV}}{f^2 S_{HH} + \sqrt{1-f^2}f(S_{HV} + S_{VH}) + (1-f^2)S_{VV}} \quad (26)$$

$$= 20 \, \text{Log}(r), \text{ where } r \text{ is the fractional expression.} \quad (27)$$

The prime notation is employed to differentiate this expression from that of Seliga and Bringi[20] which defines $Z_{DR} = 10 \, \text{Log} \, Z_H/Z_V$ or in amplitude notation corresponding to $20 \, \text{Log} \, S_{HH}/S_{VV}$;

---

20   Seliga and Bringi, Op. cit.

differential reflectivity uncorrected for antenna isolation. Three cases are of interest: scattering from collections of 1) spheres, 2) horizontal dipoles, or 3) precipitation particles.

2.3.3.2.1 **Case 1.** Rayleigh scattering from a homogeneous, uniform, infinite collection of spheres:

$$S_{HH} = S_{VV} , \quad S_{VH} = S_{HV} = 0$$

then

$$Z'_{DR} = 20 \, \text{Log} \, \frac{(1-f^2) + f^2}{f^2 + (1-f^2)} = 0.$$

For observation of a collection of perfectly spherical hydrometeors, inter-channel isolation within the feed and antenna assembly is unimportant.

2.3.3.2.2 **Case 2.** Scattering from a homogeneous, uniform, infinite, aligned collection of horizontal dipoles:

$$S_{VV} = S_{VH} = S_{HV} = 0$$

then

$$Z'_{DR} = 20 \, \text{Log} \, \frac{1-f^2}{f^2} . \tag{28}$$

Z'_{DR} is wholly a measurement of the feed and antenna assembly isolation and independent of the backscatter amplitude; furthermore in the limiting example of $f = 1/\sqrt{2}$, Z'_{DR} becomes identical to that of the previous case. Hence, as the inter-channel isolation decreases, observed backscatter appears to be that of a collection of Rayleigh spheres.

2.3.3.2.3 **Case 3.** Rayleigh scattering from a homogeneous, uniform, infinite collection of nearly spherical hydrometeors:

$$S_{HH} \neq S_{VV} , \quad S_{VH} = S_{HV} < S_{HH} .$$

39

The range of uncorrected differential reflectivity is 0 dB $< Z_{DR} < 5$ dB or $1 < S_{HH}/S_{VV} < 1.78$ for Rayleigh scattering in rain with negligible propagation effects; the uncertainty in these measurements is 0.1 dB $< \delta Z_{DR} < 0.3$ dB[21,22]. The difference between corrected and uncorrected differential reflectivity should be less than, or in the limit equal to, the measurement uncertainty, i.e.,

$$|Z_{DR} - Z'_{DR}| < \delta Z_{DR} . \tag{29}$$

From Equation (27), this inequality becomes

$$\frac{1}{r} \frac{S_{HH}}{S_{VV}} < Log^{-1}\left[\frac{\delta Z_{DR}}{20}\right] . \tag{30}$$

The inequality now becomes of interest for several cases in which the maximum measurable differential reflectivity is observed. If we approximate the results of Krehbiel and Brook[23] wherein S_{VH} varied from less than the measurement limit to as much as 15 dB less than S_{HH} or $S_{VH} = S_{HV}$ and $0 < S_{VH} < 0.2 S_{HH}$.

Employing: $Z_{DR} = 5$ dB which implies $\dfrac{S_{HH}}{S_{VV}} = 1.778$

$$\delta Z_{DR} = 0.3 \text{ dB},$$

and solving the resulting quadratic equation, we find the antenna isolation becomes

f < 0.1188 or equivalently a one way ICR of -18.5 dB.

21 Ibid
22 J. I. Metcalf, "Theory and Experimental Concepts for Coherent Polarization-Diversity Meteorological Radar," Georgia Institute of Technology, Engineering Experiment Station, Final Report, Project B-529, 30 Sept. 1980.
23 P. R. Krehbiel and M. Brook, "Coherent, Dual Polarized Observations of the Radar Return from Precipitation," submitted to Radio Science, 1982.

Therefore, to achieve capability of aforementioned measurement the one way antenna isolation must be better than -19 dB. Further results of calculation of isolation versus values of S_{HH}, S_{VH} and δZ_{DR} are tabulated in Table 3.

2.3.4 INTER-CHANNEL POLARIZATION PHASE UNCERTAINTY

Consider the circular polarization description of the generalized polarization ellipse (Figure 8). Polarization of any electromagnetic wave can be described by a left hand circular vector $\vec{L}$, a right hand circular vector $\vec{R}$, and a phase angle γ between these rotating vectors. Hydrometeors tend to orient themselves along some fall or canting angle with respect to the local vertical; certain variations of precipitation have a higher percentage of orientation than other varieties. Radar backscatter also contains this orientation angle information in the phase angle between the two vectors. For Rayleigh scattering the absolute value of the phase angle, γ, can be shown to be twice the canting angle α. Since γ is also the phase angle sensed between the two receiver channels, and since the desired canting angle uncertainty should be less than one half the canting angle processor quantization error, so that the required system phase uncertainty becomes equal to or less than the quantization error. That is, if $\Delta\alpha$ and $\Delta\gamma$ represent the uncertainties in α and γ, respectively, then $2\Delta\alpha = \Delta\gamma$ with $\Delta\gamma$ the maximum tolerable channel-to-channel phase uncertainty of the system. From previous measurements[24], the quantization error $\Delta\alpha$ was less than 3/4 degree. To review these measurements on an pulse-to-pulse basis requires that the phase uncertainty between the two antenna/receiver channels be held to less than

24   G. C. McCormick and A. Hendry, "Polarization Properties of Transmission Through Precipitation Over a Communication Link," Journal De Recherches Atmospheriques, 8 1974, pp. 175-187.

TABLE 3. MINIMUM ANTENNA ISOLATION REQUIRED TO ACHIEVE MEASUREMENT ACCURACY δZ_{DR} IN RAIN WITH 1 AND 5 dB DIFFERENTIAL REFLECTIVITY

minumum isolation	$\dfrac{S_{HV}}{S_{HH}}$	δZ_{DR}	Z_{DR}
−8.3 dB	0.0	0.3 dB	1 dB
−9.3	0.1	0.3	1
−9.9	0.2	0.3	1
−13.0	0.0	0.1	1
−14.9	0.1	0.1	1
−16.6	0.2	0.1	1
−15.5	0.0	0.3	5
−18.5	0.1	0.3	5
−21.2	0.2	0.3	5
−20.2	0.0	0.1	5
−25.5	0.1	0.1	5
−29.6	0.2	0.1	5

1.5 degrees; however, in this design we shall attempt to decrease this amount to one degree so that McCormick's and Hendry's efforts may be improved upon.

2.4 EQUIVALENCE OF LINEARLY- AND CIRCULARLY-POLARIZED BACKSCATTER

In the previous subsections, the antenna isolation requirements were considered for linear polarization diversity differential reflectivity measurements. In that scheme, all the cross terms of the scattering matrix are unmeasured; their only effect has been shown to impose an error on the differential reflectivity measurement if the antenna isolation is not sufficiently high. The next logical consideration is of the uncertainties imposed upon an entire linear scattering matrix measurement scheme due to insufficient antenna isolation, system phase uncertainty, and receiver amplitude uncertainty. However, if it can be shown that the linear and circular scattering matrices differ only by a transformation matrix consisting of unity values, then the uncertainty formulations for circularly polarized scattering developed in the previous subsections shall be applicable to linearly polarized scattering.

Consider the transformation from linearly- to circularly-polarized electric field vectors,

$$
\begin{aligned}
\dot{E}_R &= (\dot{E}_x + j\dot{E}_y)/\sqrt{2} \\
\dot{E}_L &= (\dot{E}_x - j\dot{E}_y)/\sqrt{2}
\end{aligned}
\quad \text{or} \quad
\begin{bmatrix} \dot{E}_R \\ \dot{E}_L \end{bmatrix} = M \begin{bmatrix} \dot{E}_x \\ \dot{E}_y \end{bmatrix}
\tag{30}
$$

where $M = \dfrac{1}{\sqrt{2}} \begin{bmatrix} 1 & j \\ 1 & -j \end{bmatrix}$. An inverse matrix exists such that $M^{-1} = \dfrac{1}{\sqrt{2}} \begin{bmatrix} 1 & 1 \\ -j & j \end{bmatrix}$, and

$$
\begin{bmatrix} \dot{E}_x \\ \dot{E}_y \end{bmatrix} = M^{-1} \begin{bmatrix} \dot{E}_R \\ \dot{E}_L \end{bmatrix}
\tag{31}
$$

43

By straightforward linear algebra it can be shown that the same matricies are valid for transformation of like elements of the scattering matrix. That is

$$S_{circular} = M \, S_{linear} \tag{32}$$

and

$$S_{linear} = M^{-1} S_{circular} \,. \tag{33}$$

2.5 EQUIVALENCE OF VSWR AND ISOLATION OF A HYBRID COUPLER

An ideal hybrid coupler is a four-port device which may be represented schematically by the diagram shown in Figure 9. The device is symmetric and all four ports can receive inputs in any combination. If energy is fed into ports 1 and 3, for example, then the energy entering each port is split, with half of it proceeding to the directly-opposite port (2 and 4, respectively) and half of it undergoing a -90° phase shift before reaching the diagonally-opposite port (4 and 2, respectively). Thus the energy at port 2 is the sum of half the input to port 1 and half the input (shifted by -90°) to port 3, while that at port 4 is the sum of half the input (shifted by -90°) to port 1 and half the input to port 3.

It may be seen that if the energy to port 3 has the same magnitude as that to port 1, but lags it in phase by 90°, then the two components arriving at port 2 will be 180° out of phase and cancel each other, while the components arriving at port 4 will be in phase and add together. Thus an ideal hybrid coupler with perfect impedance matching at all four ports will have perfect isolation between ports 1 and 3 and between ports 2 and 4.

If there are mismatched connections at the ports however, there will be multiple internal reflections in the device which will degrade the isolation. The calculations which follow first analyze the general case of four arbitrary, except for frequency

which must be the same at all ports, inputs and four arbitrary
mismatches. Then the maximum mismatch (assuming this is equal at
all four ports) with a desired input isolation is determined for
the case of two equal inputs separated in phase by 90°.

2.5.1 General Case

The approach will be to assume four (complex) reflection
coefficients, ρ_1, ρ_2, ρ_3, and four input signal voltages V_{1i},
V_{2i}, V_{3i}, V_{4i} (Figure 9). These input signal voltges are
considered to be those signals which actually enter the device,
since the part of the incident voltage which is reflected back
out by the mismatch is not of interest. The total voltage just
inside each port will be the sum of an input voltage, an outward-
bound voltage, and a portion of the latter which is reflected
back into the device.

It is also possible to write down what the voltages on the
various branches of the device will be (assuming perfect power
splitting and phase shifting); these are also shown in the
figure. The solution to the problem is obtained by setting the
outward-bound voltage at each port equal to the sum of the
voltages reaching it from each of the two possible paths. Thus:

$$V_{1o} = \frac{1}{\sqrt{2}} \left(V_{2i} + \rho_2 V_{2o} e^{-2j\beta L} - j \left(V_{4i} + \rho_4 V_{4o} e^{-2j\beta L} \right) \right)$$

$$V_{2o} = \frac{1}{\sqrt{2}} \left(V_{1i} + \rho_1 V_{1o} - j \left(V_{3i} + \rho_3 V_{3o} \right) \right)$$

$$V_{3o} = \frac{1}{\sqrt{2}} \left(V_{4i} + \rho_4 V_{4o} e^{-2j\beta L} - j \left(V_{2i} + \rho_2 V_{2o} e^{-2j\beta L} \right) \right)$$

$$V_{4o} = \frac{1}{\sqrt{2}} \left(V_{3i} + \rho_3 V_{3o} - j \left(V_{1i} + \rho_1 V_{1o} \right) \right).$$
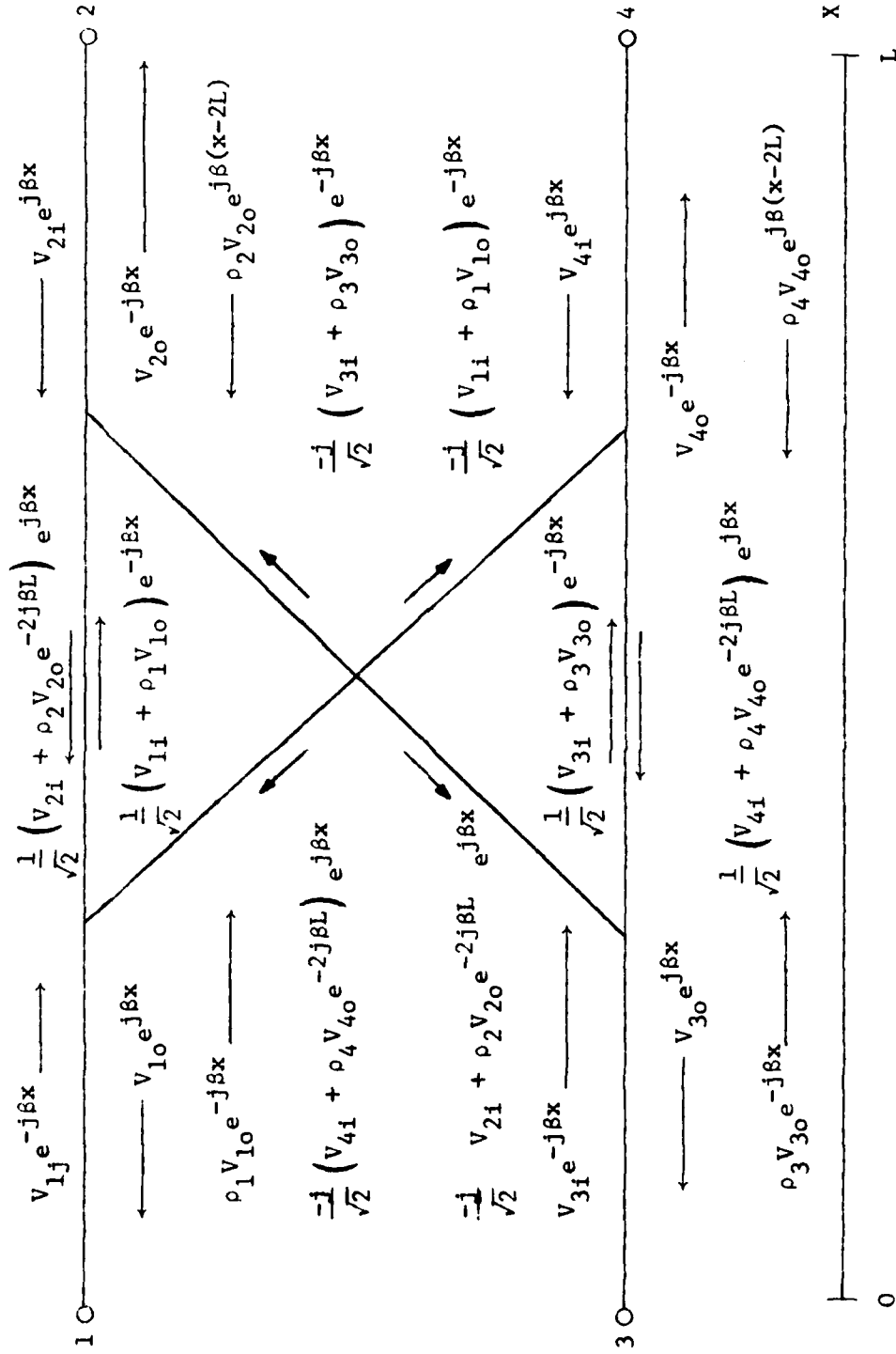
Figure 9. Voltage values and direction flow within a non-perfectly terminated hybrid coupler.

$V_{1i}e^{-j\beta x}$

$V_{1o}e^{j\beta x}$

$\rho_1 V_{1o}e^{-j\beta x}$

$\frac{-1}{\sqrt{2}}\left(V_{4i} + \rho_4 V_{4o}e^{-2j\beta L}\right)e^{j\beta x}$

$\frac{-1}{\sqrt{2}}\,V_{2i} + \rho_2 V_{2o}e^{-2j\beta L}\;e^{j\beta x}$

$V_{3i}e^{-j\beta x}$

$V_{3o}e^{j\beta x}$

$\rho_3 V_{3o}e^{-j\beta x}$

$\frac{1}{\sqrt{2}}\left(V_{2i} + \rho_2 V_{2o}e^{-2j\beta L}\right)e^{j\beta x}$

$\frac{1}{\sqrt{2}}\left(V_{1i} + \rho_1 V_{1o}\right)e^{-j\beta x}$

$\frac{1}{\sqrt{2}}\left(V_{3i} + \rho_3 V_{3o}\right)e^{-j\beta x}$

$\frac{1}{\sqrt{2}}\left(V_{4i} + \rho_4 V_{4o}e^{-2j\beta L}\right)e^{j\beta x}$

$V_{2i}e^{j\beta x}$

$V_{2o}e^{-j\beta x}$

$\rho_2 V_{2o}e^{j\beta(x-2L)}$

$\frac{-1}{\sqrt{2}}\left(V_{3i} + \rho_3 V_{3o}\right)e^{-j\beta x}$

$\frac{-1}{\sqrt{2}}\left(V_{1i} + \rho_1 V_{1o}\right)e^{-j\beta x}$

$V_{4i}e^{j\beta x}$

$V_{4o}e^{-j\beta x}$

$\rho_4 V_{4o}e^{j\beta(x-2L)}$

1 2 3 4

x

0 L

In the above equations, the various voltage amplitude terms (designated V_{1o}, V_{2i}, etc.) each include an arbitrary phase term and a time-dependence term of the same frequency for all the voltages. The wave number β is also the same for all the voltages. The use of the $1/\sqrt{2}$ term implies exact power splitting at the branch points, while the $-j$ term indicates that a perfect $-90°$ phase shift is undergone through the diagonal branches.nally, the $e^{-2j\beta L}$ terms (L is the length of the device) in the first and third equations are required for the proper phase relationship when reflections occurs at $x = L$ (ports 2 and 4).

The above set of equations can be put into matrix form:

$$
\begin{array}{l} V_{1o} \\ V_{2o} \\ V_{3o} \\ V_{4o} \end{array}
= \frac{1}{\sqrt{2}}
\begin{bmatrix}
0 & 1 & 0 & -j \\
1 & 0 & -j & 0 \\
0 & -j & 0 & 1 \\
-j & 0 & 1 & 0
\end{bmatrix}
\begin{array}{l} V_{1i} \\ V_{2i} \\ V_{3i} \\ V_{4i} \end{array}
$$

$$
+ \frac{1}{\sqrt{2}}
\begin{bmatrix}
0 & \rho_2 e^{-2j\beta L} & 0 & -j\rho_4 e^{-2j\beta L} \\
\rho_1 & 0 & -j\rho_3 & 0 \\
0 & -j\rho_2 e^{-2j\beta L} & 0 & -\rho_4 e^{-2j\beta L} \\
-j\rho_1 & 0 & \rho_3 & 0
\end{bmatrix}
\begin{array}{l} V_{1o} \\ V_{2o} \\ V_{3o} \\ V_{4o} \end{array}
\quad .
$$

Rearranging with $V_o = [V_{1o}, V_{2o}, V_{3o}, V_{40}]^t$ and $V_i = [V_{1i}, V_{2i}, V_{3i}, V_{4i}]^t$, we have

$$
\begin{bmatrix}
\sqrt{2} & -\rho_2 e^{-2j\beta L} & 0 & j\rho_4 e^{-2j\beta L} \\
-\rho_1 & \sqrt{2} & j\rho_3 & 0 \\
0 & j\rho_2 e^{-2j\beta L} & \sqrt{2} & -\rho_4 e^{-2j\beta L} \\
j\rho_1 & 0 & -\rho_3 & \sqrt{2}
\end{bmatrix}
V_o
$$

$$= \begin{bmatrix} 0 & 1 & 0 & -j \\ 1 & 0 & -j & 0 \\ 0 & -j & 0 & 1 \\ -j & 0 & 1 & 0 \end{bmatrix} V_i .$$

Designating the matrix on the left-hand side as A, the solution is given by

$$V_o = A^{-1} \begin{bmatrix} 0 & 1 & 0 & -j \\ 1 & 0 & -j & 0 \\ 0 & -j & 0 & 1 \\ -j & 0 & 1 & 0 \end{bmatrix} V_i ,$$

so that

$$V_o = \left(\frac{1}{\det A} \right) \begin{bmatrix} 2e^{-2j\beta L}(\rho_2-\rho_4 & 2\sqrt{2}(1-\rho_3\rho_4 e^{-2j\beta L}) & -2j(\rho_2+\rho_4)e^{-2j\beta L} & -2\sqrt{2}j(1+\rho_2\rho_3 e^{-2j\beta L}) \\ -2\rho_2\rho_3\rho_4 e^{-2j\beta L}) & & & \\ 2\sqrt{2}(1-\rho_3\rho_4 e^{-2j\beta L}) & 2(\rho_1 - \rho_3 & -2\sqrt{2}j(1+\rho_1\rho_4 e^{-2j\beta L}) & -2j(\rho_1+ \rho_3) \\ & -2\rho_1\rho_3\rho_4 e^{-2j\beta L}) & & \\ & & & \\ -2j(\rho_2 + \rho_4)e^{-2j\beta L} & -2\sqrt{2}j(1+\rho_1\rho_4 e^{-2j\beta L}) & -2e^{-2j\beta L}(\rho_2-\rho_4 & 2\sqrt{2}(1-\rho_1\rho_2 e^{-2j\beta L}) \\ & & +2\rho_1\rho_2\rho_4 e^{-2j\beta L}) & \\ & & & \\ -2\sqrt{2}j(1+\rho_2\rho_3 e^{-2j\beta L}) & -2j(\rho_1 + \rho_3) & 2\sqrt{2}(1-\rho_1\rho_2 e^{-2j\beta L}) & -2(\rho_1 - \rho_3 \\ & & & +2\rho_1\rho_2\rho_3 e^{-2j\beta L}) \end{bmatrix} V_i$$

48

with the determinant of A as

$$2\{ (1-\rho_1\rho_2 e^{-2j\beta L})(1-\rho_3\rho_4 e^{-2j\beta L}) + (1+\rho_1\rho_4 e^{-2j\beta L})(1+\rho_2\rho_3 e^{-2j\beta L}) \}$$

It will be shown in Section 3.4 that the case of interest for this radar modification is when:

$$\rho_3 = \rho_1 \quad , \quad \rho_4 = \rho_2$$
$$V_{3i} = jV_{1i}, \quad V_{2i} = V_{4i} = 0 \ ,$$

so that

$$V_{2o} = \frac{1}{\det A} \ 4\sqrt{2} \ V_{1i}$$

and

$$V_{4o} = \frac{1}{\det A} \ \{ \ -4\sqrt{2} \ j\rho_1\rho_2 \bar{e}^{2j\beta L} \ V_{1i} \ \} \ .$$

If the coupler isolation is defined as

$$I = | \ \frac{V_{2o}}{V_{4o}} \ |^2 \ ,$$

then the isolation as a function of reflection coefficient becomes

$$I(\rho) = 20 \ \text{Log}(\rho_1\rho_2) \ . \tag{34}$$

ANTENNA MODIFICATION

3.1 INTRODUCTION

In this section, the antenna modifications of the polarization diversity addition to the AFGL 10 centimeter Doppler radar will be considered. The details of these modifications will be kept sufficiently general so they may be applied to other systems and designs. Specific recommendations will be presented in the areas of the antenna configuration, polarizer, and feed antenna, while general parameters of other elements of the antenna will be considered to improve overall peformance, specifically in the area of circular polarization. It will be recommended that the antenna geometry be changed to a Cassegrain with four support spars and a sloped septum polarizer be employed with a corrugated feed horn. Furthermore, attention to overall axial symmetry will be stressed.

3.2 CONSIDERATION OF PRESENT ANTENNA CONFIGURATION

In theory, the present antenna could be modified to accommodate dual circular polarization operation by replacement of the present feed assembly and by the addition of a second waveguide run, however, this configuration would present certain performance restrictions which can be overcome by a Cassegrain antenna. These restrictions are a result of: (1) blockage and attending unsymmetrical diffraction due to an expanse of microwave components at or near the feed position, (2) nonconstant differential waveguide lengths due to thermal and mechanical instabilities, (3) varying cross-polarization sidelobe levels as a result of mechanical instabilities, and (4) higher than anticipated cross-polarization emanating from the tripod mounting structure. Spillover reception from such a front fed modification would present no performance restriction since in

the operational range limit of this radar the target return would have an equivalent noise temperature of the same order as that viewed in the spillover area. However, when linear polarization is considered, the minimum cross-polarization isolation requirement of -23 dB is uncomfortably close to the practical isolation limit expected from the present structure. We shall return to these four performance restricting elements after a cursory overview of theoretical aspects of reflector antenna cross-polarization.

3.2.1 CROSS POLARIZATION CHARACTERISTICS OF REFLECTOR ANTENNAS

A study of cross-polarization will begin with Silver[25] who presented the radiation field equations of a linearly polarized pencil beam antenna. He eluded to a detailed analysis by Condon[26] in which the cross-polarization pattern was shown to have maxima which lie in 45° planes between the principal axis of the antenna. These maxima consist of a set of pencil beam-like lobes on each arm of these planes, with the first maxima occurring at the co-polarized first null position.

This study then proceeds to Jones[27] who presented an exact solution for cross-polarization characteristics of the front fed paraboloid using an electric dipole, magnetic dipole, and Huygens or plane wave feed antenna. In addition, expressions for the total gain and efficiency factors were given for the overall antenna employing these various feeds. The results for the characteristics of a paraboloid excited by a short electric dipole are given in Table 4. The gain of this antenna is,

25   S. Silver, Ed., Microwave Antenna Theory and Design, (New York, NY: McGraw-Hill Co.,1949) pp. 417-423.
26   E. V. Condon, "Theory of Radiation from Paraboloid Reflector Antennas," Westinghouse Report No. 15, 1941.
27   E. M. T. Jones, "Paraboloid Reflector and Hyperboloid Lens Antennas," IRE Transactions - Antennas and Propagation, Vol. AP-2, July 1954, pp. 119-127.

TABLE 4. COMPUTED PATTERN CHARACTERISTICS AND GAIN FACTOR OF PARABOLOIDS
EXCITED BY A SHORT ELECTRIC DIIPOLE (from Jones 1954)

f/D	H-Plane Half-Power Beam-Width (Degrees)	E-Plane Half-Power Beam-Width (Degrees)	Position of Cross-Polarization Maximum	E-Plane First Side-Lobe Level(dB)	Cross-Polarized Lobe Max. Level(dB)	Gain Factor
0.25	1.6	2.20	1.8	-36.5	-15.8	0.41
0.30	1.6	2.00	1.8	-32.0	-18.1	0.37
0.40	1.6	1.75	1.8	-24.7	-22.2	0.32
0.46	1.6	1.75	1.8	-22.9	-24.3	0.28
0.60	1.6	1.75	1.8	-20.0	-28.0	0.19

$$G = \left(\frac{\pi D}{\lambda}\right)^2 \left\{ 6 \left[0.123 \, \frac{D}{\lambda} - 0.023 \left(\frac{D}{\lambda}\right)^3 + 0.0003 \left(\frac{D}{\lambda}\right)^5 \right]^2 \right\} \qquad (35)$$

which has been defined by $G = 4\pi$ (power radiated per unit solid angle by the aperture)/(total power radiated by the feed) so that this gain equation will have to be reduced by any energy loss due to feed spillover. The results for a paraboloid reflector with a magnetic dipole feed are identical with the sole exception that the E and H plane antenna patterns are to be interchanged. The term in braces in Equation (35) is the gain or efficiency factor. A plane wave feed is next considered and it is chosen such that the E and H plane patterns are identical (definition of Huygens source). With this feed, the gain becomes,

$$G = \frac{\pi D}{\lambda}^2 \left\{ 14.5 \left(\frac{B}{\lambda f}\right)^2 \left[0.246D - 0.0918D^2 + 0.0096D^5 \right]^2 \right\} \qquad (36)$$

where B = E-plane dimension of feed antenna. Jones then interpreted that for equal E and H fields the cross-polarized component of the fields are equal in magnitude and of opposite sign within each of the paraboloid quadrants (Figures 10 and 11) so that, "it is noticed that the far zone field has no cross-polarized radiation fields."

Continuing our chronological trek through literature, we stopped at a paper by Watson and Ghobrial[28], the results of which disagree with the preceding profound statement by Jones as well as future statements by others including Ghobrial. Although it is beyond the scope of this report to logically reconstruct this paper, in summary it is shown that: cross-polarization is a function of the electric field, the magnitude of the first cross-

28 P. A. Watson and S. I. Ghobrial, "Off-Axis Polarization Characteristics of Cassegrain and Front-Fed Paraboloidal Antennas," IEEE Transactions on Antennas and Propagation, Vol. AP-20, No. 6, November 1972, p. 691.
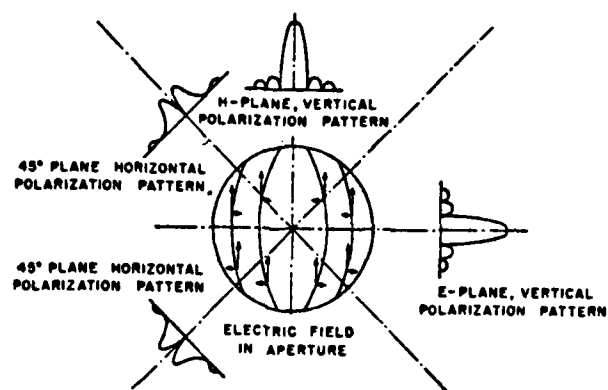
Figure 10.   Electric field in the paraboloid
             reflector aperture and resulting
             far-zone radiation patterns when
             the paraboloid is excited by a
             vertically oriented electric dipole.
             From Jones (1954).
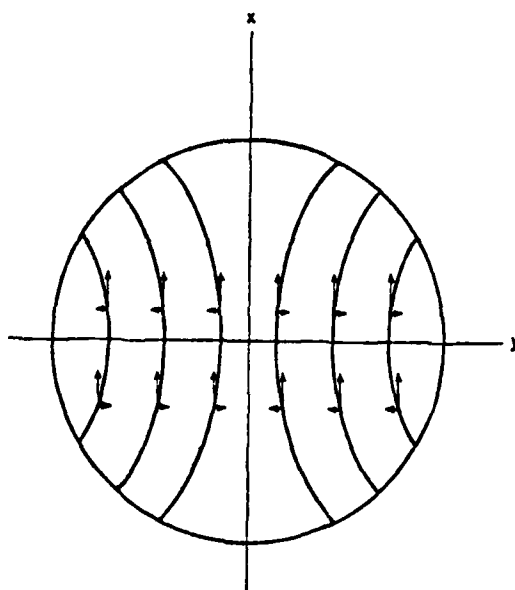
Figure 11.   Electric field in paraboloid
reflector aperture when para-
boloid is excited by a short
magnetic dipole lying along
y axis. From Jones (1954).

polarization lobe is far greater than that given by Jones, and the off-axis cross-polarization behavior of a Cassegrain antenna is superior to that of a front fed antenna, "due to the fact that the convex subreflector compensates to a high degree of cross-polarization caused by the concave main reflector." Later, Ghobrial and Futuh[29] refuted the last statement by showing that the polarization properties of Cassegrain antennas are identical to that of their identical front fed antennas.

During early 1973, Ludwig[30] presented a paper on three then prevailing differing definitions of cross-polarization. Again it is beyond the scope of this report to examine this information in detail. It is interesting to note that, according to the third definition of Ludwig, zero cross-polarization will result with a Huygens source feed, and a physically circular feed with equal E and H plane amplitude and phase patterns is a Huygens source feed. Furthermore, he successfully argued that the cross-polarization currents on a paraboloid illuminated by infinitesimal electric dipole are incorrectly frequently attributed to reflector curvature. The electric dipole itself has the cross-polarization which increases rapidly with increasing dipole pattern (as viewed by the reflector) angle. Cross-polarization is then reduced by increasing the focal length of the paraboloid so that the reflector views less off-axis (i.e., cross-polarized) dipole energy. Finally he shows that the measurement of cross-polarized pattern may actually be a measurement of the co-polarization pattern coupled into the sensing antenna by incorrect choice of measurement coordinate system.

---

29   S. I. Ghobrial and M. M. Futuh, "Cross-Polarization in Front-Fed and Cassegrain Antennas with Equal f/D Ratio," 1976 Region V IEEE Conf. Digest, April 1976, p. 277.

30   A. C. Ludwig, "The Definition of Cross-Polarization," IEEE Transactions on Antennas and Propagation, Vol. AP-21, No. 1, January 1973, p. 116.

The next stop is an expedient paper by Dijk[31], et al. Here not only do the results for a short electric dipole feed agree with that of Jones, but also a practical example using an approximation of a Huygens source is given. Finally, polarization loss efficiency factor curves are presented for both open waveguide and electric dipole feeds as a function of subtended half-angle between the feed and the reflector. The polarization efficiency is defined by the ratio of total cross- and co-polarized antenna gain to the antenna gain if the cross polarized energy was zero everywhere. This definition is in accordance with Potter[32] which appears to be the definition employed by everyone since the Dijk paper. Figures 12 - 14 present curves of polarization loss efficiency factor versus subtended half-angle for an electric dipole feed employed in a front fed paraboloid, Cassegrain antenna of various magnification factors, and a front fed paraboloid excited by an open waveguide structure operating in the TE_{10} mode, respectively. One should note that a Cassegrain antenna with a magnification factor of 1 is not presented, but it was shown by Ghobrial[33] that if it were it would be identical to that of a front fed parabolic reflector. However, our interest in this paper is Figure 14 and a synopsis of accompanying discussion of "a practical example."

In this example, they first consider a Huygens source and show that by definition of this source the dimensions of the waveguide must be such that $\beta_{10}/k = 1$. In practice, this can not be attained as

31 J. Dijk, C. T. W. van Diepenbeek, E. J. Maanders, and L. F. G. Thurlings, "The Polarization Losses of Offset Paraboloid Antennas," IEEE Transactions on Antennas and Propagation, Vol. AP-22, No. 4, July 1974, p. 513.

32 P. D. Potter, "Application of Spherical Wave Theory in Cassegrainian-fed Paraboloids," IEEE Transactions on Antennas and Propagation, November 1967, pp. 727-736.

33 Ghobrial and Futuh, Op. cit.
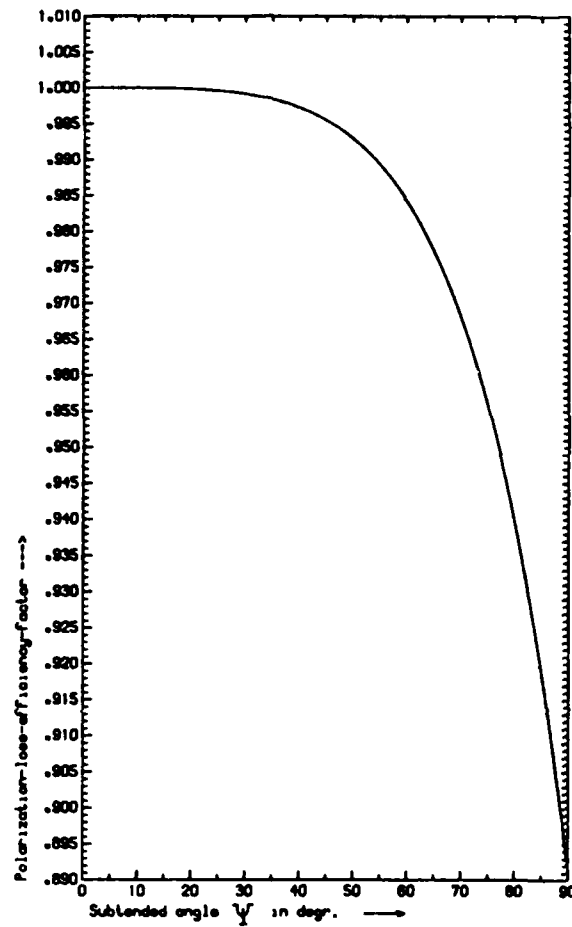
Figure 12. Polarization loss efficiency factor of a front fed
parabolic reflector employing an electric dipole
feed. (Dijk, et al., 1974)
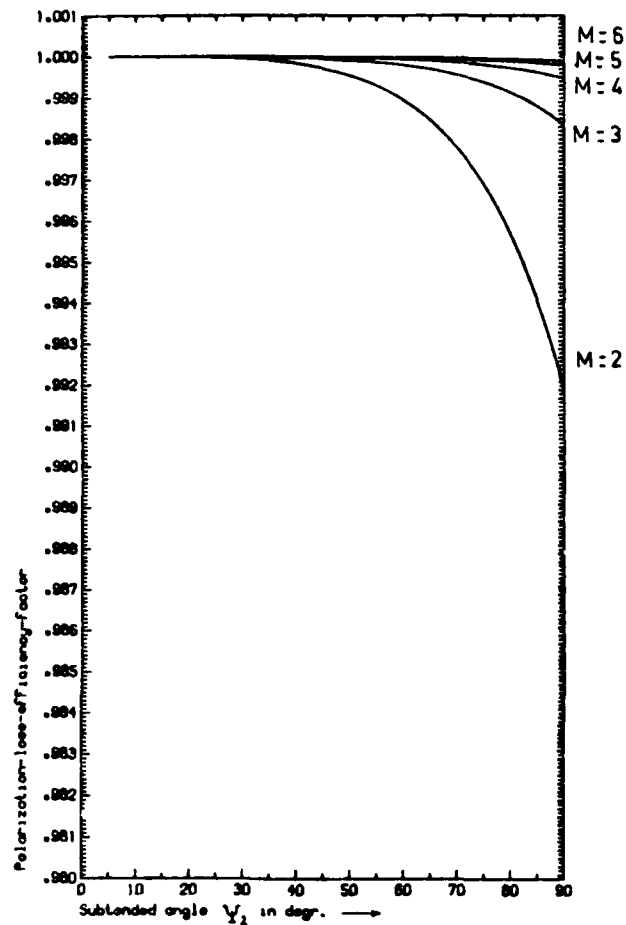
Figure 13. Polarization loss efficiency factor of axisymmetric Cassegrainian antenna employing an electric dipole feed. (Dijk, et al., 1974)

60
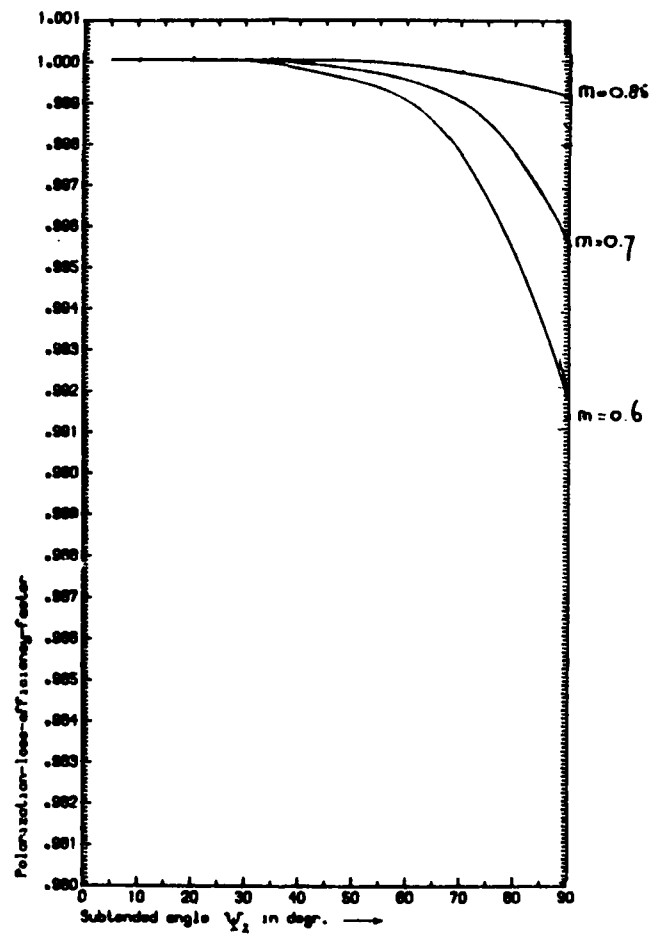
Figure 14. Polarization loss efficiency factor of a circularly symmetrical paraboloid antenna illuminated by open waveguide excited with the TE_{10} mode. (Dijk, et al. 1974)

61

$$\frac{\beta_{10}}{k} = \frac{\cdot \lambda}{\lambda_{g10}} \quad , \tag{36}$$

where λ_{g10} is the wavelength in the waveguide. From Silver[34] for the TE_{10} mode

$$\lambda_{g10} = \frac{\lambda}{[1 - (\lambda/2A)^2]^{1/2}} \quad , \tag{37}$$

then $\beta_{10} = k$ only for $\lambda \ll A$. Nonetheless, the effort is not without merit as they continue to calculate the polarization efficiency for various almost Huygens source open waveguide feeds. The general proportion of the lowest and highest operating frequency of any waveguide to the cutoff frequency of that waveguide are 1.25:1 and 1.90:1, or in terms of wavelength they are $\lambda/\lambda_{g10} = 0.60$ and 0.85, respectively. From Equation (37), we may readily obtain any intermediate values of this ratio, namely

$$\lambda/\lambda_{g10} = M = [1 - (\lambda/2A)^2]^{-1/2} \tag{38}$$

For the purposes of this calculation, it is also been shown in the literature that a horn feed antenna may be thought of as an open waveguide feed with A equal to the maximum dimension of the horn. From Equation (38) and by interpolating M in Figure 14, the polarization efficiency of any axisymmetric reflector antenna may be determined. It should be stressed that these are theoretical ideas which do not include the effects of the feed support structure, waveguide run, or other perturbations on or near the reflector surface.

Our journey continues to the effort of Ghobrial[35] for an approximation to the cross-polarization calculations of Jones.

---

34   Silver, Op. cit.
35   S. I. Ghobrial, "Off-axis Cross-Polarization and Polarization Efficiencies of Reflector Antennas," IEEE AP-27, July 1979, p. 460.

Not only is there good agreement between these calculations, but also from his method he derives an expression for peak cross-polarization which may be determined from the overall polarization efficiency, η,

$$\text{peak cross-polarization (dB)} = 10 \, \text{LOG}_{10} |0.29 \, (1/\eta - 1)| \, . \qquad (39)$$

The impression is that, for an axisymmetric reflector antenna without a feed support structure, the overall polarization isolation or integrated cross-polarization ratio may be determined by a measurement of the level of one of the main cross-polarization lobes.

Thus far, we have investigated reflector antennas with linearly polarized feeds. Our journey concludes with a recent text by P. J. Wood[36] which develops insight into the cross polarization properties of reflector antennas with circularly polarized feeds. First, we should review the physics of the purely circularly polarized wave. That wave can be mathematically constructed to contain two equal linear electric fields in phase quadrature. It can also be constructed from equal electric and magnetic components in time quadrature if it is understood that the amplitude of the magnetic field is considerably less than that of the electric field, while the total energy of the fields are equivalent. This effect might be exploited by manufacturing a low power circularly polarized array using alternate electric dipole and slot (magnetic dipole) antennas. Such a feed antenna is a Huygens source so that in theory no cross-polarization should exist in the far field of the driven reflector antenna. Wood,[37] on the other hand, has shown

36   P. J. Wood, Reflector Antenna Analysis and Design, IEE, London and New York, 1980.

37   Ibid

by his vector diffraction analysis method that such cross-polarization lobes do exist in phase quadrature with the co-polarization lobes and they have an absolute peak level of 8 dBi independent of reflector diameter. Obviously, these lobes vanish in the optical limit, $\lambda/D \to 0$. For the AFGL antenna, the peak lobe exists approximately 35 dB below the main beam.

Since polarization efficiency is the ratio of total co-polarized energy to the total radiated energy, a relationship may be constructed between polarization efficiency and one-way integrated cancellation ratio,

$$ICR = \text{isolation} = ICPR = 10 \, LOG_{10}|1 - \eta/\eta| \, , \qquad (40)$$

so that

$$ICR|_{\text{one-way}} = \text{peak cross-polarization in dB} - 10 \, LOG_{10}(0.29)$$

or

$$ICR|_{\text{one-way}} = \text{peak cross-polarization} + 5.38 \, dB. \qquad (41)$$

The outcome of the above is interesting. Since the theoretical level variation of all first cross-polarized lobes among themselves is non-existent as is the level variation of the second cross-polarized sidelobes, and since the amplitude ratio between the first and second cross-polarized sidelobes is a constant, then using the Ghobrial approximation only the absolute level of one lobe need be measured to determine the antenna integrated cancellation ratio.

3.2.2 BLOCKAGE AND UNSYMMETRICAL DIFFRACTION

In the previous subsection, consideration was given to the theoretical aspects of antenna cross-polarization. We now attack

64

the more practical considerations. It has been seen, that depending upon the feed arrangement and the choice of theory, the circular cross-polarization lobes should disappear; usually this is not the case. Experimentally, it has been found that excessive aperture blockage will contribute diffracting surfaces which increase cross-polarization and reduce overall antenna efficiency. Reduction in antenna efficiency for the Cassegrain configuration due to aperture blockage is given by the ratio the square of the subreflector to main reflector diameters, and in general the efficiency reduction can be discounted as this ratio provides an almost unmeasurable effect on the total antenna gain. Diffraction from the main reflector edge, subreflector edge, feed horn edge, and support structure edges on the other hand can contribute energy into both the cross- and co-polarized sidelobes. Although quantitative calculations of this effect are beyond the scope of this report, these calculations are performed by consideration of the edge currents that exist on the diffracting edges. The diffraction contribution can be reduced by various methods, some of which are: (1) elimination of edges, (2) occulation of edges, and (3) employment of a symmetrical design. As an example of the former, a choke flange is often used around a linear feed horn to suppress currents that exist at the horn's edge. In the proposed design for the AFGL radar, a shroud around the polarizer and rear of the corrugated horn will be utilized to occlude those reflecting surfaces. In the case of the latter consideration, detailed attention will be given to the overall axial symmetry of the entire antenna structure.

3.2.3 WAVEGUIDE LOCATION

While consideration is given to the merits of the various antenna geometries, equal consideration must be given to the equipment configuration imposed by those geometries. If the AFGL front fed antenna geometry is retained, then either two phase matched waveguide runs from the back of the reflector to the

65

polarizer fed horn assembly will be required, or the entire RF switch/microwave package/receiver package will have to be located at the prime surface. Obviously, the latter is impossible as it will impose severe blockage. Less obvious is the impossibility of placing only the feed horn at the focus with the polarizer behind the main reflector, as this configuration would place severe VSWR requirements upon the waveguide connections (see subsections 2.5 and 3.4).

Employment of two matched waveguide runs imposes thermal as well as mechanical constraints. The thermal requirement is easily calculated by assuming a waveguide run of 800 centimeters of WR-284. At the frequency of operation, the wavelength in this waveguide is 17.0 centimeters so that each waveguide run extends over 47 wavelengths. For a phase stability of one degree overall, the phase error must be less than 2.1×10^{-2} degrees per wavelength in guide, which in turn implies a waveguide expansion of 10^{-3} centimeters per wavelength or a maximum allowable coefficient of linear expansion of 5.9×10^{-5}. If aluminum waveguide is considered, whose coefficient of linear expansion is 2.3×10^{-5} per degree C, then the maximum tolerable differential temperature between the two waveguide runs is $2.6°$. Since the two waveguides would most likely be located on opposite sides of the antenna to preserve sidelobe and cross-polarization lobe reduction symmetry, this total differential temperature would have to be maintained within approximately the inner two-thirds volume of the radome. Furthermore, mechanical distortion imposed by the slewed antenna would only reduce this temperature differential constraint to a more challenging value so that, based on these considerations alone, a Cassegrain is preferable as all the abbreviated waveguide can be enclosed within the shroud behind the feed horn to not only provide a temperature controlled environment but also reduce slewing forces.

3.2.4 MECHANICAL STABILITY

In addition to the aforementioned mechanical requirements of the waveguide, the general requirements of the AFGL reflector must also be considered. The manufacturer of the reflector has been contacted and, although they could not apriori predict antenna degradation due to modification to a Cassegrain configuration and predict degradation due to slewing, they have offered to perform this analysis via their computer-aided design analysis department and program STARDYNE for a nominal sum. However, they do feel that this reflector has sufficient structure to not require the modifications performed on the Alberta Research Council radar reflector.

The AFGL reflector (Serial No. 728) was manufactured and pattern tested at H&W Engineering (formerly Radiation Systems, Inc.) in Cohassett, Massachusetts, in 1977. This 24-foot diameter reflector is a scaled down 30 foot diameter design and utilizes the same 1-1/2" square tubing members and hub of the original design. Jim Hayes, company co-owner and chief engineer, suspects that the hub has four internal plates radially spaced at 90° angles between the inner and outer hub cylinders. Prior to any mechanical analysis of the antenna structure, he requested that he be permitted to drill a few non-structural inspection holes into the hub to confirm the location of these plates. The hub has eight pickup bolts spaced radially at 22.5° intervals on a bolt circle of 74.5 inches. The entire antenna weighing approximately 2500 pounds is constructed of 24 panel assemblies. Misalignment of these assemblies is not possible as the panel attachment screw holes are individually through-drilled during construction. Three spar attachment plates and four pull attachment plates are located on the surface of the reflector, however, these plates are not attached to the surface but rather to the structure behind. Although the pull plates and spar plates are slightly different in appearance, their use is interchangeable. The spar attachment holes on the spar plates

are located 71-1/4 inches from reflector surface edge measured along the reflector contour, while the attachment holes on the pull plates are located 68-3/4 inches in from the reflector surface edge. Because the reflector is far more rugged design than that employed at Red Deer, Alberta, Canada, it is the opinion of H&W that the additional rear strut assemblies required by the Alberta radar antenna will be unnecessary. However, Jim Hayes feels that deletion of this additional truss work can only be determined after structural analysis.

3.3 OPTIMUM ANTENNA CONFIGURATION

In the previous subsections, two antenna geometries have been discussed, with the conclusion that a Cassegain affords the best compromise between focal length, feed location, decreased blockage and symmetry to produce favorable co- and cross-polarized sidelobe architecture. A third configuration, offset Cassegrain, has been briefly mentioned during the project as a possible geometry to totally eliminate illuminator blockage, thereby further reducing these urwanted lobes. In an axisymmetric antenna with a dipole feed, cross-polarization is generated in the aperture electric field by off-axis observation of the feed antenna; this cross-polarization has a symmetry property that it is oppositely directed in adjacent quadrants. Then by symmetry, cross-polarization cannot exist in the principal planes of the antenna, but does achieve a maximum value in two planes located midway between the principal planes. As has been discussed, if a feed is constructed such that equal electric and magnetic dipole patterns are placed on the reflecting surface (Huygens source), a second set of cross-polarized electric field vectors is generated by the magnetic field in the aperture which are equal and opposite to those generated by the electric field (Figures 10 and 11). Obviously, if these vectors are not symmetric, radiation of cross-polarized energy will exist. In the case of an asymmetric reflector, such

68

an unsymmetry is accomplished because the distance between the subreflector and the upper quadrants is greater than the distance between the subreflector and the lower quadrants. In theory, this distance variation can be ameliorated by an offset subreflector; but in practice, the best achievement of such an arrangement has yielded two -34 dB cross-polarization sidelobes symmetrically displaced from the principle axis.[38] The virtue of such an antenna is its capacity for a great reduction in the near co-polarized sidelobes; in the aforementioned example, a 17 dB improvement was achieved versus the level expected for a conventional shaped Cassegrain antenna.

In light of these achievements, this geometry was considered, but the cost of an appropriate development program quickly dispelled further attention. The antenna of choice then remains an axisymmetric Cassegrain with a yet to be determined focal length.

3.3.1 INTEGRATED CROSS-POLARIZATION RATIO

Throughout the preceding discussion various terms, notably the isolation f, have be employed to describe system cross-polarization conditions in the linear polarization mode. An alternate figure of merit, analagous to ICR, developed by Georgia Tech is the integrated cross-polarization ratio (ICPR). This one-way calculation is defined as the ratio total cross-polarized power transmitted by the antenna to the total co-polarized power transmitted, and is a useful definition of both circular and linear polarizations; ICPR is equivalent to one-way ICR. Our previous discussion of isolation (ICPR) of reflector antennas in the linear polarization mode has been theoretically based, however investigation of the ICPR of reflector antennas has also

---

38   E. J. Wilkinson and B. H. Burdine, "A Low Sidelobe Earth Station Antenna for the 4/6 GHz Band," GTE International Systems Corp. Report, 1980.

been performed utilizing the Engineering Experiment Station (EES) computer models.

EES has developed computer programs which use the E-field formulation to calculate the co- and cross-polarized fields radiated by the feed for analyzing the pattern performance of single reflector and double reflector antennas.[39] These computer programs have been validated over the past several years not only with measured data Georgia Tech has obtained but also with measured and theoretical data that have appeared in the literature. For front-fed antennas, the feed antenna induces currents on the reflector which are integrated by the program to obtain the co- and cross-polarized fields radiated by the reflector. In the case of Cassegrain antennas, physical optics is employed within the program to determine the field reflected by the subreflector; this reradiated field in turn induces currents on the main reflector that are then integrated to obtain the co- and cross-polarized components of main reflector radiation.

The single reflector program was applied to calculate the co- and cross-polarized pattern of the present AFGL antenna with its 288 inch diameter and 115 inch focal length, and 3.25 inch by 3.63 inch feed horn. The program predicted peak cross-polarized lobes occurring along 45° planes having an amplitude value of -24 dB with respect to the co-polarized on-axis level. this value is close to the theoretical value calculated by Jones[40] for an electric dipole feed. ICPR was then calculated for this antenna and also for parabolic reflectors of the same diameter, but with longer focal lengths. Integration of the antenna pattern was performed to limits of the -3 dB, -10 dB, first null and second null positions of the co-polarized pattern to assess cross-

---

39   D. G. Bodnar, J. W. Cofer, and N. T. Alexander, "Computer-Aided Design of Scanning Reflector Antennas." 1974 Antenna Propagation Symposium, Atlanta, Georgia.

40   Jones, Op. cit.

polarization contribution to the total radiated power. The results presented in Table 5 show that, while a -20 dB ICPR can be obtained with the existing AFGL reflector, any further improvement requires a reflector with a longer focal length. These results are also plotted against those of the literature in Figure 15; as expected the actual results employing a feed horn have a lesser ICPR than the theoretical predictions, but are somewhat better than a dipole feed.

3.3.2 FOCAL LENGTH

It was shown in subsection 2.3.3.2 that a minimum isolation between -20 dB and -30 dB is required to measure a differential reflectivity of 5 dB within an uncertainty of 0.1 dB, and as will be discussed in Section 4, 0.1 dB is approximately the limit of expected amplitude uncertainity within the microwave and receiver package. Using -25 dB as a respectable isolation (ICPR) requirement, it is obvious from Figure 15, a minimum focal length of 160 inches is required with 173 inch focal length (f/D = 0.6) a safer value. This is based upon linear polarization considerations only; cross-polarization in the circularly polarized mode is only the result of antenna imperfections and is independent of focal length.

3.3.3 SUBREFLECTOR

While the specific detail of design for the hyperbolic subreflector is not a subject of this report, an interesting addition to the subreflector shape was provided by E. J. Wilkinson of GTE International Systems Division. The center of their subreflector of circularly polarized earth station antennas are closely conical shaped so that a "hole" exists in the backscatter pattern. This "hole" prevents backscattered energy from re-entering the feed by radiating that energy beyond the rim of the main reflector. This is an important item in the design as if a mismatch exists within the polarizer any energy, re-

TABLE 5. CALCULATED VALUES OF ICPR FOR A 288 INCH AXISYMMETRIC REFLECTOR ANTENNA WITH A RECTANGULAR HORN FEED

Focal Length	f/D	-3.0 dB	-10.0 dB	First Null	Second Null	Integrated over Entire Pattern-- Theorectical Value with Dipole Feed
115.2"	0.4	-35.8 dB	-26.6 dB	-20.8 dB	-20.3 dB	-17.6 dB
172.8	0.6	-42.2	-34.1	-28.6	-26.8	-23.0
230.4	0.8	-47.1	-38.9	-33.3	-31.6	-27.0
288.0	1.0	-50.9	-42.6	-37.1	-35.3	-31.0

72
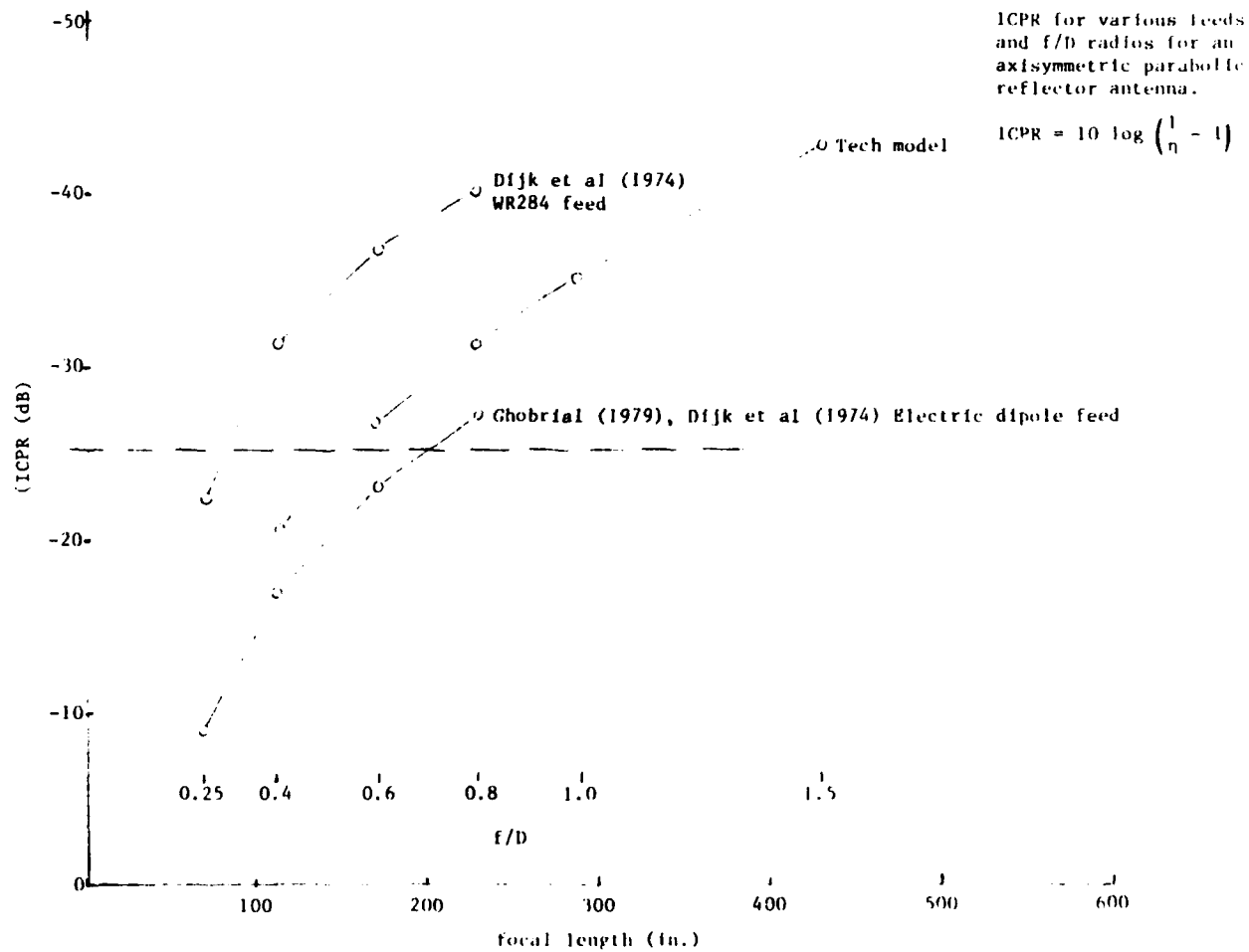
Figure 15.   ICPR for various feeds and f/D for an axisymmetric
parabolic reflector antenna.

73

entering the polarizer via the feed will be reflected at the mismatch and retransmitted with the opposite polarization sense. This phenomenon does not occur in linear polarization and is the principle reason why all new communications satellites are using linear polarization for frequency "reuse" operation. To prevent diffraction effects, this conical section should have a smooth taper into the hyperbolic subsection of the subreflector; the use of absorbing material in place of the conical section should not be considered as it would provide an additional diffracting edge.

3.3.4 SUBREFLECTOR AND FEED MOUNTING STRUCTURE

Although not a direct consideration of the specific antenna geometry, the feed and subreflector mounting structure has a significant influence upon the side and cross-polarization lobe integrity. Maintenance of overall antenna symmetry is the foremost requirement to reduce cross-polarization if the proper feed assembly is used; symmetry can not be preserved with a tripod secondary reflector mount. Either a bipod and support wires or a quadrapod structure is required. Furthermore, it has been shown that the mount's attachment points must be located as far to the rim of the main reflector as possible. This reduces lobe structure as not only is there less blockage due to the spars but also, if a reasonable illumination taper is employed, the energy level impinging upon the attachment points are further reduced. So as to understand the experimentally determined importance of the secondary reflection mounting configuration, an interview was arranged with Wilkinson of GTE International Systems in May 1981:

> Subreflector Support Assembly. In GTE's advertising we have noted that the bipod support structure with two support wires has been employed to support this subreflector. What are the advantages of this arrangement?

In the early days of satellite antennas, GTE went to a bipod support structure as the antenna cone angle was small, which caused spherical wave blockage. The bipod structure was an attempt to reduce this blockage. The blockage reduced antenna gain, two large struts were employed to reduce blockage and wires were added for stability. Of course the shallow cone angle was due to having the mounting emanating from the most central location on the reflector. A larger cone angle is achieved by bringing the attachment points further out to the edge of the reflector. GTE has never found a bipod structure to perform better than a quadrapod structure. They have found, however, that the quadrapod structure does affect the sidelobes; and that minimum sidelobes occur midway between the mounting struts. The sidelobes are higher in the planes of the quadrapod. This effect occurs only for the far out sidelobes, however, not just the first two or three.

Effect of Structure on Axial Ratio. How does a quadrapod structure affect the axial ratio?

We have never found an effect on axial ratio from a quadrapod structure, however, a strong correlation exists between the feed axial ratio and the final antenna axial ratio. In fact, as long as symmetry is employed in the antenna the overall axial ratio will be very close to the feed axial ratio. Antenna symmetry can be determined by deep nulls and no optical distortion, when this is the case then the effect of blockage on cross-polarization is very small. However, our stringent cross-polarization requirement does not

exist very far off axis; only down to the -1 dB level. GTE does measure the axial ratio over the entire beam to this -1 dB level, and they achieve 0.5 dB axial ratio if the feed axial ratio is less than or equal to 0.2 dB. It can be seen that the antenna does add some degradation but it is very small. In the past few years, confidence in these antennas has become sufficiently high that the axial ratio of the entire antenna assembly is no longer measured during construction but is only measured during the final testing following installation. Only the performance of the feed assembly is evaluated before the system is shipped.

Optimum Shape of Support Spars. What spar cross section should be employed to reduce the backscatter into the feed assembly?

No special cross section has been shown to reduce cross-polarization backscatter from the support Spars.

From the foregoing, it can be seen that a quadrapod mount consisting of cylinderical spars attached to the reflector rim offers the optimal sidelobe and cross-polarization reduction condition. Furthermore, no structure visible to the subreflector should be employed to support the feed assembly as such a support would detract from overall symmetry. This requires the feed support be wholly contained within a shroud that is, with respect to secondary reflector, occluded by the feed horn.

3.4 POLARIZER ASSEMBLY

Three polarizers were considered for this modification: (1) lossless power divider with an orthomode transducer, (2) short slot hybrid coupler, orthomode transducer combination, and (3) sloped septum hybrid. Each consideration (Figure 16) employed

| Phase Shifter State | Transmitted Polarization by Excitation of | |
	Port 1	Port 2
Out	RHC	LHC
In	Horiz.	Vert.
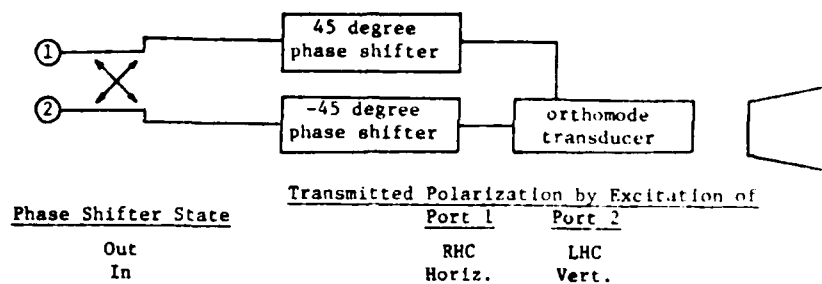
a. Short slot hybrid coupler/orthomode transducer polarizer.
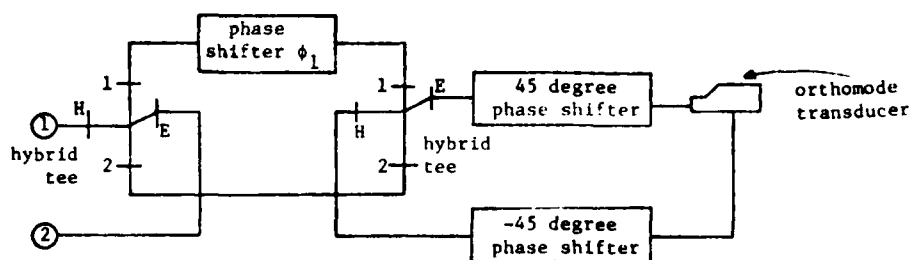
b. Lossless power divided/orthomode transducer polarizer.

| Transfer Switch State | Transmitted Polarization by Excitation of | |
	Port 1	Port 2
Hybrid Coupler Out (as shown)	LHC	RHC
Hybrid Coupler In	Vert.	Horiz.
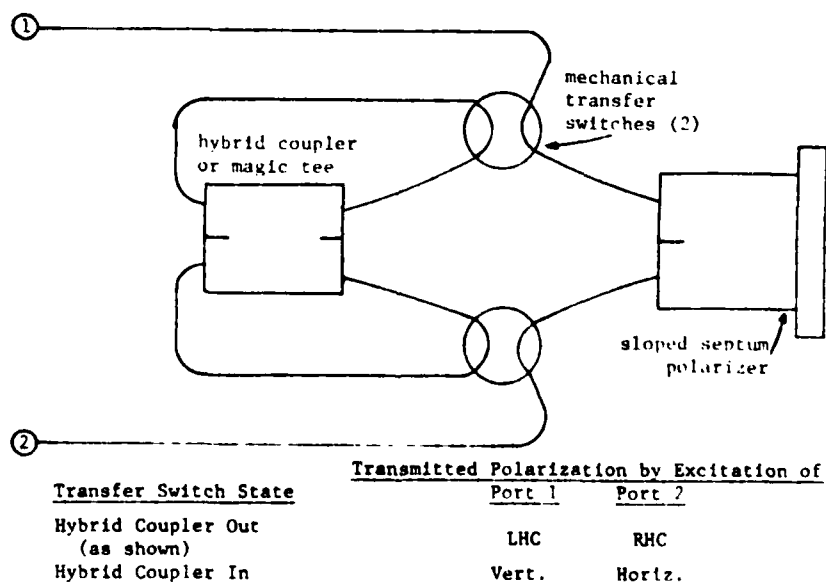
c. Sloped septum polarizer. Polarizer is rotated 45° with respect to local vertical.

Figure 16. Various polarizer configurations. Transducer or septum rotated 45° with respect to local vertical.

attending phase shifters and attenuators to accommodate all modes of linear or circular polarization transmission as well as reception of transmitted and orthogonal polarizations. The selection criteria of the appropriate scheme were based upon the requirement of a minimum 35 dB isolation for circular polarization and 25 dB isolation for linear polarization.

Thus far, no single item of the general design has been shown to limit the overall integrated cancellation ratio of a polarization diversity radar system to less than -40 dB, however, if consideration is given to the VSWR of the components attached to hybrid junction within any polarizer consideration and the equivalence of hybrid junction isolation with two-way ICR, then it can be shown that such a ICR is most likely unachievable, while a -35 dB ICR is a realistic anticipation. The validity of this realization exists within the one-to-one mapping of VSWR and isolation of a hybrid junction (subsection 2.5). From that subsection, the isolation of hybrid is given by,

$$I = 20 \; Log_{10} \; (\rho_1 \rho_2), \tag{34}$$

with VSWR related to the reflection coefficient by,

$$\rho = \frac{1 - VSWR}{1 + VSWR} \; .$$

In Table 6, values of isolation versus VSWR of the two pairs of ports are presented. When reviewing Table 6, it must be realized that a component VSWR requirement of equal to or less than 1.02:1 overall is generally unachievable in microwave components operating at the frequency of interest for any reasonable bandwidth, with the sole exception of a corrugated horn. Achievable minimum VSWR for special order variants of these components over a small percentage bandwidth is usually in the 1.05:1 to 1.07:1 range. This will be a significant driving function for the polarizer choice. We shall analyze each

TABLE 6.   ISOLATION VS VSWR OF A HYBRID COUPLER

Isolation	Maximum VSWR of Input Ports*	Maximum VSWR of Ouput Ports**
-40 dB	1.01	1.041
	1.02	1.020
	1.04	1.010
-37 dB	1.01	1.084
	1.02	1.041
	1.05	1.016
	1.07	1.012
-35 dB	1.01	1.136
	1.02	1.066
	1.05	1.026
	1.07	1.019
	1.10	1.013
-32 dB	1.01	1.290
	1.02	1.136
	1.05	1.053
	1.07	1.038
	1.10	1.027
	1.20	1.014
-30 dB	1.01	1.503
	1.02	1.225
	1.04	1.086
	1.07	1.061
	1.10	1.043
	1.30	1.015
-27 dB	1.01	2.339
	1.02	1.505
	1.05	1.178
	1.07	1.125
	1.10	1.087
	1.30	1.031
	2.00	1.012
-25 dB	1.01	4.489
	1.02	1.939
	1.05	1.298
	1.07	1.206
	1.10	1.142
	1.30	1.050
	2.00	1.019

*   The two input ports have identical VSWR

** The two output ports have identical VSWR

polarizer configuration assuming an attached corrugated horn with a VSWR value of 1.025:1, require a polarizer isolation of -35 dB for circular polarization, and then from Table 6 determine that the high speed RF switch attached to ports 1 and 4 must have a VSWR of 1.05:1 or less.

3.4.1 SHORT SLOT HYBRID AND ORTHOMODE TRANSDUCER POLARIZER

The reflection from the feedhorn will have little effect upon the isolation performance of this configuration as the isolation is a function of the VSWR of the combined components in each arm including phase shifter, waveguide flanges and bends, linear-circular polarization transfer switch, and orthomode transducer, the combined value of which must be less than the minimum 1.1:1 VSWR achievable for the transducer alone. Although the combined VSWR may be significantly reduced by an appropriate choice and location of matching stubs, such a choice would present a formidable task in attempting to "match" all components, and questions of such a microwave package's mechanical and thermal stability would certainly arise.

3.4.2 LOSSLESS POWER DIVIDER AND ORTHOMODE TRANSDUCER

The input E and H arms of the hybrid tees in the lossless power divider as shown in Figure 16b do not suffer the same isolation constraints of a hybrid junction unless the reflections from the arms 1 and 2 are quadrature. The divider can certainly be constructed so that such a condition is not achieved over a small bandwidth. However, taken as an entity the lossless power divider, when analyzed, exhibits the same characteristics of the single hybrid junction, so that the previous nonachievable condition is also enforced for the microwave components between the power divider and the orthomode transducer. If less isolation could be tolerated, then this polarizer does offer the flexibility of transmission in any ellipticity and reception in that polarization as well as the orthogonal polarization.

80

3.4.3 SLOPE SEPTUM POLARIZER

Obviously, the polarizer of choice would employ as few microwave components between itself and the feed antenna so that the advantage of the low VSWR of the feed antenna could be utilized. Therefore, such a device must be capable of directly generating the proper circular polarization with each waveguide input. A sloped septum polarizer is such a device. It is described in relatively few papers[41,42] and at least one patent.[43] The polarizer is a true hybrid coupler with two input ports and a common output port; exciting one input port causes the excitation voltage to be equally divided with one division receiving a 90° phase lag prior to entering the square common waveguide output port. Linear polarization is achieved by adding a hybrid coupler to provide an appropriate 90° phase shift and allow equal amplitude excitation of the input ports (Figure 16c). This device also obeys the VSWR versus isolation requirements of the previous polarizers such that a minimum of attached components must exist in the high isolation circular polarization mode, while more attached components are tolerated in the less demanding linear polarization mode. Since transfer switches with a VSWR of less than 1.05:1 are obtainable, a review of Table 4 demonstrates the possibility of constructing a −35 dB isolation feed assembly utilizing this polarizer if a very low VSWR corrugated horn feed antenna is employed.

41 D. Davis, O. J. Digiondomenico, and J. A. Kempic, "A New Type of Circularly Polarized Antenna Element," Symposium Digest, 1967 G-AP, pp. 26-33.

42 Ming Hui Chen and G. N. Tsandoulas, "A Wide-Band Square-Waveguide Array Polarizer," IEEE Transactions on Antennas and Propagation, Vol. AP-21, May 1973, p. 389.

43 J. V. Rootsey, "Tapered Septum Waveguide Transducer," U.S. Patent No. 3,958,193, May 18, 1976.

3.5 FEED ANTENNA

Three horn antennas were considered for this modification. In the previous paragraphs, it was shown that the VSWR, cross-polarization, and axial ratio demands required a corrugated horn, but for completeness the three antennas should be described. The first, a pyramidal horn, can be easily attached to the polarizer, requires no square-to-circular waveguide transition, and is inexpensive to manufacture. However, it has been shown theoretically such an antenna will give rise to relatively high off-axis cross-polarization lobes in two orthogonal planes rotated 45° with respect to the principal axis[44]. The same effect was noted experimentally by GTE[45]. The second antenna under consideration is a circular multitaper horn which will provide the required reduced cross-polarization at the expense of -20 dB co-polarized sidelobes and a narrow bandwidth. Since the third antenna, a corrugated horn, can provide all the requirements of this design, but at a relatively high cost, the multitapered design should receive further investigation as it is inexpensive to manufacture.

3.6 SUMMARY

3.6.1 ELECTRICAL

In this section, the theoretical and practical aspects of the polarization diversity antenna modification to the AFGL S-band Doppler weather radar have been considered, however, the information in this report has been sufficiently general so that it is applicable to other frequencies and designs. An outline of the specific recommendations of choice for this modification is presented in Table 7.

---

44   E. A. Nelson, "Polarization Diversity Array Design (PDAD)," GE Aerospace Electronic Sys. Dept., Utica, NY, March 1972.
45   Wilkinson and Burdine, Op. cit.

TABLE 7. RECOMMENDATIONS FOR ANTENNA MODIFICATION
OF S-BAND AFGL WEATHER RADAR

Requirement	Recommendation
Antenna configuration	Cassegrain with f/D ≈ 0.6
Number of support spars	4
Support spar cross-section	Circular
Feed/polarizer supports	Entire assembly must be covered by axisymetric shroud
Secondary reflector	Hyperbola with center half-conical section
Secondary reflector pattern taper	About -10 dB on reflector edges
Feed antenna	Corrugated horn
Feed antenna VSWR	< 1.025:1
Polarizer	Sloped septum
VSWR at polarizer	< 1.05:1
Anticipated ICR	-35 dB
Anticipated ICPR	Better than -25 dB

3.6.2 MECHANICAL

Little mention has been made of the mechanical requirements of this modification, however, it is recommended that a complete static and dynamic structural analysis be performed simultaneously with the antenna component design effort. The manufacturer of the reflector, H&W Engineering of Cohassett, Massachusetts, has provided a reasonable cost estimate to provide such a computer-aided mechanical analysis. This analysis will ensure that the structure is sufficiently stiff to prevent significant distortion as the antenna is slewed and thereby maintain the integrated cancellation ratio and sidelobe requirements.

SECTION 4
MICROWAVE PACKAGE AND RECEIVER

4.1 INTRODUCTION

In this section, we shall no longer evaluate by the best-of-the-multiple approach concept, but shall consider the requirements to obtain a solution for converting the antenna output energy into a baseband signal. That is, we shall confine the discussion to the hardware necessary to produce the desired measurement accuracy. From the antenna through the IF amplifier chain, little deviation is recommended from this design (Figure 17). Following this, however, as other equivalent phase detection and line driving schemes exist, these items could be modified as required. Within this section, little mention will be made of the transmitter as it is not to be modified save a possible slight power reduction.

In reviewing Section 4.2, the reader should always be aware of the 1.2 megawatt peak power output of the transmitter as well as the unusual maximum expected average power of 1950 watts. This average power is a result of not only a maximum PRF of 1300 Hertz and a pulse width of 1 microsecond, but also is a result of the combined energy of two transmitters, one of which operates at 1/4 the PRF of the "power channel" transmitter. The pulses of these two transmitters are sufficiently separated in time to prevent a doubling of the peak power output.

Furthermore, the reader should remember the constraints put forth in Section 2 of an overall amplitude uncertainty less than or equal to 0.1 dB and phase uncertainty less than or equal to 1 degree. Both of these limits will require careful amplitude and phase balancing of all channels, careful temperature and mechanical control, as well as an effective calibration scheme. This section will detail a microwave package and receiver electronic design which should perform at those limits, while
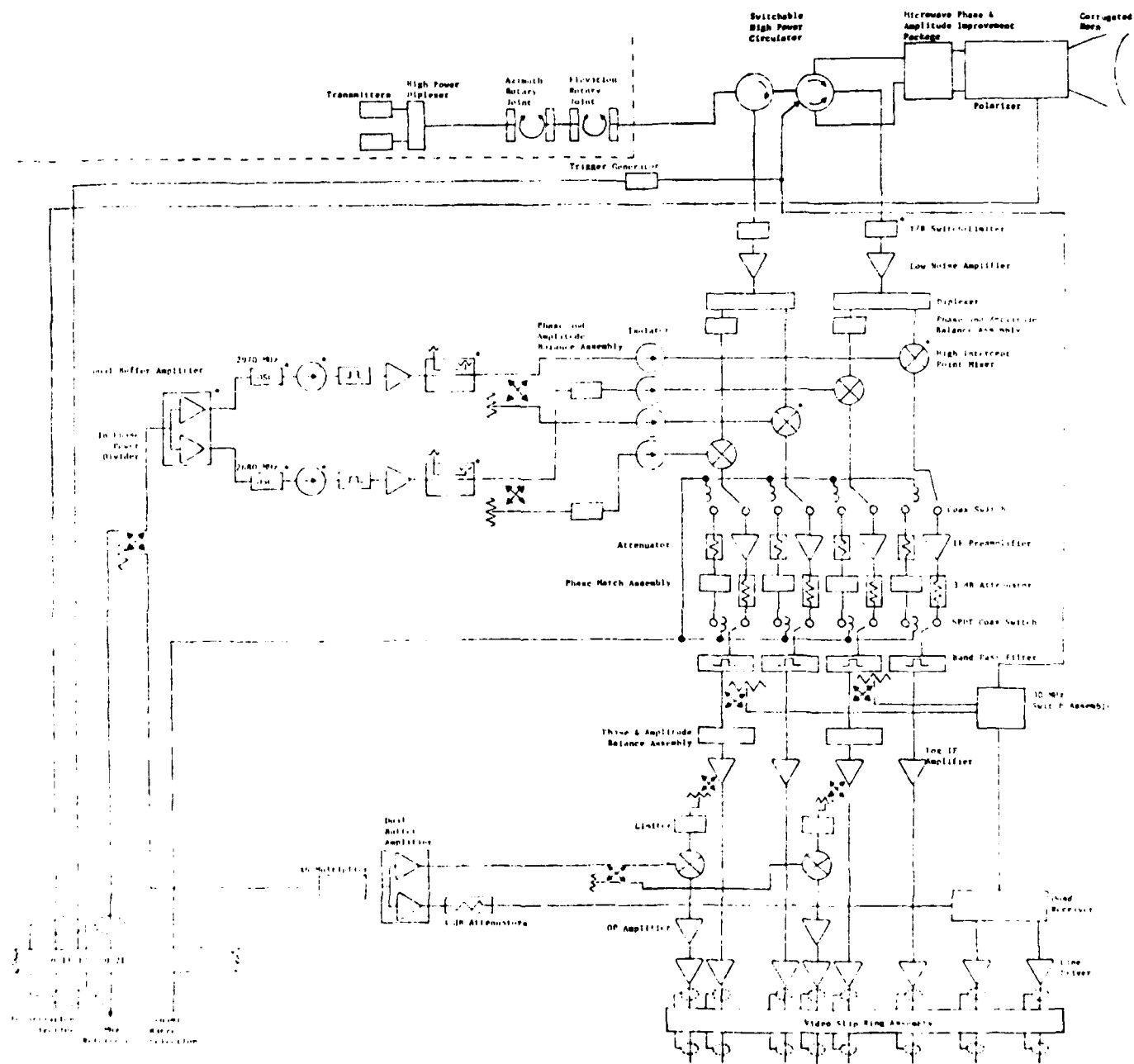
Figure 17. Recommended modification of microwave package and receiver.

Appendix B will list the components chosen for the design. The study of an effective onsite calibration scheme is left for the future.

4.2 MICROWAVE PACKAGE

The microwave package contains those components which interface with the transmitter, receiver, and polarizer, and as such must be capable of operating at the transmitter power level as well as be able to withstand heating due to losses while critically maintaining phase and amplitude balance of both transmitted and received signals. This can only be accomplished if the aforementioned VSWR versus isolation requirements are maintained and the microwave package/receiver through the second IF amplifier is thermally stabilized by placement in a temperature-controlled container that is located as close as possible to the antenna feed assembly.

4.2.1 TEMPERATURE REQUIREMENTS

In most systems with stringent phase and amplitude tracking requirements, the operating temperature of the system enclosure is chosen such that under the highest ambient temperature conditions dissipated transmitter energy is radiated away and thermal stability is maintained by heaters alone; such a choice is not available for the AFGL weather radar modification. In this instance, the operating temperature of choice is dictated by maintenance of phase stability of the most unstable component. Georgia Tech believes that component to be the microwave circulator and has performed a cursory phase versus temperature experiment on the present unit. As shown in Figure 18, the optimum operating temperature for this device is 42.5°C to 45°C. This temperature is uncomfortably close to the maximum expected ambient temperature inside the radome of approximately 36°C so that a complete heat exchanger system is recommended to maintain a mean temperature of 44°C. The deviation from this

87
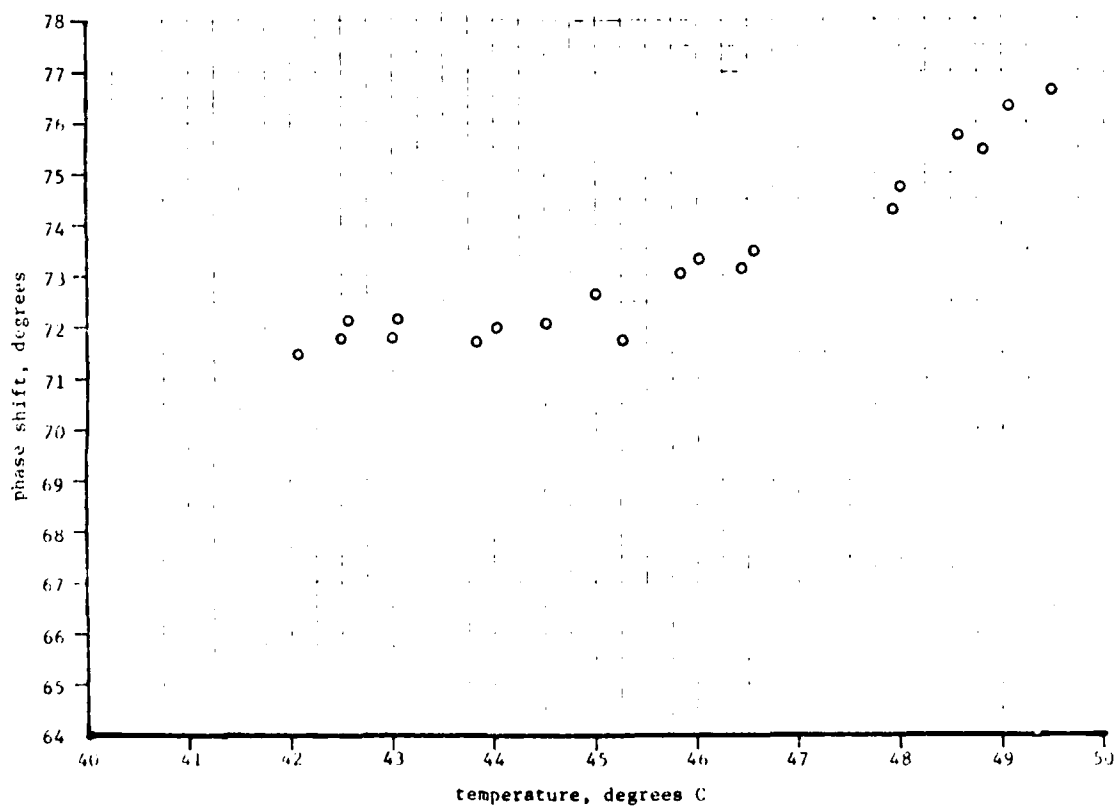
Figure 18. Phase shift vs. temperature change
for Microwave Associates Model 8H02
Circulator. Serial No. 76.

END

FILMED

DTIC
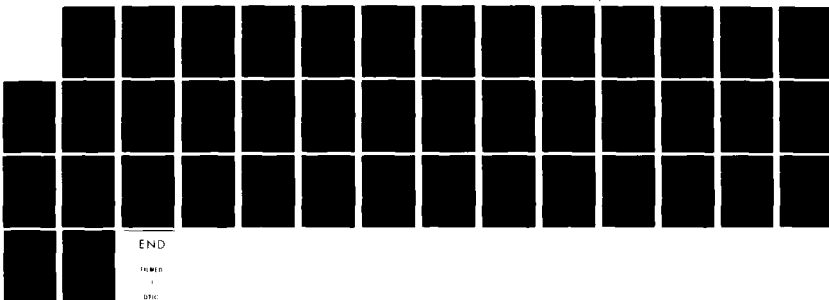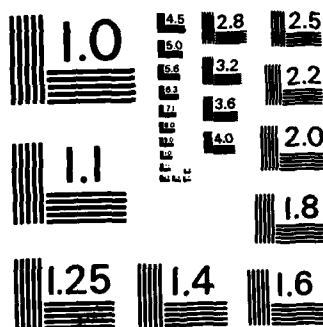
MICROCOPY RESOLUTION TEST CHART

NATIONAL BUREAU OF STANDARDS-1963-A

mean allowable by the heat exchanger will require further study. Furthermore, it is suggested that a more extensive set of measurements over a wider range be performed upon the circulator to not only confirm Figure 18, but also to determine if other optimum operating temperatures exist.

Determination of the capacity of the heat exchanger has yet to be accomplished; however, some points of attention are the dissipated transmitter energy due to loss of each component in the transmitter to antenna path and dissipated switching energy of the high power RF switch. Both of these items will involve moderate amounts of localized heating which could cause one of the receiver paths to differentially expand with respect to the other path, thereby creating a phase imbalance. Prior to the fabrication of the microwave package/receiver container, a thorough thermodynamic analysis should be executed.

4.2.2 MICROWAVE IMPROVEMENT NETWORK

In an attempt to improve the VSWR of the components prior to the polarizer, a microwave improvement network has been included into the design. Various candidate matching or isolation improvement schemes exist for this package, but the choice of the specific solution depends upon the achieved characteristics of the RF switch and the feed antenna (subsections 2.5, 3.4, and 3.5). One scheme under consideration[46] which will improve only isolation and overall phase error has been under study at Georgia Tech. This device as shown in Figure 19a with a variant in Figure 19b was strongly favored as it is employed in the National Research Council of Canada (NRC) K_u-band polarization diversity weather radar. Over the past few months, we have attempted to improve the isolation of the stock hybrid coupler (Figure 20) and

---

46   J. S. Hollis, T. G. Hickman, and T. J. Lyon, "Polarization Theory," Microwave Antenna Measurements Handbook, Chapter 3, 1970, Scientific-Atlanta, Atlanta, Georgia.
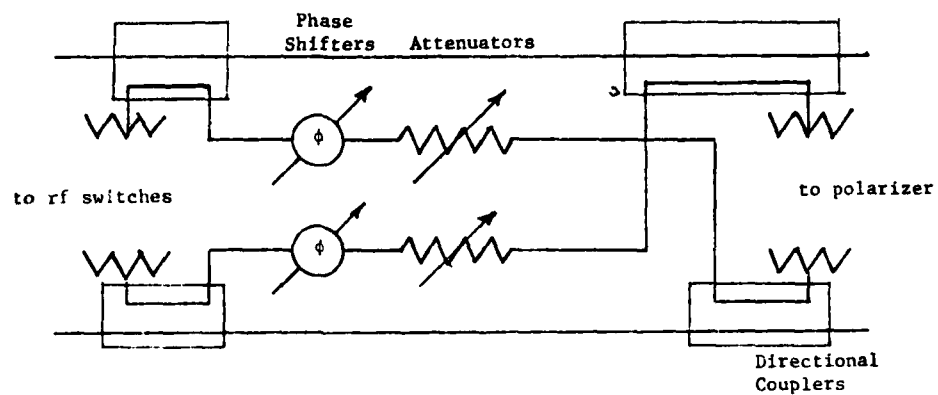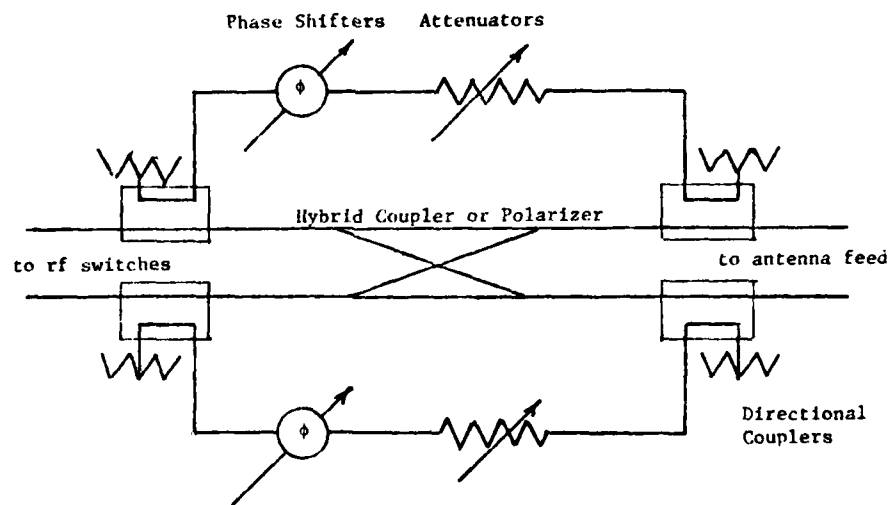
Figure 19. Potential isolation improvement networks from
Microwave Antenna Measurements Handbook.

90
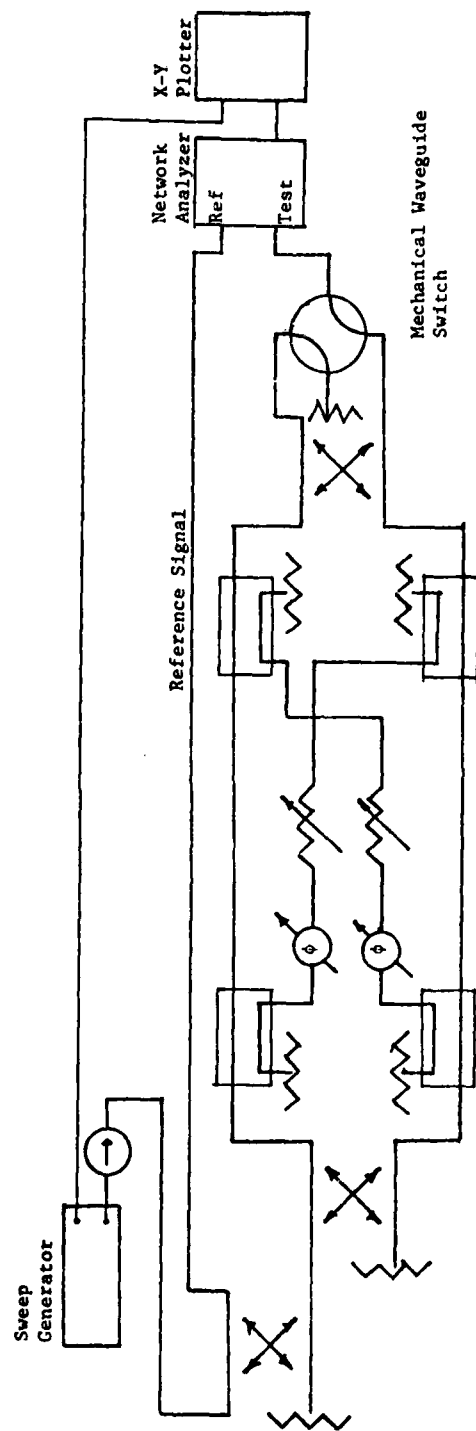
Figure 20. Microwave improvement network as tested.

have determined that, unless the waveguide lengths on all arms are exactly the same, the network has far to narrow a bandwidth to be of use. Furthermore, for reasonable values of coupling and attenuation wherein the actual transmitter power is considered, little isolation improvement is realized.

Another form of microwave improvement device consisting of various shorted matching stubs similar to that employed in the Alberta radar can be constructed from waveguide and waveguide tee junctions. To be effective, these stubs require a precise length and location which are a function of the magnitude and phase angle of all reflections within the microwave package; obviously then the length, location, and number of stubs can be determined only after the characteristics of the other microwave components are determined. Then by resorting to the intimacies of a Smith Chart, it is theoretically possible to achieve a perfect match (1.0:1 VSWR) and the attending isolation at a single frequency at the expense of lessor isolation at all other frequencies.

4.2.3 HIGH POWER RADIO FREQUENCY SWITCH

The radio frequency (RF) switch is the only other device currently thought to limit the performance of this modification as its isolation requirement must be equal to or better than the two-way ICR specification. To date, only a -33 dB isolation between output ports has been achieved in a K_u-Band device; however, three ferrite switch manufacturers are of the opinion that a -35 dB isolation is possible, and another manufacturer contends that a diode switch with this isolation is achievable.

The basic high speed waveguide switch employs a configuration of phase shifters, magic tee, and short slot hybird (Figure 21) so that the switching of transmitted energy between output ports is achieved by appropriate setting of the phase shifters. Reception of backscatter is also available with the orthogonal polarizations in the respective E and H arms of the

92
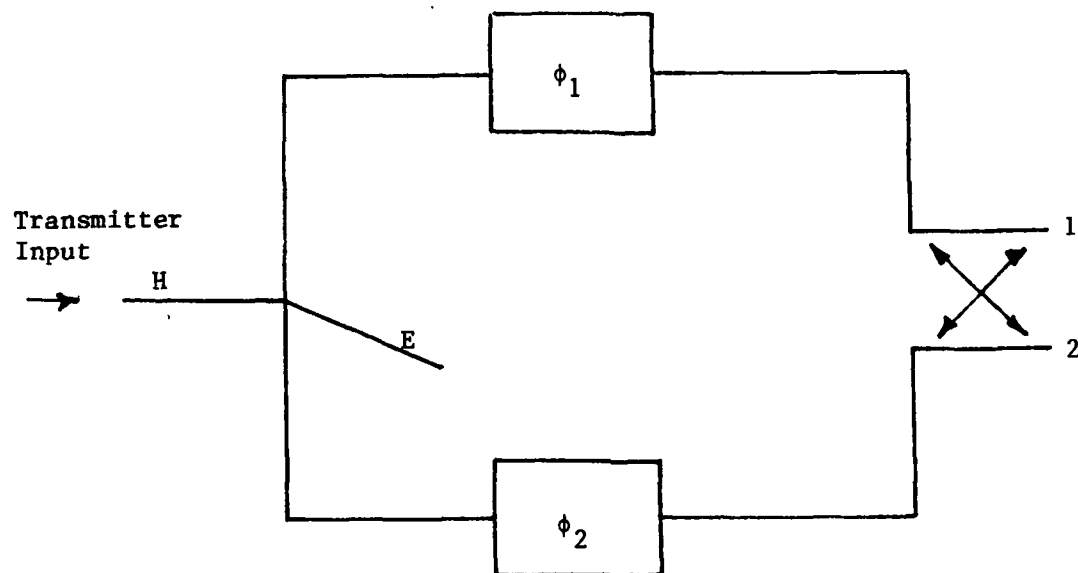
Phase Shifter Setting	Transmitted Energy Exit Point
ϕ_1 +45 deg.	
ϕ_2 -45 deg.	2
ϕ_1 -45 deg.	
ϕ_2 +45 deg.	1

Figure 21.   Basic high speed radio frequency switch.

magic tee. Although each of the ferrite designs is different, two manufacturers, Electromagnetic Sciences and Premiere Microwave Corporation (manufacturers names and addresses are given in Appendix B), have essentially the same approach to realizing the isolation requirement; three switches connected in a series parallel configuration are proposed. Raytheon, on the other hand, intends to emulate the previous successful approach of the K_u-Band switch, wherein a microprocessor based update network will sample the main and isolated ports and upon a prearranged schedule adjust the current in each of the phase shifters to correct for isolation deficiency. Since all variations employ a hybrid coupler in their design, the isolation limitation is a function of our nemesis, VSWR; in this case, both external and internal to the switch. Therefore, not only must the VSWR presented by each port of the switch be tightly specified so that isolation of the polarizer can be guaranteed, but the VSWR seen by each port of the switch must also be carefully controlled.

The power requirements of the switch just exceeded those which might lower its procurement cost. The peak and average powers presented to the switch are given by the transmitter output less an expected waveguide and microwave component loss of 1.9 dB (Table 8); however, if a least loss case of neglecting the rotary joint attenuation is assumed, then the maximum power output expected at the switch is 0.81 MW, with an average power 1.32 W, which exceeds by 2 dB a lower construction cost 500 W ferrite switch. Atlantic Microwave also expressed similar reservations due to the cost of components for their proposed 1.0 MW diode switch and implied that a 500 W unit may be offered at a considerable cost reduction. It is therefore suggested that a reduced power output be considered as an option within the RFQ issued for this device.

Another option exists within the design framework of each ferrite phase shifter, which trades switching time and drive

94

TABLE 8. LOSS IN TRANSMISSION LINE OF S-BAND AFGL WEATHER RADAR

ITEM	LOSS	
High Power Diplexer	0.46 dB	*
Azimuth Rotary Joint	0.10 dB	
Elevation Rotary Joint	0.10 dB	
Waveguide	0.94 dB	
Circulator	0.30 dB	*
	1.90 dB	

* measured value

power requirements versus insertion loss. According to Raytheon,[47] two phase shifter designs exist at this power level; a marginal design capable of phase change in less than 2 microseconds and a slower design with switching times approaching 0.1 milliseconds which may offer less loss and greater power handling abilities. Switching time is mandated by the greatest range of operation as transmitted polarization cannot be altered until the final expected return cell has passed into the receiver. From a rudamentary calculation, it does not appear that microsecond switching speed is necessary, but a final determination based upon the transmitter as well as processing requirements must be considered.

Finally the consideration of a mechanical switch should be broached. Of the varieties that exist, none can approach the switching time or other performance characteristics of an electronic device. Shutter switches are in the 10 millisecond region, rotary switches are an order of magnitude slower, and the most ingeneous fast rotating devices do not afford the liberty of variable PRF and cannot attain the sufficiently low VSWR demanded by the polarizer.

4.2.4 OTHER MICROWAVE COMPONENTS

Two additional microwave components exist in the microwave package, the circulator and the transmit/receive (TR) switch. While phase versus temperature measurements have previously been considered within this subsection, no phase or amplitude balance information has been ascertained for the TR switch-limiter assemblies. According to the manufacturer, Microwave Associates of Burlington, Masschussetts, 1.0 degree phase tracking and 0.1 dB amplitude balance cannot be assumed. Georgia Tech advocates that a complete set of phase balance, amplitude balance, and VSWR

---

47   D. Milne, manager Ferrite Devices Division, Raytheon Co., Northborough, MA, personal communication, 1981.

versus temperature measurements be completed for these existing devices before they are incorporated into the radar modification.

As a final recommendation of the microwave package, Georgia Tech urges that only copper waveguide with similar metal flanges and elbows (i.e., brass) be employed so that dissimilar metal corrosion from the slightly salt atmosphere will not be experienced and the thermal expansion will be less than that experienced by of aluminum waveguide.

4.3 RECEIVER

The suggested receiver (Figure 18) consisting of four subassemblies will be discussed through, but not including, the processor. Critical phase and amplitude balance is maintained throughout by careful component selection, thermal control as the receiver is physically located wthin the microwave package container, and phase/amplitude trimmer assemblies inserted at strategic locations. Gross phase and amplitude mismatch errors will be eliminated in software via a look-up table. While this design has retained a maximum of present components as well as present operating features, the reader will notice that some existing hardware is altered to either maintain phase and amplitude balance or to improve inter-channel isolation.

4.3.1 GENERAL RECEIVER REQUIREMENTS
4.3.1.1 Channel-to-Channel Isolation

This last point must not be ignored because, as the system isolation is weakened beyond a certain point, overall performance will suffer. Choosing as a goal a maximum of 10% data corruption and utilizing the full 35 dB isolation offered by the antenna feed assembly, then the minimum channel-to-channel isolation must be 45 dB. This value confirms that of McCormick[48] who observed

---

48 G. C. McCormick, National Research Council of Canada (retired) Granville Ferry, Nova Scotia, Canada, personal communication, 1981

data corruption as the isolation of the NRC K_u-Band radar receiver deteriorated to 45 dB; he suggested that to avoid a conspicuous data error a minimum 55 dB isolation is necessary. Three deisolation mechanisms exist: (1) cross coupling in the local oscillator channel (subsection 4.3.1), (2) coupling via faulty coaxial cables, and (3) coupling via the DC power lines. Coupling via faulty coaxial cables can be reduced by employing only copper semi-rigid cables and utilizing a layout which places high level components as far as possible from low level components. In the case of the latter, it is recommended that the layout follow the relative component placement of the block diagram. Power supply coupling can be reduced by having a separate power supply for each receiver channel, by careful anodizing of the aluminum enclosure, and by insisting that insulated wire, not the enclosure, carry return currents; in no case should a cable shield be employed as a component "ground" or return.

4.3.1.2 Noise Figure

Noise figure is a measure of overall system sensitivity. Sensitivity can be defined as the minimum signal above the noise floor from which usable data is proccessable. Since the noise figure of a system specifies the system's internal noise, for other fixed overall receiver parameters, an improvement in noise figure results in an improvement in sensitivity. A low system noise figure is important as improvement in noise figure provides the same improvement as a likewise increase in transmitter power at a considerably reduced cost.

The noise power level of a beamfilling weather radar is related to the source temperature and the receiver effective temperature by

$$W_n = K_b \, B(T_s + T_{eff}),$$
(42)

where: K_b = Boltzmann's constant

$\quad\quad\quad$ = 1.38×10^{-23} Joules/K°

$\quad\quad$ B = effective receiver bandwidth and

$\quad\quad$ T_s = source temperature.

The noise figure of an amplifier is defined by IEEE Standard 62IRE.7.S2 adopted in 1962 with respect to 293°K as

$$NF = 10 \log \left(\frac{T_{eff}}{293} + 1 \right) , \quad\quad\quad (43)$$

with the quantity in brackets also known as noise factor. Combining Equations (42) and (43), we have the overall noise floor,

$$\text{Noise floor} = 10 \log \left\{ K_b B - T_s + 293 \left[\log^{-1} \left(\frac{nf}{10} \right) - 1 \right] \right\}. \quad (44)$$

It can be seen from Equation (44) that, for situations where $T_s = 0(T_{eff})$, improvements in noise figure yield slightly better improvements in overall sensitivity than would be expected from the noise figure improvement alone, so that a noise floor of -109.2 dBm/MHz is expected from the observation of ice clouds at -40°C (223°K) with an overall 5 dB noise figure, while a 3 dB improvement in overall noise figure will result in a noise floor of approximately -112.7 dBm/MHz; this is equivalent to more than a doubling of radar range. Another factor which will contribute to sensitivity degradation in the superhetrodyne receiver is reception of the other mixer sideband. Since its bandpass characteristics are identical to the desired sideband, it contributes 3 dB of noise. The unwanted sideband can be suppressed either by a preselector located either prior to the front-end low noise amplifier or between the amplifier and the mixer, or by a sideband suppression mixer. If a preselector is located prior to the amplifier, it adds a front-end insertion loss which is equivalent to an increase in noise figure by the

99

value of the insertion loss. Usually, however, the preselector loss is only on the order of 1 dB, so that an overall improvement results. On the other hand, if a preselecting filter is placed between the amplifier and the mixer, little sensitivity degradation will result due to the preselection insertion loss as the overall receiver noise figure is normally determined by the receiver preamplifier and the losses associated with the circuitry between the antenna and the receiver. While this location is appealing by sensitivity considerations alone, it does not offer preselection of those out-of-band signals which might cause receiver overload (subsection 4.3.1.3). A sideband suppression mixer also suffers this fault as well as affording the minimal preselection of the mixer. However, in order to preserve the phase characteristics of the receiver (Section 4.3.1.4) a sideband suppression mixer may be the preselector of choice.

4.3.1.3 Dynamic Range

Two definitions of dynamic range exist: (1) overall dynamic range defined as the operating range of the receiver from the noise floor to the 1 dB compression point, and (2) the spurious free dynamic range (SFDR) defined as the operating range from the noise floor up to a power level at which spurious signals are processable. By reviewing the expected return energy for each form of hydrometeor (Figures 3 to 7) and assuming a minimum radar range of 1 kilometer, the required receiver 1 dB compression point can be determined. From the further assumptions of a transmitter level of +88 dBm and two-way antenna gain of +84 dB, the maximum expected signal at the receiver input becomes approximately -8 dBm.

In the general case of a linear receiver, or for those receivers which contain logarithmic amplifiers, signal compression usually first occurs in the RF or IF preamplifier stages. Care must be exercised to determine the correct choice

of these components as: (1) the 1 dB compression point defined as the point at which 1 dB of nonlinearity is observed at the amplifier output for a linear increase in signal level at the amplifier input is an order of magnitude more coarse than our requirement. As a rule of thumb, the 0.1 dB compression point (the linearity requirement for this modification) is approximately 10 dB less than the 1 dB compression point; (2) most amplifier manufacturers define the 1 dB compression point as an output value; therefore, the system designer must be careful to subtract the amplifier gain from this value so that the 1 dB compression point may be referenced to the amplifier input.

Utilizing a 4 MHz bandpass (subsection 4.3.1.4), this design requires a dynamic range extending from the noise floor of -107 dBm to a 1 dB compression point of +2 dBm, or approximately 109 dB. A dynamic range of this magnitude is impossible to achieve, so that surreptitious methods must be undertaken to expand the receiver's dynamic range. Generally, an automatic gain control (AGC) voltage is available to reduce the RF and IF amplifier gain as the return signal level is increased, however, AGC removes the power level measurement capabilities of the receiver. One method to circumvent this situation is to calibrate and monitor an AGC voltage while the receiver circuitry attempts to maintain a constant output level. This method is prone to error at the upper and lower limits of input signal. Another method, chosen for this design, circumvents the limited receiver dynamic range by minimizing the RF amplifier gain and electronically removing the IF preamplifier when the expected return approaches receiver compression; the computer is cognizant of this condition and adjusts its processing accordingly.

The dynamic range of a receiver is also limited by spurious responses which are accepted by the processor. Two sources of spurious responses exist: (1) internally generated signals as a result of totally external sources and (2) IF responses that are the products of unwanted local oscillator signals and external sources.

Amplifier spurious response generation results from the internal products of harmonic frequencies which are, in turn, internally generated. In the case of this modification, only a few spurious frequencies or intermodulation products (IMP) are created in the low noise amplifier that are receptive by the mixer. Those products are given by[49]

$$f_{spur} = \pm nf_1 \pm mf_2, \text{ where } n,m \text{ are integers.} \tag{45}$$

For the frequencies of operation of 2710 and 2760 MHz, only those values for $n,m = 1,2$ are receptable as shown in Table 9. In most single frequency receivers, the spurious responses are of no concern if a signal of opportunity does not exist at a reponsive frequency. However, if an examination of the receptable frequencies by the mixer is undertaken (Table 10), a possible corruption of power channel by velocity channel data, and vice versa, does exist as the spurious frequency generated from one channel is in the nearby spectrum receivable by the other channel. To determine if a processable cross-channel signal level exists, a fourier transform of the transmitted pulse shape must be undertaken so that the return energy level within the cross-channel bandpass can be calculated, following which the IMP response level of the low noise amplifier must be ascertained. At present, the exact pulse shape is unknown so that this calculation can only be approximated. In the next subsection (4.3.1.4), a worst case approximation and IMP elimination by IF filtering is considered. The IMP response also can be eliminated by connecting a preselector before the low noise amplifier, but this will result in an increased phase uncertainty and phase dispersion as well as a slight sensitivity reduction. Therefore,

---

49   F. C. McVay, "Don't Guess the Spurious Level," _Electronic Design_, Vol. 3, 1 February 1967, pp. 70-73.

TABLE 9. SPURIOUS FREQUENCIES GENERATED WITHIN THE LOW NOISE
AMPLIFIER FROM HARMONIC FREQUENCIES

	Harmonic Frequency		Spurious Frequency	
N,M	Nf_1	Mf_2	$2f_1 - f_2$	$2f_2 - f_1$
1	2710 MHz	2760 MHz	2660 MHz	2810 MHz
2	5420 MHz	5520 MHz		

Table 10. FREQUENCIES RECEIVABLE BY MIXER.

Local Oscillator Frequency	
LO_1	LO_2
2680 MHz	2790 MHz
2710 MHz	2760 MHz
2650 MHz	2820 MHz

it is suggested that a frequency spectral analysis of the transmitter output be performed prior to receiver finalization with consideration given to the tradeoff between spurious response and phase uncertainty data corruption.

Further spurious responses which require consideration exist within this design. Because of the phase tracking accuracy requird by this radar, a master oscillator/final amplifier transmitter with associated phase locked loop oscillators is employed; identical oscillators are also utilized in the local oscillator chain. This type of oscillator is notoriously rich in spurious response generation not only at the output frequency plus or minus the reference oscillator frequency, but also at other unrelated frequencies. Since these levels are sufficiently intense (-72 dBC) to activate additional reception of unwanted signals, a high Q cavity filter should be placed between the local oscillator and the mixer to reduce unwanted reception.

4.3.1.4 IF Filter

The IF filter fulfills two missions: it limits the overall system noise figure by determining system bandwidth, and it provides the required selectivity. Exact choice of an IF filter is not a trivial task as the filter together with the RF amplifier essentially determines the total receiver performance. An acceptable video halfpower bandwidth is 1.2 times the transmitted pulse width, to fully receive an amplitude modulated signal the IF bandwidth must be twice the video halfpower bandwidth, or in this design 2.4 MHz. However, it will be shown that a minimum halfpower IF bandwidth of 4 MHz is required for this receiver. First, it is necessary to determine the filter skirt selectivity requirement.

The importance of filter skirt selectivity cannot be overstressed; many designs do not extend filter specifications beyond the bandwidth of the halfpower points which in no manner specifies the attenuation provided at frequencies further deviant

from the center frequency. Consider the intermodulation products which can be generated within the RF amplifier and appear as an image signal to the mixer to be down converted into the IF bandpass. The degree of data corruption caused by these IMP depends on many factors such as the range, type of hydrometeors observed, the spectral distribution of the transmitter pulse, and the intended purpose of the measurement. If one were to assume a rectangular one microsecond transmitter pulse, then the relative magnitude of the intruding IMP can be understood. Since only 10 MHz separates the intermediate frequency and IMP signals at the output of the mixer, it can be seen from Table 11 that relatively intense signals have the potential to exist on the filter skirts and even within the filter passband.

Before proceeding, we must show that both the Doppler and power channel return pulses can occur simultaneously at all four mixers. This condition takes place whenever two precipitation cells separated by $c\tau/2$ exist along the axis of the antenna, where τ is the power transmitter to Doppler transmitter inter-pulse spacing. Next we review the specifications of the existing LNA (Table 12) to determine the minimum return signal necessary to create a third order IMP. With a 4 MHz halfpower IF bandwidth, the output noise floor given by observing cool precipitation is approximately -77 dBm, so that with a 25 dB intercept point, a -9 dBm signal (-39 dBm into the amplifier) is required to generate an IMP at the noise floor (Figure 22). Since a 1 dB increase in input level will cause a 3 dB increase in output level for third order IMP, a -38 dBm return into the receiver will begin to cause data corruption if the signal is allowed to enter the IF amplifier and detector network. When the total path loss including backscatter loss is less than the additive values of transmitter power (88 dBm), two-way antenna gain (84 dB), and the value at which data corruption is viable, the received energy will support IMP. From a review of Figures 3 and 4, it can be seen that a return signal exceeding this amount

TABLE 11. RELATIVE LEVEL OF SPECTRAL SIDELOBES OF A
RADAR EMPLOYING A 1.0 μs RECTANGULAR PULSE

Frequency (MHz)	Relative Power of Lobe Peak
f_o	reference
± 1.5	-13.5 dB
± 2.5	-17.9
± 3.5	-20.8
± 4.5	-23.0
± 5.5	-24.8
± 6.5	-26.2
± 7.5	-27.4
± 8.5	-28.5
± 9.5	-29.5
± 10.5	-30.4

TABLE 12. MICROMEGA LOW NOISE AMPLIFIER SPECIFICATIONS

NOISE

Gain 30 dB

Noise Temperature 90°K

Intercept Point +25 dBm (output)

1 dB Compression Point +15 dBm (output)
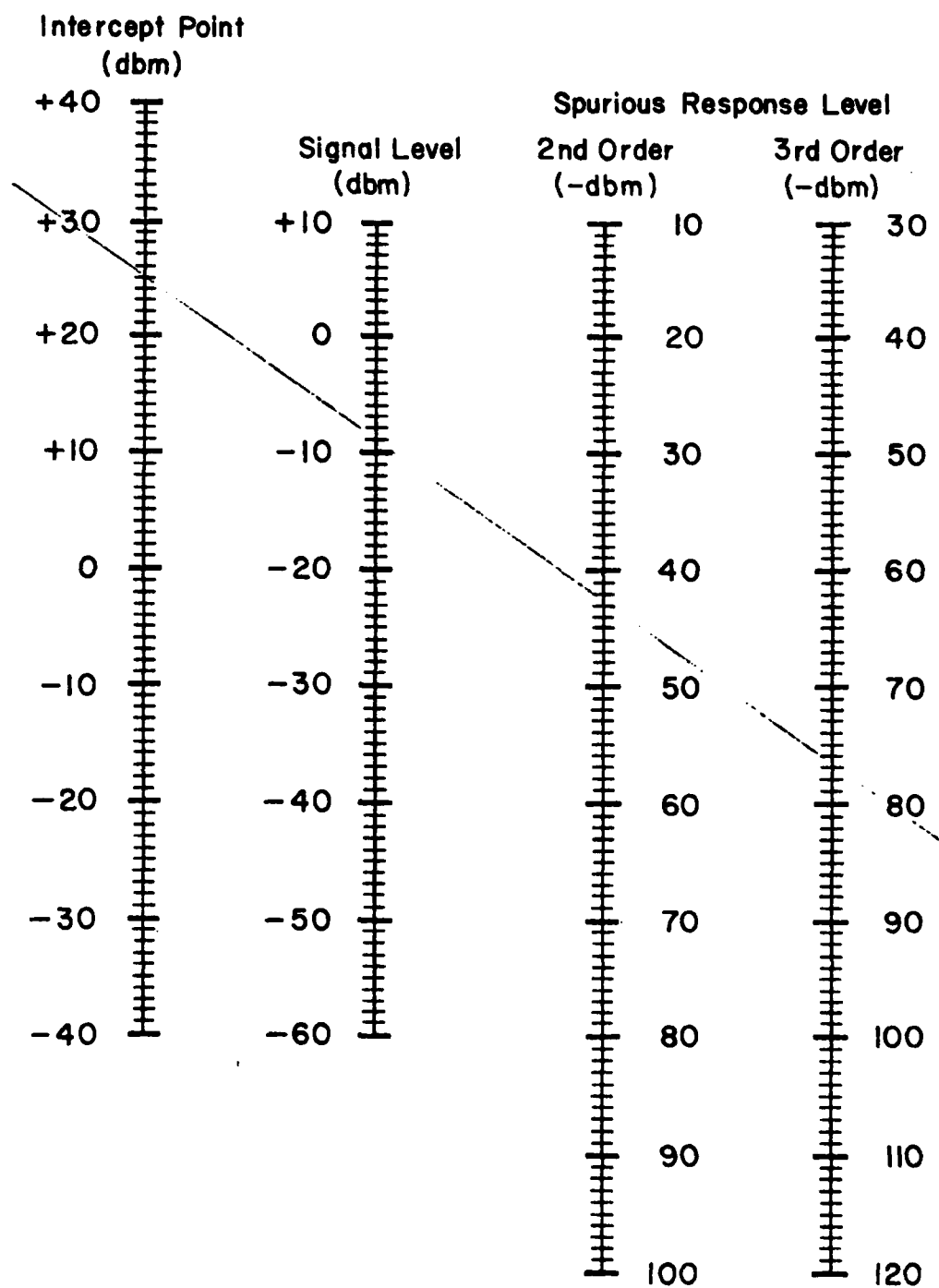
Figure 22. Intermodulation distortion nonograph.
From Electronic Design, 1 Feb. 1967.
The diagonal line indicates the conditions at which
intermodulation distortion exists at the noise floor
for the LNA.

can be infrequently expected. The elimination of this IMP then depends upon correct choice of interpulse spacing τ or filter selectivity; should control of τ be impractical, then the filter skirt selectivity must be chosen so that the interfering pulse "sidebands" detailed in Table 10 are attenuated into the noise. This condition may not be possible as good skirt selectivity and phase dispersion are divergent from one another in discrete component planar filters.

Three varieties of these filters exist: Chebishev, Butterworth, (the limiting case of Chebishev with zero passband amplitude ripple) and Elliptic. In the case of the former, two fundamental designs exist: flat amplitude ripple or flat phase ripple across the passband. Another variable of the filter is shape factor for which, among its various definitions, a useful definition is the ratio of the -60 dB bandwidth to the -3 dB bandwidth. If we wish to attenuate the main lobe of the IMP by 60 dB, the required shape factor is 2.5. The theoretical maximum attenuation with an infinite number of elements, flat phase design filter, for this shape factor is an insufficient 23 dB[50]. A flat amplitude ripple design with a shape factor of 2.5 requires a minimum of 6 poles and will experience an intolerable 100 degree phase dispersion across its 3 dB bandwidth. Although designs with lesser number of elements (with lesser phase dispersion) are given in the reference, they are unrealizable due to the high component Q requirment. Flat amplitude filters can be matched to each other to provide an overall phase error of 1 degree, but without an external compensation network such matching is only practical within ±0.6 of the halfpower bandwidth[51], so that a 4 MHz half power bandwidth is then

---

50 Reference Data for Radio Engineers, VI Edition, (Indianapolis, Indiana: Howard W. Sams and Co. Inc., 1975) pp. 8-17.
51 Ibid, Figure 4.

required to provide adequate phase tracking over a 2.4 MHz bandwidth. A comparison of these filters with the class of filters described by Bessel functions, also known as Elliptic filters, "shows very small deviation between the two cases"[52]. Four options exist then for the choice of filter and reduction of IMP: (1) choose a discrete element design and attempt to reduce phase dispersion by attaching a phase equalizing network, (2) consider a non-planar design such as a SAW filter, (3) raise the intermediate frequency so that the IMP is sufficiently removed from the IF passband to be severely attenuated, or (4) carefully adjust τ and the radar PRF so that the IMP signal is not created within the amplifier.

4.3.2 INDIVIDUAL RECEIVER SECTIONS, INCIDENTAL NOTES
4.3.2.1 Diplexer

In the previous subsection, the demands of the preselector and LNA were demonstrated. Little information can be added concerning the reciever "front-end", save a note on the diplexer. This device should be capable of a minimum of filtering; its primary function is to provide isolation between the receiver channels. The reader should be aware that many diplexers are constructed of high pass/low pass filters and as such will afford no attenuation for large bands of frequencies as well as provide minimal attenuation within 15 percent of the "split" frequency; such devices could be replaced by a less costly hybrid coupler. The proper diplexer must contain two bandpass filters which are a compromised design between low phase dispersion and reasonable skirt selectivity.

---

52 M. S. Ghausi, Principles and Design of Linear Active Circuits, (New York, NY: McGraw-Hill Book Co., 1965).

4.3.2.2 Local Oscillator and Mixer

The local oscillator chain retains all of the present components while adding additional components to provide increased isolation, phase balance, and amplitude balance. The increased losses of these items require a slight amplification of the local oscillator signal level so that the mixers will be operated in their lowest distortion region. By additionally increasing this amplification, high intercept point mixers can be employed with the result that the overall receiver intercept point (or 1 dB compression point) is wholly determined by the RF amplifier. To maintain coherency the original radar utilized phase locked loop oscillators, a filter following this oscillator is required to reduce the high spurious output of the oscillator from entering the mixer as these spurious responses will allow the receiver to capture unwanted signals. Since spurious signals occur within 600 kHz of the local oscillator frequency, only a high Q, thermally stable, cavity filter is indicated. Isolation of reflected energy between this filter and oscillator is also necessary to prevent oscillator "pulling" and generation of additional spurious responses.

4.3.2.3 IF Amplifier and Filter

Because of the expected high level of return energy for some targets and because AGC cannot be used, disconnecting the IF preamplifier for intense returns to achieve an additional 20 dB of dynamic range has been proposed. Additionally, a small attenuator is to be employed prior to the logarithmic amplifier in this mode of operation to optimize the overall dynamic range as well as provide channel-to-channel amplitude balance. The function of the attenuator shown between the bandpass filter and the IF preamplifier in the more sensitive mode of operation is to prevent IF preamplifier oscillation and pulse ringing that has been observed in past designs. This attenuator could also be optimized to maximize the dynamic range.

110

4.3.2.4 Phase Detection and Video Amplification

The proposed phase detector is only conceptually shown and may not be the detection scheme of choice. The video amplifiers however are a proven Georgia Tech design and not only have internal compensation for the amplitude dispersion of the long coaxial cable run to the data processor but also have sufficient output to overcome the losses imposed by the smaller coaxial cables.

SECTION 5
SUMMARY & RECOMMENDATIONS

This section summarizes in Tables 13-16 the technical design requirements of the polarization diversity modification to the AFGL S-band Doppler weather radar; within these tables is also the reasonable level of expected performance.

Recommended components to achieve these characteristics are listed in Appendix A.

TABLE 13.   SUMMARY OF SYSTEM REQUIREMENTS

Integrated cancellation ratio (ICR)	-35 dB min
Allowable error in ICR	3 dB max
Maximum expected ICR	-37 dB
Integration limits of ICR	through 2nd copolarized sidelobe
Integrated cross-polarization ratio (ICPR)	-23 dB min
Maximum expected ICPR (based upon component VSWR)	-30 dB
Allowable error in differental reflectivity	0.1 dB
Antenna overall VSWR	$\leq$ 1.025:1
Microwave package overall VSWR	consistent with isolation
Overall phase tracking error	$\leq$ 1.0 degree
Overall amplitude tracking error	
scattering matrix measurement	$\leq$ 0.23 dB
differential reflectivity measurement	$\leq$ 0.10 dB

TABLE 14.   SUMMARY OF ANTENNA REQUIREMENTS

Requirement	Recommendation
Antenna configuration	Cassegrain with f/D ≈ 0.6
Number of support spars	4
Support spar cross-section	Circular
Feed/polarizer supports	Entire assembly must be covered by axisymetric shroud
Secondary reflector	Hyperbola with center half-conical section
Secondary reflector pattern taper	About -10 dB on reflector edges
Feed antenna	Corrugated horn
Feed antenna VSWR	≤ 1.025:1
Polarizer	Sloped septum
VSWR at polarizer	≤ 1.05:1
Anticipated ICR	-35 dB
Anticipated ICPR	Better than -25 dB

TABLE 15. SUMMARY OF MICROWAVE PACKAGE REQUIREMENTS

RF Switch isolation	output arms	35 dB min
	input arms	35 dB min
RF switch VSWR	ports towards antenna	1.05:1 max
	ports towards transmitter	consistent with
	and receiver	isolation req't
Improvement package		as required
Waveguide material		copper WR284
Temperature of operation		43°C ± 1/2°C
Recommended components		see Appendix A

TABLE 16. SUMMARY OF RECEIVER REQUIREMENTS

Phase stability	$\leq$ 1.0 deg
Amplitude stability	$\leq$ 0.1 dB
Dynamic range	109 dBm
Spurious free dynamic range	TBD
Noise floor inc. microwave pkg. loss	-106 dBm
Temperature of operation	43°C
Recommended coaxial cable	0.141" Dia. semirigid
Recommended component connectors	APC-7 or APC-3.5
Recommended components	see Appendix A

REFERENCES

1. Skolnik, M. I., Radar Handbook, pp. 2-4, New York, NY: McGraw-Hill, 1970.

2. Metcalf, J. I., Holm, W. A., Bodnar, D. G., Martin, E. E., Trebits, R. N., and Steinway, W. J., "Design Study for a Coherent Polarization-Diversity Radar," Georgia Institute of Technology, Engineering Experiment Station, AFGL-TR-80-0262 Air Force Geophysics Laboratory, 1980, AD A096757.

3. Ibid

4. Ibid

5. Dwight, H. B., Tables of Integrals and Other Mathematical Data, Fourth Edition, New York, NY: The Macmillan Co., 1969.

6. Probert-Jones, J. R., "The Radar Equation in Meteorology," Quart. J. Roy. Meteor. Soc., 88, 1960, pp. 485-495.

7. Metcalf, J. I., "Interpretation of Simlulated Polarization Diversity Radar Spectral Functions", submitted to Radio Science 1982.

8. Metcalf, et al., Op. cit.

9. McCormick, G. C., and Hendry, A., "Principles for the Radar Determination of the Polarization Properties of Precipitation," Radio Science, Vol. 10, No. 4, April 1975, pp. 421-434.

10. Metcalf, J. I., and Echard, J.D., "Coherent Polarization-Diversity Radar Techniques in Meteorology," Journal of the Atmospheric Sciences, Vol. 35, No. 10, October 1978, pp. 2010-2019.

11. Cohen, M. H., "Radio Astronomy Polarization Measurements," Proc of IRE, Vol. 46, Jan. 1958, pp. 172-182.

12. Kraus, J. D., Radio Astronomy, New York, N.Y.: McGraw-Hill, 1966, Chapter 4.

13. Jasik, editor, Microwave Antenna Handbook, See Section 17.8 by Offutt, Warren B.

14. Ibid

15. Allan, L. E., Markell, R. C., and McCormick, G. C., "A Variable Polarization Antenna," National Research Council of Canada Publication ERB-768, June 1967.

16. Jasik, Op. cit.

17. J. I. Metcalf, personal communication, 1982

18. Seliga, T. A., and Bringi, V. N., "Potential Use of Radar Differential Reflectivity Measurements at Orthogonal Polarizations for Measuring Precipitation," Journal of Applied Meteorology, Vol. 15, January 1976, pp. 69-76.

19. Bringi, V. N., Seliga, T. A., and Mueller, E. A., "First Comparisons of Rain Rates Derived from Radar Differential Reflectivity and Disdrometer Measurements," IEEE GE-20 No. 2, April 1982, p. 201.

20. Seliga and Bringi, Op. cit.

21. Ibid

22. Metcalf, J. I., "Theory and Experimental Concepts for Coherent Polarization-Diversity Meteorological Radar," Georgia Institute of Technology, Engineering Experiment Station, Project B-529 Final Report, 30 September 1980.

23. Krehbiel, P. R., and Brook, M., "Coherent, Dual Polarized Observations of the Radar Return from Precipitation," submitted to Radio Science, 1982

24. McCormick, G. C., and Hendry, A., "Polarization Properties of Transmission Through Precipitation ,Over a Communication Link," Journal De Recherches Atmospheriques, 8 1974, pp. 175-187.

25. Silver, S., Ed., Microwave Antenna Theory and Design, New York, NY: McGraw-Hill, 1949, pp. 417-423.

26. Condon, E. V., "Theory of Radiation from Paraboloid Reflector Antennas," Westinghouse Report No. 15, 1941.

27. Jones, E. M. T., "Paraboloid Reflector and Hyperboloid Lens Antennas," IRE Transactions - Antennas and Propagation, Vol. AP-2, July 1954, pp. 119-127.

28. Watson, P. A., and Ghobrial, S. I., "Off-Axis Polarization Characteristics of Cassegrain and Front-Fed Paraboloidal Antennas," IEEE Transactions on Antennas and Propagation, Vol. AP-20, No. 6, November 1972, pp. 691-698.

29. Ghobrial, S. I., and Futuh, M. M., "Cross-Polarization in Front-Fed and Cassegrain Antennas with Equal f/D Ratio," 1976 Region V IEEE Conf. Digest, April 1976, p. 277.

30. Ludwig, A. C., "The Definition of Cross-Polarization," IEEE Transactions on Antennas and Propagation, Vol. AP-21, No. 1, January 1973, p. 116-119.

REFERENCES (continued)

31. Dijk, J., van Diepenbeek, C. T. W., Maanders, E. J., and Thurlings, L. F. G., "The Polarization Losses of Offset Paraboloid Antennas," IEEE Transactions on Antennas and Propagation, Vol. AP-22, No. 4, July 1974, pp. 513-520.

32. Potter, P. D., "Application of Spherical Wave Theory in Cassegrainian-fed Paraboloids," IEEE Transactions on Antennas and Propagation, November 1967, pp. 727-736.

33. Ghobrial and Futuh, Op. cit.

34. Silver, Op. cit.

35. Ghobrial, S. I., "Off-axis Cross-Polarization and Polarization Efficiencies of Reflector Antennas," IEEE Transactions on Antennas and Propagation, Vol. AP-27, No. 4, July 1979, p. 460-466.

36. Wood, P. J., Reflector Antenna Analysis and Design, IEE, London and New York, 1980.

37. Ibid

38. Wilkinson, E. J., and Burdine, B. H., "A Low Sidelobe Earth Station Antenna for the 4/6 GHz Band," GTE International Systems Corp. Report, 1980.

39. Bodnar, D. G., Cofer, J. W., and Alexander, N. T., "Computer-Aided Design of Scanning Reflector Antennas," 1974 AP Symposium, Atlanta, Georgia.

40. Jones, Op. cit.

41. Davis, D., Digiondomenico, O. J., and Kempic, J. A., "A New Type of Circularly Polarized Antenna Element," Symposium Digest, 1967 G-AP, pp. 26-33.

42. Ming Hui Chen and Tsandoulas, G. N., "A Wide-Band Square-Waveguide Array Polarizer," IEEE Transactions on Antennas and Propagation, Vol. AP-21, May 1973, pp. 389-391.

43. Rootsey, J. V., "Tapered Septum Waveguide Transducer," U.S. Patent No. 3,958,193, May 18, 1976.

44. Nelson, E. A., "Polarization Diversity Array Design (PDAD)," General Electric Co., Aerospace Electronic Systems Dept., Utica, NY, March 1972.

45. Wilkinson and Burdine, Op. cit.

46. Hollis, J. S., Hickman, T. G., and Lyon, T. J., "Polarization Theory," Microwave Antenna Measurments Handbook, Chapter 3, 1970, Scientific Atlanta, Atlanta, Ga.

47. D. Milne, manager Ferrite Devices Division, Raytheon Co., Northborough, MA, personal communication, 1981.

48. McCormick, G. C., National Research Council of Canada (retired) Granville Ferry, Nova Scotia, Canada, personal communication, 1981.

49. McVay, F. C., "Don't Guess the Spurious Level," _Electronic Design_, Vol. 3, February 1, 1967, pp. 70-73.

50. _Reference Data for Radio Engineers_, VI Edition, Indianapolis Indiana: Howard W. Sams and Co. Inc., 1975, pp. 8-17.

51. Ibid, Figure 4.

52. Ghausi, M. S., _Principles and Design of Linear Active Circuits_, New York, N.Y.: McGraw-Hill, 1965.

BIBLIOGRAPHY

Bickel, S. H., "Some Invariant Properties of the Polarization Scattering Matrix," IRE Transactions - Antennas and Propagation, August 1965, pp. 1070-1072.

Bodnar, Donald G., "Cross-Polarized Characteristics of Monopulse Difference Patterns," Universite' Laval, Québec, Canada, 1980 International Symposium Digest, Volume II, IEEE Antennas and Propagation, pp. 477-480.

Boerner, Wolfgang M., "Use of polarization in electromagnetic inverse scattering," Radio Science, Vol. 16, No. 6, November-December 1981, pp. 1037-1045.

Bringi, V. N., Seliga, T. A., and SriRam, M. G., "Statistical Characteristics of the kDifferential Reflectivity Radar Signal," 19th Conference on Radar Meteorology, Am. Met. Soc., April 15018, 1980, pp. 692-696.

Chu, Ta-Shing, and Turrin, R. H., "Depolarization Properties of Offset Reflector Antennas," IEEE Transactions on Antennas and Propagation, Vol, AP-21, No. 3, May 1973, pp. 339-345.

Cohen, Marshall H., "The Cornell Radio Polarimeter," Proc. IRE, Vol. 46, January 1958, pp. 183-190.

Collin, Robert E., Foundations for Microwave Engineering, New York, NY: McGraw-Hill, 1966.

Copeland, J. R., "Radar Target Classification by Polarization Properties," Proc. IRE, July 1960, pp. 1290-1296.

"Engineering Study of Radar Modifications For Dual-Polarization Meteorological Measurements," Proposal No. RI-RAD-1052, Georgia Institute of Technology, Engineering Experiment Station, 28 April 1980.

Evans, J. V., and Hagfors, T., "Study of Radio Echoes from the Moon at 23 Centimeters Wavelength," Journal of Geophysical Research, Vol 71, No. 20, October 15, 1966, pp. 4871-4889.

Gent, H., Hunter, I. M., and Robinson, N. P., "Polarization of radar echoes, including aircraft, precipitation and terrain," Proc. IEE, Vol. 110, No. 12, December 1963, pp. 2139-2148.

Ghobrial, S. I., "Co-Polar and Cross-Polar Diffraction Images in the Focal Plane of Paraboloidal Reflectors: A Comparison Between Linear and Circular Polarization," IEEE Transactions on Antennas and Propagation, Vol. AP-24, NO. 4, July 1976, pp. 418-424.

Ghobrial, Samir I., "Cross-Polarization in Satellite and Earth-Station Antennas," Proc. IEEE, Vol. 65, No. 3, March 1977, pp. 378-387.

Hendry, A., and Allan, L. E., "Apparatus for the Real-Time Display of Correlation and Relative Phase Angle Data from the Alberta Hail Studies Radar," National Research Council of Canada, Radio and Electrical Engineering Division, Ottawa, Canada, January 1973.

Hood, A. D., and McCormick, G. C., "Radar for Study of Hailstorms," Bulletin of the Radio and Electrical Engineering Division, National Research Council of Canada, Vol. 17, No. 1, Ottawa, Canada, March 1967, pp. 13-19.

Jacobsen Johannes, "On the Cross Polarization of Asymmetric Reflector Antennas fo Satellite Applications," IEEE Transactions on Antennas and Propagation, March 1977, pp. 276-283.

Kauffman, J. F., Croswell, William F., Jowers, Leonard J., "Analysis of the Radiation Patterns of Reflector Antennas," IEEE Transactions on Antennas and Propagation, Vol. AP-24, No. 1, January 1976, pp. 53-65.

Keen, K. M., "A Measurement Technique for Modeling the Effects of Feed Support Struts on Large Reflector Antennas," IEEE Transactions on Antennas and Propagation, Vol. AP-28, No. 4, July 1980, pp. 562-564.

King, R. J., "Crossed-Dipole Method of Measuring Wave Tilt," Radio Science, Vol. 3 (New Series), No. 4, April 1968, pp. 345-350.

Kreutel, Randall W. Jr., DiFonzo, Daniel F., English, William J., and Gruner, Robert W., "Antenna Technology for Frequency Reuse Satellite Communications," Proc. IEEE, Vol. 65, No. 3, March 1977, pp. 370-377.

Kumar, Dr. Akhileshwar, "Reduce Cross-Polarization in Reflector-Type Antennas," Microwaves, March 1978, pp. 48-51.

Leung, S. K., "The Alberta Hail Project Radar Systems," Atmos. Sci. Rept. 77-4, Alberta Research Council, May 1977.

Levy, R., "Hybrid Junctions," Electronic & Radio Engineer, August 1959, pp. 308-312.

Long, M. W., "A Radar Model for Land and Sea," Prepared for Proceedings of the Open Symposium of URSI, La Baule, France, 28 April - 6 May, 1977, Appendix 1.

Martin, Alan G., "Short Backfire Antenna for Doppler Sensing," Microwave Journal, October 1981, pp. 93-96.

BIBLIOGRAPHY (continued)

McCormick, G. C., "An Antenna Designed for the Investigation of Precipitation Phenomena," Bulletin of the Radio and Electrical Engineering Division, National Research Council of Canada, Vol. 14, No. 4, Ottawa, Canada, December 1964, pp. 15-18.

McCormick, G. C., "An Antenna for Obtaining Polarization-Related Data with the Alberta Hail Radar," Proc. 13th Radar Meteor. Conf., Amer. Meteor. Soc., 1968, pp. 340-347.

McCormick, G. C., "Feed for a Spherical Reflector," Bulletin of the Radio and Electrical Engineering Division, National Research Council of Canada, Vol. 16, No. 4, Ottawa, Canada, December 1966, pp. 37-38.

McCormick, G. C., "Polarization Errors in a Two-Channel System," Radio Science, Vol. 16, No. 1, January-February 1981, pp. 67-75.

McCormick, G. C., and Hendry, A., "Techniques for the Determination of the Polarization Properties of Precipitation," Radio Science, Vol. 14, No. 6, November-December 1979, pp. 1027-1040.

McLyman, Colonel W. T., "28-Channel Rotary Transformer," Technical Support Package, Pasadena, Ca, Jet Propulsion Laboratory, NASA contract no. NAS 7-100, January 1981.

Metcalf, James I., "Propagation Effects on a Coherent Polarization-Diversity Radar," Radio Science, Vol. 16, No. 6 November-December 1981, pp. 1373-1383.

Metcalf, J. I., "Rain Backscattering Effects in Coherent Polarization-Diversity Radar Signals," Preprints of 20th Conf. on Radar Meteor., Amer. Meteor. Soc., 1981, pp. 649-655.

Metcalf, James I., Brookshire, Stephen P., Morton, Thomas P., "Polarization-Diversity Radar and Lidar Technology in Meteorological Research," Georgia Institute of Technology, Engineering Experiment Station, AFGL-TR-78-0030, Air Force Geophysics Laboratory, 1978.

Metcalf, J. I., and Morton, T. P., "Applications of Polarization-Diversity Radar and Lidar Technology in Meteorology," AFGL-TR-78-0031, Air Force Geophysics Laboratory, 1978.

Newell, Reginald E., Geotis, Spiros G., and Fleisher, Aaron, "The Shape of Rain and Snow at Microwavelengths," Cambridge 39, Mass., Massachusetts Institute of Technology, Research Report No. 28, September 1957.

BIBLIOGRAPHY (continued)

Peebles, Peyton Z. Jr., "Radar Rain Clutter Cancellation Bounds Using Circular Polarization," _IEEE International Radar Conference_, 1975, pp. 210-214.

Rumsey V. H., "Horn Antennas with Uniform Power Patterns Around Their Axes," _IEEE Transactions on Antennas and Propagation_, September 1966, pp. 656-658.

Ryan, Charles E. Jr., "Review and Evaluation of Antenna Test Ranges," Atlanta, Georgia, Georgia Institute of Technology, Engineering Experiment Station, Preliminary Report, 8 May 1975.

"The Scientific - Atlanta Antenna Calculator," _S/A Application Notes_, Atlanta, GA, Scientific-Atlanta, Inc.

Smith, Paul L. Jr., Hardy, Kenneth R., and Glover, Kenneth M., "Applications of Radar to Meteorological Operations and Research," _Proc. IEEE_, Vol. 62, No. 6, June 1974, pp. 724-745.

Stutzman, Warren L., Overstreet, William P., "Axial Ratio Measurements of Dual Circularly Polarized Antennas," _Microwave Journal_, Technical Feature, October 1981, pp. 75-78.

APPENDIX A. RECOMMENDED MAJOR COMPONENTS, SUGGESTED VENDORS

ITEM	No.	Unique Specifications	VENDOR/MODEL/PRICE/DELIVERY Vendor #1	Vendor #2	Vendor #3	EXCEPTIONS TO SPECIFICATIONS Vendor #1	Vendor #2	Vendor #3	Comments
A. ANTENNA									
1. Feed & Subreflector Support Assembly			H&W Eng.						Static & dynamic analysis of entire antenna $8850 add'l
2. Hyperbolic Subreflector			H&W Eng. $4000						
B. POLARIZER – Use either Hybrid Polarizer item 3 or polarizer from major items 4 through 6									
3. Hybrid	1	Circ. Pol. Isol.: 40 dB; Linear Pol. Isol.: 26 dB; Instantly switchable from linear to circ.	Atlantic Microwave #34,600 7-9 mos.						
*4. Dual Mode	1	Min. Isol.: ≥ 50 dB; Freq.: 2.735 GHz; Bandwidth: 2%; Insertion Loss: ≤ 0.1 dB	MDL 284TR56B $602 12-16 wks.	Trak $1685 10 wks.	Atlantic Microwave $2500				
*5. 45° Phase Shifter	2	Switch time: ≈ 1 sec.; Peak Power: 1/2 MW; Avg. Power: 1 KW	Atlantic Microwave $1250						
*6. Short Slot Hybrid	1	Freq: 2.735 GHz; Bandwidth: 2%, Isol.: > 40 dB; Insertion Loss: ≤ 0.05 dB; Amp Bal: ± 0.2 dB; No Flanges	MDL 285H592B $342	Arra AW1199 $1200	Atlantic Microwave $2500	> 30 dB Isolation guar. 0.10 dB balance	30 dB Isolation	40 dB Isol. at 1 freq. Amp Bal: ±0.1 dB. Std. Coupler; Isol. 30 dB, Amp Bal. 0.25 dB $135	
C. MICROWAVE PACKAGE									
*7. 20 dB 90° Directional Coupler	4	Power Capability: ≥ 1.2 MW; VSWR ≤ 1.07:1	Arra 284-620B-20 $1200	MDL $1950 10 mos.	Waveline 274-20 $1200 10-12 wks.				VSWR requirement may increase cost
*8. High Power Circulator	1	Must phase & amplitude track present unit	Microwave Associates about $10,000	Litton No Bid		May req. $3,000 add'l to measure present unit			May not be buildable; two circulators may be required
*9. Medium Power Termination	2	Power = 100 W; VSWR ≤ 1.2:1; WR 284 flange	Airtron #284C $930 150 days	Arra 284925B $295	Passive Microwave Components $300	1.5 KW Avg. Aluminum body	1200 watts		Not required if additional circulator is not required
10. Switchable High Power Circulator/ RF Switch Assembly	1	Isolation: 37 dB; 40 dB Design Goal; Switch Time: 10 µs; Power: 1 MW peak, 2 KW avg.; Insertion Loss: 1 dB	Raytheon $80,000 budgetary / Vendor #4 Premier Microwave $55,000 incl. drivers budgetary	Electro Magnetic Sciences $190,000 incl. drivers	Atlantic Microwave $140,000 includes drivers	Isolation: 35 dB 27 dB Design Goal Switch time: 7 µs	Isolation: 40 dB min Power: 1.2 MW pk Switch time: 20 ns max.	A 0.5 MW pk, 500 W avg. switch is available for $75,000	Vendors 1,2,4 utilize ferrite devices Vendor 3 would construct a diode device Recommend all vendors to give final RFQ
11. Trigger Generator	1	Provide Switch pulse to Circulator	to be constructed $200 est. comp. cost 3 man-month design & construction						

* Items marked by * are not or may not be required in the recommended configuration.

APPENDIX A. RECOMMENDED MAJOR COMPONENTS, SUGGESTED VENDORS (continued)

ITEM	No.	Unique Specifications	VENDOR/MODEL/PRICE/DELIVERY			EXCEPTIONS TO SPECIFICATIONS			Comments
			Vendor #1	Vendor #2	Vendor #3	Vendor #1	Vendor #2	Vendor #3	
D.1 RECEIVER, RF COMPONENTS									
12. Diplexer	1	Frequency: 2600-2800 MHz Split out 2710 & 2760 MHz 0.1 dB amplitude error pair phase tracking: 1 deg.	Microphase $2700 + $600 NRE 14 weeks	Delta Micro. $1250 each 8-10 weeks					The microphase design might be inappropriate see Section IV
13. T/R Switch Limiter	1	Must phase & amplitude track existing unit Phase track ≤ 3 deg. Phase uncertainty ≤ 1 deg.	Microwave Associates $4250			Requires Measurements of present unit $3000 Add'l			
14. Low Noise Amplifier	2	Noise Fig. ≤ 2.3 dB Frequency: 2709-2762 MHz 12-15 dB Gain 1 dB comp. pt. = 15 dBm 3/4° phase tracking 1/2 dB amplitude tracking	Avantek ABG4330M1C3 $1020/Pair 120 days	Bunker-Ramo #70149 $1500 90 days		Avantek 11-14 dB Gain 1 dB comp =13 dBm 2° phase tracking 0.5 amplitude tracking	phase tracking $250 to $500 Add'l noise temp. 90°K		
15. Phase Shifter	4	Frequency: 2660-2790 MHz remotely adjustable coaxial	Arra 9428 (A)-28 9428 (B)-28 $725	Merrimac PSIM-3-30 $175	Lorch VP401C $90	Motorized "A": 608/GHz "B": 30°/GHz	Not remotely adjustable	Not remotely adjustable	connector should be APC 3.5 or APC-7 recommend remotely adjustable
16. Mixer	4	1 dB comp. pt., +15 dB Noise Figure: 8 dB Internal image suppression amplitude tracking: 0.1 dB phase tracking: 1 deg. RF to LO isolation ≥ 20 dB	RHG 1 RDM 2.8E03PN	Triangle FA 107i $1650/pair		Phase tracking: 10 deg.	RF to LO isolation > 35 dB Phase tracking ± 0.75 deg.		
17. Power Dividers	8	Frequency: 30 MHz In Phase Outputs Phase Balance: 1 deg. Amplitude Balance: 0.2 dB	Merrimac PDM-20-50 $45	Anzac THV-50 $70	Arra 0200-2 $130				
18. Filters	one each freq	Power level ≥ 13 dBm Insertion Loss ≤ 7 dB Q: ≥ 268. Min atten. at f_0 ± 5 MHz: 20 dB Freqs: 2680 & 2790 MHz	Delta Microwave $450 each frequency						
19. Amplifier	2	Frequency: 2650-2790 MHz Gain 5-7 dB Input Level 11-14 dBm Output Level > 21 dBm 1 dB comp. pt. > 21 dBm	Avantek APG 4001 $445 120 days			2-4 GHz Gain: 6 dB 1 dB comp. pt.: 30 dBm Noise Fig: 7 dB			
20. Coaxial In Phase Power Divider	2	Frequency: 2-4 GHz Connector: SMA	Anaren 40266 $160	MiniCircuits ZAPD-4 $44.95	Arra N4200-2 $130				only 4 req'd if different phase detector is employed
21. 50 Ω Terminations	2	Connector: SMA Power: 1/2 W VSWR ≤ 1.2:1	Merrimac TM-9K $25	Elcom CT-51 $11.50	Midwest 2444M $21				
22. Isolator	4	Isolation: > 20 dB Frequency: 2.6-2.8 GHz Connectors: SMA VSWR ≤ 1.2:1	RYT 200209 $150	PMC D4185 (waveguide) $1225					

APPENDIX A. RECOMMENDED MAJOR COMPONENTS, SUGGESTED VENDORS (continued)

D.3 RECEIVER, IF AMPLIFIERS AND PHASE DETECTOR

ITEM	No.	Specifications	VENDOR/MODEL/PRICE/DELIVERY Vendor #1	Vendor #2	Vendor #3	EXCEPTIONS TO SPECIFICATIONS Vendor #1	Vendor #2	Vendor #3	Comments
23. By Pass Relay	8	Indicator contacts Frequency: 30 MHz coaxial Connector: SMA	Transco 919C70200 $136 Stock	Engleman SW0510 $250					
24. IF Preamp 30 MHz	4	Noise Figure: ≤ 3 dB 3 dB Bandwidth: 4 MHz Gain: 25 dB Phase Tracking: 1.0 deg Amplitude tracking: 0.1 dB	RHG P/N not assigned $1915 + 1900 NRE						Atlantic Microwave should also be considered
25. Variable Attenuators	6	Frequency: 30 MHz Continuously adjustable Maximum range: 3 dB	RHG VCA 500 $275 90 days	Arra 0682-1SF $120		voltage controlled			
26. 3 dB Attenuators	5		NARDA 4772-3						
27. 30 MHz Filters	4	1 dB bandwidth: 4 MHz Ins. loss: < 3.5 dB; ≥ 25 dB at ±5 MHz; fₒ: 30 MHz Phase dispersion: ≤ 1.0 deg.	Cir-Q-Tel FBT/216-30/ 4-10/50-28A/ 28A $584 each	Lark DP 30-X4-6AA $219 6 weeks		10 Pole Bessel Group delay ≤ 100ns 10 Pole Butterworth Group delay ≤ 1200ns also avail. @ $346 ea.	Butterworth		Bessel function filters have insufficient skirt selectivity. Group delay & skirt selectivity must be reconsidered
28. 30 MHz SAW Filters	1	Connectors: SMA Ins. loss: > 40 dB Power level: ≤ + 20 dBm Switch time: = 100 ns	Transco $494	Daico P.M100C1052-CPO $1000 10 weeks					
29. Log IF Amplifiers	4	Center Freq.: 30 MHz Dynam.: Range: 90 dB	RHG P/N not assigned $935						
30. IF Limiters	2	Frequency: 30 MHz Phase uncertainty ≤ 3/4°	RHG ICDX30 $725						
31. X6 Multiplier/ Buffer Amplifier	1	Frequency Input: 5 MHz Frequency Output: 30 MHz	Austron $1200 90 days						unit is the same as, but separate from present multiplier
32. 30 MHz Dual Buffer Amp.	1	Spec. Identical to existing units	Austron $850 90 days						
33. 30 MHz Mixer			Mini Circuits ZEM2FM-H 12FY = $50	Anzac MD-525-4 $180	Merrimac DMM-2A-250 $65	Vendor #4 Engleman MLK101-M/MLK102.5 $65 / $45			
34. Line Driver	8	Bandwidth: 4 MHz with coaxial line equalizer	Georgia Tech Part no. A2134-0011						
35. Video Slip Ring Assembly	1	8 video rings 4 10 amp power rings 6 control rings	Weldon $3,990			Add'l $600 NRE required			Add'l video rings should be considered for use as spares

APPENDIX B. SUGGESTED VENDORS, ADDRESSES, AND CONTACTS

Company	Product	Telephone No.	Contact	Address
Acme Microwave Corp.	Waveguide	(516) 567-2992		1595 Ocean Ave., Bohemia, L.I., NY 11716
Airtron/Litton	Waveguide/Components	(201) 539-5500	Bob Vance	200 E. Hanover Ave., Morris Plains, NJ 07950
Alpha Industries, Inc./TRG	Components	(617) 935-5150 Ext. 201	George Gill	20 Sylvan Rd., Woburn, MA 01801
Amplica, Inc.	Amplifiers	(805) 498-9671		950 Lawrence Dr., Newbury Park, CA 91320
Anaren Microwave, Inc.	Micro. Low Power Comp.	(315) 476-7901	Lou Nielsen	185 Ainsley Dr., Syracuse, NY 13205
Andrew Corp.	Antennas	(703) 442-8771	Mr. Savalle	10500 W. 153rd St., Orlando Park, IL 60462
Anzac	Components	(617) 273-3333		80 Cambridge St., Burlington, MA 01803
Arra, Inc.	Components	(516) 231-8400	Carl Solomon	15 Harold Ct., Bay Shore, NY 11706
Atlantic Microwave	Components, Mixer	(617) 779-5525	Ed Saltzberg	Rt. 117, Bolton, MA 01740
Austron, Inc.	Crystal Oscillator	(405) 452-8709	Phil Mabrey	1915 Kramer Lane, Austin, TX 78758
Avantek	Amplifiers	(408) 249-0700	J. Danielson	3175 Bowers Ave., Santa Clara, CA 95051
Bendix Corp.	Connectors	(607) 563-5384		Sidney, NY 13838
Bunker Ramo Corp.	Connectors	(404) 394-6298		No. 7 Dunwoody Park, Suite 107, Atlanta, GA 30338
Cir-Q-tel, Inc.	IF filters	(301) 946-1800	Dick Wainwright Paul Leo	10504 Wheatley St., Kensington, MD 20795
DAICO	IF/RF Components	(213) 631-1143	Robert Kramer	2351 E. Del Amo Blvd., P.O. Box 5225, Compton, CA 90220 90224
Delta Microwave	Filters/Diplexers	(213) 889-6582	Dick Reed	755M LakeField Rd., Unit K, Westlake Vil., CA 91361
Elcom Systems, Inc.	Components	(516) 667-5800		127F Brook Ave., Deer Park, NY 11729
Englemann Micro. Co.	Microwave Components	(201) 334-5700	Mr. Bailey	Skyline Dr., Montville, NJ 07045
Electromagnetic Sciences	Ferrite Devices	(404) 448-5770	J.L. Banks	125 Technology Park, Norcross, GA 30092

APPENDIX B. SUGGESTED VENDORS, ADDRESSES, AND CONTACTS (continued)

Company	Product	Telephone No.	Contact	Address
Ford Aerospace	Antennas	(415) 494-7400	F.B. Bellit	3939 Fabian Way, Palo Alto, CA 94303
Frequency Sources	Solid State Oscillators	(408) 727-8500	Ed Brown	3140 Alfred St., Santa Clara, CA 95050
H&W Industries	Reflectors	(617) 383-1200	Jim Hayes	155 King Skt., P.O. Box 322, Cohasett, MA 02025
K&L Microwave, Inc.	Filters	(301) 749-2424		408 Coles Circle, Salisbury, MD 21801
K&W	Filters	(714) 571-8444	Art Brand	4565 Russner St., San Diego, CA 92111
Kings BNC	Coaxial Connectors	(914) 793-5000		40 Marbledale R., Tuckahoe, NY 10707
Lamda	Power Supplies	(516) 694-4200		515 Broad Hollow Rd., Melville, L.I., NY 11747
Lark Engineering	Filters	(714) 493-9501	Bill Wheeler	26401 Calle Rolando, San Juan Capistrano, CA 92675
Lorch Electronics Corp.	Components	(201) 569-8282	Alan Drumbar	105 Cedar Lane, Englewood, NJ 07631
MDL	Microwave Components	(617) 665-0060	Ernie Banister	10 Michigan Dr., Natick, MA 01760
Maury Microwave Corp.	Microwave Components	(714) 978-4715		8610 Helms Ave., Cucamonga, CA 91730
Merrimac	Passive Coaxial Comp.	(201) 575-1300		41 Fairfield Place, West Caldwell, NJ 07006
Microphase Corp.	Multiplexers	(203) 661-6200	H. Schumacher	P.O. Box 1166, Greenwich, CN 06830
Microwave Associates	Ferrite Devices	(617) 272-3000	Auston Dobson	South Ave., Burlington, MA 01803
Microwave Cavity Lab.	Components	(312) 354-4350		10 N. Beach Ave., La Grange, IL 60525
Midwest Microwave	Components	(313) 971-1992	Bill Stockman	3800 Packard Rd., Ann Arbor, MI 48104
Milliflect (Fowler Mktg.)	Antennas	(415) 791-5188	Al Fowler	7752 Enterprise Dr., Newark, CA 94560
Mini-Circuits	Mixers	(212) 769-0200		2625 E. 14th St., Brooklyn, NY 11235
NARDA	Coaxial Components	(404) 451-6161	E.G. Holm	4185 Clairmont Rd., Chamblee, GA 30341
Omni Spectra	Passive Coaxial Components/Connectors	(603) 424-4111		21 Continental Blvd., Merrimack, NH 03054

APPENDIX B. SUGGESTED VENDORS, ADDRESSES, AND CONTACTS (continued)

Company	Product	Telephone No.	Contact	Address
Passive Microwave Technology	Passive Coaxial Components	(213) 999-3111	George Grund	8030 No. 1 Remmet, Conoga Park, CA 91304
Phelps Dodge	Antennas	(201) 462-1880	Dan Applegate	Rt. 79, Marlboro, NJ 07746
Premier Microwave Corp.	Microwave Components Ferrite Devices	(914) 939-8900		33 New Broad St., Port Chester, NY 10573
RHG Electronics Lab	IF Components/Mixers	(516) 242-1100	Sid Wolin	161 E. Industry Ct., Deer Park, NY 11729
Raytheon	Ferrite Devices	(617) 393-7300	Dawson Micne	Bearfoot Rd., Northboro, MA 01532
Scientific Atlanta	Antennas/Pedestals	(404) 449-2000		3845 Pleasantdale Rd., Atlanta, GA 30340
Seavey Engineering	Antennas	(617) 383-9722	John Seavey	339 Beachwood St., Cohassett, MA 02025
Spincraft	Antennas	(617) 667-2771		Iron Horse Ind. Pk., High St., N. Billerica, MA 01862
Tecom	Antennas	(213) 341-4010	Jim Olsen	21526 Osborne St., Canoga Park, CA 91304
Teloric/Berkeley	Filters	(714) 494-9401		2825 Laguna Canyon Rd., Box 277, Laguna Beach, CA 92665
TRAK	Microwave Components	(813) 884-1411	Toby Gant	4726 Eishenhower Blvd., Tampa, FL 33614
Transco Products, Inc.	Switches	(213) 822-0800	Larry Neeley	4241 Glencoe Ave., Benice, CA 90291
Triangle Microwave	Microwave Components	(201) 984-1423	Mr. Rabinowitz	11 Great Meadow Lane, E. Hanover, NJ 07936
A.J. Tuck Co.	Waveguide Components	(203) 775-1234	Tore Anderson	Tuck Rd., Brookfield, CN 06804
Vectron Labs. Inc.	Crystal Oscillators	(203) 853-4433		166 Glover Ave., Norwalk, CN 06850
Watkins-Johnson Co.	RF Components	(415) 493-4141	George Graham	3333 Hillview Ave., Stanford Industrial Park, Palo Alto, CA 94304
Waveline, Inc.	Test Equip./Micro. Comp.	(201) 226-9100	Don Morsillo	P. O. Box 718, W. Caldwell, NJ
Weinschel Engineering	Instr./Attenuators	(301) 948-3434	Jerry Spero	Gaithersburg, MD 20760
Weldon	Slip Ring Assemblies	(203) 348-6271		Irving & Selleck Streets, Stanford, CN 06902

A PROGRAM TO CALCULATE AVERAGE ANTENNA GAIN
DUE TO BEAMFILLING OF AN EXTENDED TARGET

Given the 3 dB beamwidth this program determines the mainbeam gain vs assumed filled beamwidth using a gaussian antenna pattern approximation. The program is written in Microsoft Basic.

```
10      REM AVGPWR
20      CLS
30      Input "3dB BEAMWIDTH IN DEGREES?"; B
35      A = 1.66511/B
40      Input "ANGLE OVERWHICH POWER IS TO BE AVERAGED?"; T(1)
45      T = T(1)/2
50      DIM P(10)
60      N(1) = 1
70      GO SUB 80
80      FOR N=1 to 10
90      PRINT "N="; N
100     N(2) = N(1)*N
110     PRINT "N!="; N(2)
120     N(4) = (A*T) ↑ (2*N)
130     PRINT "(AT) ↑ 2N="; N(4)
140     N(3) = ((-1) ↑ N)
150     PRINT "(-1) ↑ N = "; N(3)
160     N(5) = (2*N)+1
170     PRINT "2N+1 = "; N(5)
180     P(N) = ((N(4))*(N(3)))/((N(2))*(N(5)))
190     PRINT "P(N) = "; P(N)
200     FORM=1 to 3000: NEXT M
210     CLS
220     P(0) = P(0) + P(N)
230     P  = P(0) + 1
240     PRINT "SO FAR THE SUMMATION EQUALS ";P
250     PRINT "THE NEXT NUMBER IS: "
260     N(1)=N(2)
270     IF N=10 THEN GO TO 300
280     NEXT N
290     RETURN
300     PRINT "FOR BEAM ANGLE "; T ;" DEGREES"
310     Q =(20*(0.43429*(LOG(P))))
320     PRINT "THE AVERAGE POWER IS REDUCED BY: "; Q ; " DB"
```